

Application of Translational Addition Theorems to Electrostatic and Magnetostatic Field Analysis for Systems of Circular Cylinders

by

Adam Machynia

A Thesis submitted to the Faculty of Graduate Studies of
The University of Manitoba
in partial fulfilment of the requirements of the degree of

Master of Science

Department of Electrical and Computer Engineering
University of Manitoba
Winnipeg

Copyright ©2012 by Adam Machynia

Abstract

Analytic solutions to the static and stationary boundary value field problems relative to an arbitrary configuration of parallel cylinders are obtained by using translational addition theorems for scalar Laplacian polar functions, to express the field due to one cylinder in terms of the polar coordinates of the other cylinders such that the boundary conditions can be imposed at all the cylinder surfaces. The constants of integration in the field expressions of all the cylinders are obtained from a truncated infinite matrix equation.

Translational addition theorems are available for scalar cylindrical and spherical wave functions but such theorems are not directly available for the general solution of the Laplace equation in polar coordinates. The purpose of deriving these addition theorems and applying them to field problems involving systems of cylinders is to obtain exact analytic solutions with controllable accuracies, thereby, yielding benchmark solutions to validate other approximate numerical methods.

Acknowledgements

In the first place I would like to thank Prof. Ioan M.R. Ciric for his ideas, support, continuing enthusiasm and encouragement without which I may never have completed this research. I consider myself privileged to have had the opportunity to work under his guidance.

Special thanks for the financial assistance of the University of Manitoba Faculty of Graduate Studies in the form of a Graduate Fellowship and to the personnel working in the Electrical and Computer Engineering Department of the University of Manitoba, but especially to Amy Dario for her continued assistance.

Finally, my utmost gratitude to my family for their understanding and continued support.

Dedication

In loving memory of my brother, Robert.

Contents

Contents	iii
List of Figures	v
List of Tables	vii
List of Symbols	ix
1 Introduction	1
2 Laplacian potential of a system of circular cylinders	4
2.1 Harmonic solution of the Laplace equation in circular cylindrical coordinates	4
2.2 Geometry of a general system of parallel circular cylinders	5
2.3 Addition theorem for circular cylindrical scalar waves	8
3 Translational addition theorems for static and stationary fields	11
3.1 Limiting forms of the Bessel and Neumann functions for small arguments	11
3.2 Derivation of the translational addition theorems for two-dimensional circular cylindrical Laplacian functions $r^{-n} \cos n\phi$ and $r^{-n} \sin n\phi$. .	12
3.3 Derivation of the translational addition theorems for two-dimensional circular cylindrical Laplacian functions $r^n \cos n\phi$ and $r^n \sin n\phi$. . .	16
3.4 Derivation of the translational addition theorems for two-dimensional circular cylindrical Laplacian function $\ln r$	19
3.5 Numerical analysis of the series expansions in the addition theorems	21
3.5.1 Evaluation of the translational addition theorems for Laplacian functions $r^{-n} \cos n\phi$ and $r^{-n} \sin n\phi$	22
3.5.2 Evaluation of the translational addition theorems for Laplacian functions $r^n \cos n\phi$ and $r^n \sin n\phi$	27
3.5.3 Evaluation of the translational addition theorems for Laplacian function $\ln r$	29

4	Application of the addition theorems to the solution of electrostatic fields in systems of parallel circular cylinders with coplanar axes	31
4.1	Conducting cylinder parallel with a line charge	31
4.2	Two-cylinder system	37
4.3	Two-cylinder system in external electric field	47
4.4	Three-cylinder system	51
4.5	Three-cylinder system in external electric field	55
5	Application of the addition theorems to the solution of electrostatic fields in systems of parallel cylinders with arbitrary axis locations	62
5.1	Two-cylinder system arbitrarily located in the system of coordinates	62
5.2	System with N arbitrarily located cylinders	68
6	Application of the translational addition theorems to the solution of magnetostatic fields	74
6.1	Two perfectly conducting cylinders in an external magnetic field parallel to the plane of their axes and normal to them	74
6.2	Two perfectly conducting cylinders in an external magnetic field normal to the plane of their axes	80
6.3	The magnetic vector potential	84
7	Conclusion and Future Work	85
7.1	Conclusion	85
7.2	Continued research	86
A	Circular cylindrical harmonics	87
B	Two-dimensional bipolar coordinates	89
	Bibliography	92

List of Figures

2.2.1	Geometry of N parallel cylinders arbitrarily located	7
3.5.1	Point P along a circle of radius r_p when $r_p < r_{qp}$	22
3.5.2	Point P along a circle of radius r_p when $r_p > r_{qp}$	26
4.1.1	Conducting cylinder near a parallel line charge	32
4.1.2	Two straight line charges of equal and opposite sign	35
4.2.1	System of two conducting cylinders	37
4.2.2	Two conducting cylinders in bipolar coordinates (η, ξ)	44
4.3.1	Two conducting cylinders in an external electric field, $\mathbf{E}_0 = E_0 \mathbf{a}_x$	47
4.4.1	Three conducting cylinder system with given charges	52
4.4.2	Potential distribution with respect to r_1 for angles $\phi_1 = 0, \pi/6,$ $\pi/4, \pi/3$ and $\pi/2$, when $a_1 = 1$ cm, $a_2 = 2$ cm, $a_3 = 3$ cm, $d_{12} = 5$ cm, $d_{23} = 7$ cm, $d_{13} = 12$ cm, $q_{tot}^{(1)} = -2$ nC/m, $q_{tot}^{(2)} = 1$ nC/m, $q_{tot}^{(3)} = 1$ nC/m and $M = 15$	55
4.5.1	Three conducting cylinders in an external field, $\mathbf{E}_0 = E_0 \mathbf{a}_x$	56
5.1.1	Two conducting cylinders arbitrarily located in space	63
5.1.2	Potential distribution and errors between translational and bipolar methods for $a_1 = 1$ cm, $a_2 = 2$ cm, $d_{12} = d_{21} = 5$ cm, $\phi_{12} = \pi/3,$ $\phi_{21} = 4\pi/3$, $q_{tot}^{(1)} = -1$ nC/m, $q_{tot}^{(2)} = 1$ nC/m and $M = 25$	67
	(a) Potentials distribution for $\phi_1 = \pi/3, 7\pi/12$ and $5\pi/6$ over $0 < r_1 < 40$ cm	67
	(b) Percentage Error for $\phi_1 = \pi/3, 7\pi/12$ and $5\pi/6$ over $0 <$ $r_1 < 10$ cm	67
5.2.1	Three conducting cylinders arbitrarily located in space	69
5.2.2	Potential distribution with respect to r_1 for angles $\phi_1 = 0, \pi/6,$ $\pi/3, \pi/2, 2\pi/3$ and π , when $a_1 = 1$ cm, $a_2 = 2$ cm, $a_3 = 3$ cm, $d_{12} = d_{23} = d_{13} = 10$ cm, $q_{tot}^{(1)} = 1$ nC/m, $q_{tot}^{(2)} = -2$ nC/m, $q_{tot}^{(3)} = 1$ nC/m and $M = 15$	72
6.1.1	Two conducting cylinders in external magnetic field, $\mathbf{H}_0 = H_0 \mathbf{a}_x$	75

6.1.2	Magnetic field intensity components H_x and H_y plots around cylinder 1, $r_1 = a_1$ for different separation distances $d = 5$ cm, 10 cm and 20 cm between the translational and bipolar methods for $a_1 = 1$ cm, $a_2 = 2$ cm, $H_0 = 1$ A/m, and $M = 50$	79
	(a) H_x field for $d = 5$ cm	79
	(b) H_y field for $d = 5$ cm	79
	(c) H_x field for $d = 10$ cm	79
	(d) H_y field for $d = 10$ cm	79
	(e) H_x field for $d = 20$ cm	79
	(f) H_y field for $d = 20$ cm	79
6.2.1	Two conducting cylinders in external magnetic field, $\mathbf{H}_0 = H_0 \mathbf{a}_y$.	80
6.2.2	Magnetic field intensity component plots around cylinder 1, $r_1 = a_1$ between the translational and bipolar methods for $a_1 = 1$ cm, $a_2 = 2$ cm, $d = 20$ cm, $H_0 = 1$ A/m and $M = 50$	83
	(a) H_x field	83
	(b) H_y field	83
B.1	Relation between bipolar and Cartesian coordinates	90

List of Tables

3.5.1	Truncation errors of $g_1(r_p, \phi_p)_{\cos}$ and $g_1(r_p, \phi_p)_{\sin}$ for $n = 3$, $M = 20$, $\phi_{qp} = 0$ and $r_p/r_{qp} = 0.5$	23
3.5.2	Truncation errors of $g_1(r_p, \phi_p)_{\cos}$ and $g_1(r_p, \phi_p)_{\sin}$ for $n = 3$, $M = 50$, $\phi_{qp} = 0$ and $r_p/r_{qp} = 0.5$	23
3.5.3	Truncation errors of $g_1(r_p, \phi_p)_{\cos}$ and $g_1(r_p, \phi_p)_{\sin}$ for $n = 9$, $M = 50$, $\phi_{qp} = 0$ and $r_p/r_{qp} = 0.5$	24
3.5.4	Truncation errors of $g_1(r_p, \phi_p)_{\cos}$ and $g_1(r_p, \phi_p)_{\sin}$ for $n = 9$, $M = 80$, $\phi_{qp} = 0$ and $r_p/r_{qp} = 0.5$	24
3.5.5	Truncation errors of $g_1(r_p, \phi_p)_{\cos}$ and $g_1(r_p, \phi_p)_{\sin}$ for $n = 9$, $\phi_p = 72^\circ$, $\phi_{qp} = 0$ and $r_p/r_{qp} = 0.5, 0.7, 0.9$	25
	(a) for $r_p/r_{qp} = 0.5$, $\phi_q = 29.35^\circ$ and $r_{qp}/r_q = 1.0309$	25
	(b) for $r_p/r_{qp} = 0.7$, $\phi_q = 40.35^\circ$ and $r_{qp}/r_q = 0.9725$	25
	(c) for $r_p/r_{qp} = 0.9$, $\phi_q = 49.86^\circ$ and $r_{qp}/r_q = 0.8931$	25
3.5.6	Truncation errors of $g_1(r_p, \phi_p)_{\cos}$ and $g_1(r_p, \phi_p)_{\sin}$ for $n = 9$, $M = 80$, $\phi_{qp} = \pi/3$ and $r_p/r_{qp} = 0.5$	25
3.5.7	Truncation errors of $g_2(r_p, \phi_p)_{\cos}$ and $g_2(r_p, \phi_p)_{\sin}$ for $n = 6$, $M = 80$, $\phi_{qp} = \pi/3$ and $r_{qp}/r_p = 0.6$	27
3.5.8	Truncation errors of $g_3(r_p, \phi_p)_{\cos}$ and $g_3(r_p, \phi_p)_{\sin}$ for $n = 20$, $\phi_{qp} = \pi/3$ and $r_p/r_{qp} = 0.9$	28
3.5.9	Truncation errors of $g_4(r_p, \phi_p)_{\cos}$ and $g_4(r_p, \phi_p)_{\sin}$ for $n = 20$, $\phi_{qp} = \pi/3$ and $r_{qp}/r_p = 0.9$	28
3.5.10	Truncation errors of $g_5(r_p, \phi_p)$ for $\phi_{qp} = 2\pi/3$, $r_p/r_{qp} = 0.5$, and $M = 10$ and 30	29
3.5.11	Truncation errors of $g_6(r_p, \phi_p)$ for $\phi_{qp} = 2\pi/3$, $r_{qp}/r_p = 0.6$, and $M = 10$ and 30	30
4.2.1	Percentage error between the potential values of the translational and bipolar boundary value methods for $a_1 = 1$ cm, $a_2 = 2$ cm, $d = 5$ cm, $q_{tot}^{(1)} = -1$ nC/m, $q_{tot}^{(2)} = 1$ nC/m, and $M = 5$	46
4.2.2	Percentage error between the potential values of the translational and bipolar boundary value methods for $a_1 = 1$ cm, $a_2 = 2$ cm, $d = 5$ cm, $q_{tot}^{(1)} = -1$ nC/m, $q_{tot}^{(2)} = 1$ nC/m, and $M = 15$	46

4.3.1	Percentage error between the potential values of the translational and bipolar boundary value methods for $a_1 = 1$ cm, $a_2 = 2$ cm, $d = 5$ cm, $q_{tot}^{(1)} = -1$ nC/m, $q_{tot}^{(2)} = 1$ nC/m, $E_0 = 10$ V/m and $M = 25$	51
4.5.1	Relative electric field components at selected points on the cylinders in Figure ?? for different relative gaps g/a , when $\mathbf{E}_0 = E_0\mathbf{a}_x$ and zero total charge of the cylinders	58
4.5.2	Potential on each cylinder in Figure ?? for different relative gaps g/a , when $\mathbf{E}_0 = E_0\mathbf{a}_x$ and zero total charge of the cylinders	59
4.5.3	Relative electric field components at selected points on the cylinders in Figure ?? for different gap ratios g/a , when $\mathbf{E}_0 = E_0\mathbf{a}_y$ and no charge on the cylinders	61
4.5.4	Induced potential on each cylinder in Figure ?? for different relative gaps g/a , when $\mathbf{E}_0 = E_0\mathbf{a}_y$ and zero total charge of the cylinders	61

List of Symbols

∇^2	Laplacian operator.
∇	Gradient operator.
\mathbf{a}_n	Unit vector normal exterior to surface.
k	Wave number.
j	$\sqrt{-1}$
$J_n(z)$	Bessel function of integral order n and argument z .
$Y_n(z)$	Neumann function of integral order n and argument z .
$H_n(z)$	Hankel function of integral order n and argument z .
$Z_n(z)$	Cylindrical Bessel function of integral order n and argument z .
N	Number of cylinders.
p, q	Cylinder number.
ε	Permittivity.
μ	Permeability.
(x_p, y_p)	Cartesian coordinate system of the p^{th} cylinder.
(r_p, ϕ_p)	Polar coordinate system of the p^{th} cylinder.
E	Electric field intensity.
H	Magnetic field intensity.
$\delta_{n,m}$	Kronecker delta, zero if $n \neq m$, one if $n = m$.
u	General scalar function, satisfying Laplace equation. Also, scalar electrostatic potential.
a_p	Radius of the p^{th} cylinder.
V_p	Potential on the p^{th} cylinder.
ψ	Scalar wave function.
$\Gamma(n)$	Gamma function.
ρ_l	Linear charge density.
$\rho_S, \rho_S^{(p)}$	Surface charge density of the p^{th} cylinder.
$Q_{tot}^{(p)}$	Total charge on the p^{th} cylinder.
$q_{tot}^{(p)}$	Total charge per unit length on the p^{th} cylinder.
γ, τ	Shorthand notation for various functions.

(η, ξ)	Planar bipolar coordinate system.
a	Semi focal distance in bipolar coordinates.
d	Separation distance between two cylinders in bipolar coordinates.
S	Surface.
$P(x_p, y_p), P(x_n, y_n)$	Point in space, with respect to coordinate system (x_p, y_p) or (x_n, y_n) .
u_m	Magnetic scalar potential.
A_z	Magnetic vector potential, z -component.
A	Magnetic vector potential.
B	Magnetic flux density.
J	Current density.
I_p	Current on the p^{th} cylinder.
$u_p(r_p, \phi_p)$	Electrostatic potential of the p^{th} cylinder with respect to the p^{th} coordinate system.
$u_q^{(p)}(r_p, \phi_p)$	Electrostatic potential of the q^{th} cylinder with respect to the p^{th} coordinate system.
$u_{tot}^{(p)}(r_p, \phi_p)$	Total electrostatic potential with respect to the p^{th} coordinate system.
u_{tot}^{im}	Total electrostatic potential using image method solution.
u_{tot}^{bi}	Total electrostatic potential using bipolar coordinate Laplacian solution.
d_{qp}	Separation distance between the centres of the q^{th} and p^{th} cylinders.
r_{qp}	Separation distance between the origins of the q^{th} and p^{th} coordinate systems.
ϕ_{qp}	Coplanar angle of the centre of the p^{th} cylinder or origin with respect to q^{th} coordinate system (cylinder or origin).

Chapter 1

Introduction

The main focus of this thesis is on the derivation of the two-dimensional translational addition theorems for scalar Laplacian functions in polar coordinates. The theorems are then applied to some electrostatic and magnetostatic potential boundary value problems for various locations of parallel circular cylindrical conductors. Theoretically, a two-dimensional field model is an approximation for parallel conductors of finite length, when the length is much greater than the cross-sectional linear dimensions and the end effects are neglected.

Analytical solutions for boundary value field problems can only be obtained when the boundary surfaces coincide with a coordinate surface in an orthogonal system of coordinates. For the case of a single circular cylinder, the natural choice is that of the polar coordinates and for two parallel circular cylinders that of the two-dimensional bipolar coordinates. Then, existing classical methods, such as separation of variables, images [1], or conformal mapping [2], can be applied to solve for the field problem. For the general case of more than two cylinders, no set of coordinate surfaces in any orthogonal system can be made to coincide with all the cylinder surfaces. However, the combination of the method of images and inversion [3] yields analytic techniques that can be used to solve for some systems of parallel conductors.

For the general problem of N parallel circular cylinders we take a similar approach as that used in [4], where translational addition theorems for the Laplacian spherical functions were derived by particularizing the addition theorems for scalar spherical

wave functions [5]. In our case, we particularize the addition theorems for scalar cylindrical wave functions [6] to derive addition theorems for scalar Laplacian functions in polar coordinates.

Using the translational addition theorems allows for the field contributions from all the cylinders to be expressed in terms of the polar coordinates attached to each individual cylinder. Application of the boundary conditions at each cylinder surface gives a set of algebraic equations in terms of the unknown constants of integration from the field expressions of each cylinder.

The purpose of solving various field problems involving systems of parallel circular cylinders is to yield benchmark solutions, with exact analytic expressions and of controllable error, which are to be made available to the electromagnetic community for establishing the range of validity for various approximate numerical methods, such as the finite difference, finite element or boundary element methods [7]. This control of accuracy is achieved by appropriate truncation of the infinite series in the expressions for the harmonic fields and in the addition theorems.

The general problem for N arbitrarily located parallel cylinders is first formulated in Chapter 2, for Dirichlet and Neumann boundary conditions, to find solutions of Laplace's equation for given values of charges or potentials of the conducting cylinders. In Chapter 3, translational addition theorems are derived for the polar Laplacian functions $r^{-n} \cos n\phi$, $r^{-n} \sin n\phi$, $r^n \cos n\phi$, $r^n \sin n\phi$ and $\ln r$ and, then, their convergence tested numerically for numerous cases.

The translational addition theorems are then applied, in Chapters 4 and 5, to various electrostatic field problems for complete systems of parallel cylinders. For the cases of a circular cylinder in the presence of a line charge and of two cylinders, the numerical results are evaluated by comparison with results from existing exact methods: images and the separation of variables in bipolar coordinates, respectively. The translational method is also used to solve for the fields involving a charged three-cylinder complete system and for a three-cylinder grounded system in the presence of external electric fields.

A particular geometrical configuration of the cylindrical systems is considered in Chapter 4, where the cylinder axes are in the same plane, which allows for the simplification of the field expressions, where as, in Chapter 5, the parallel cylinders are arbitrarily located and the field expressions are more complex.

In Chapter 6, the addition theorems are used to solve scalar magnetostatic field problems for the case of two perfectly conducting cylinders in given external fields, of arbitrary orientations. A scalar magnetic potential is used, but it is also shown how the vector magnetic potential can be employed.

Chapter 2

Laplacian potential of a system of circular cylinders

The purpose of this chapter is to present the theoretical background necessary for the derivation and application of the addition theorems for circular cylindrical Laplacian functions. The formulation involves a set of circular cylindrical bodies under various boundary conditions.

2.1 Harmonic solution of the Laplace equation in circular cylindrical coordinates

The general form¹ of the Laplace equation is

$$\nabla^2 u(\mathbf{r}) = 0. \quad (2.1.1)$$

The natural choice when a boundary condition is given on a circle is the polar (or circular) coordinate system (r, ϕ) . For an infinitely long cylinder (2.1.1) simplifies to a two-dimensional problem with no z -dependence. The general solution to

¹For the scalar electrostatic and magnetostatic potentials we use the general notation u instead of the more common Φ in order to avoid any confusion with the notation ϕ used for the angular polar coordinate; the analysis being also applicable to other branches of engineering and physics.

(2.1.1) in circular harmonics is [see Appendix A]

$$u(r, \phi) = A_0 + B_0 \ln r + \sum_{n=1}^{\infty} (A_n r^n + B_n r^{-n}) (C_n \cos n\phi + D_n \sin n\phi). \quad (2.1.2)$$

For convenience (2.1.2) can be expressed in the alternate form

$$u(r, \phi) = A_0 + B_0 \ln r + \sum_{n=1}^{\infty} (A_n r^n + B_n r^{-n}) (C_n e^{jn\phi} + D_n e^{-jn\phi}), \quad (2.1.3)$$

where n is an integer, $j \equiv \sqrt{-1}$ and A_0, B_0, A_n, B_n, C_n and D_n are constants of integration. The general solutions for (2.1.2) or (2.1.3) are uniquely determined if one of the three boundary conditions are satisfied

$$u|_S = f_1(r, \phi), \quad (2.1.4a)$$

$$\left. \frac{\partial u}{\partial n} \right|_S = f_2(r, \phi), \quad (2.1.4b)$$

$$\left. \left(\frac{\partial u}{\partial n} + hu \right) \right|_S = f_3(r, \phi), \quad h > 0, \quad (2.1.4c)$$

where S is the boundary of the cylinder, f_1, f_2, f_3 are given functions of position on S , and $\frac{\partial}{\partial n}$ denotes the derivative with respect to the exterior normal to S . Dirichlet and Neumann boundary problems of the form (2.1.4a) and (2.1.4b), respectively, will be used for the electrostatic and magnetostatic problems in Chapters 4 to 6.

2.2 Geometry of a general system of parallel circular cylinders

Consider N parallel, non-intersecting and infinitely long circular cylinders placed in a linear, homogeneous and isotropic medium as shown in Figure. 2.2.1. Each cylinders axis is parallel with the z -axis of the circular coordinate system reducing the problem to two-dimensional circular coordinate system. The radius of the

p^{th} cylinder is a_p centred at r_{0p} with local Cartesian coordinates (x_{0p}, y_{0p}) . For convenience N circular coordinate systems are defined, the origin of each being centred at the axis of each respective cylinder. In the case of conducting cylinders, for instance, the electrostatic potential due to the presence of the p^{th} cylinder after imposing the regularity conditions for (2.1.2) at $r \rightarrow \infty$ and renaming of constants can be written

$$u_p(r_p, \phi_p) = A_0^{(p)} + B_0^{(p)} \ln r_p + \sum_{n=1}^{\infty} \frac{1}{r_p^n} \left[A_n^{(p)} \cos n\phi_p + B_n^{(p)} \sin n\phi_p \right], \quad (2.2.1)$$

where $r_p > a_p$ for all the cylinders $p = 1, 2, \dots, N$, with (r_p, ϕ_p) denoting the polar coordinates of the observation point P , and $A_0^{(p)}$, $B_0^{(p)}$, $A_n^{(p)}$ and $B_n^{(p)}$ representing the constants of integration for the p^{th} coordinate system.

For completeness, the potential for the case when the p^{th} cylinder is filled with a homogeneous material different from the outside medium after imposing regularity condition in (2.1.2) as $r \rightarrow 0$, and renaming the constants, gives

$$u_p(r_p, \phi_p) = \sum_{n=0}^{\infty} r_p^n \left[C_n^{(p)} \cos n\phi_p + D_n^{(p)} \sin n\phi_p \right], \quad (2.2.2)$$

where $r_p < a_p$ for all the cylinders $p = 1, 2, \dots, N$, with $C_n^{(p)}$ and $D_n^{(p)}$ representing constants of integration for the p^{th} coordinate system.

The resultant potential for any point outside all the cylinders due to the presence of all N cylinders and to any external applied field in the local coordinate system is then

$$u_{tot}(\mathbf{r}) = u_0(\mathbf{r}) + u_C + \sum_{p=1}^N u_p^{(0)}(\mathbf{r}), \quad r_p > a_p, \quad (2.2.3)$$

where $u_0(\mathbf{r})$ is the potential due to the applied field, $u_p^{(0)}(\mathbf{r})$ is the potential of the p^{th} cylinder expressed in the local coordinates (r_0, ϕ_0) and u_C is an arbitrary constant defined by a reference potential.

In order to impose the boundary conditions in (2.1.4) at the surface of the p^{th}

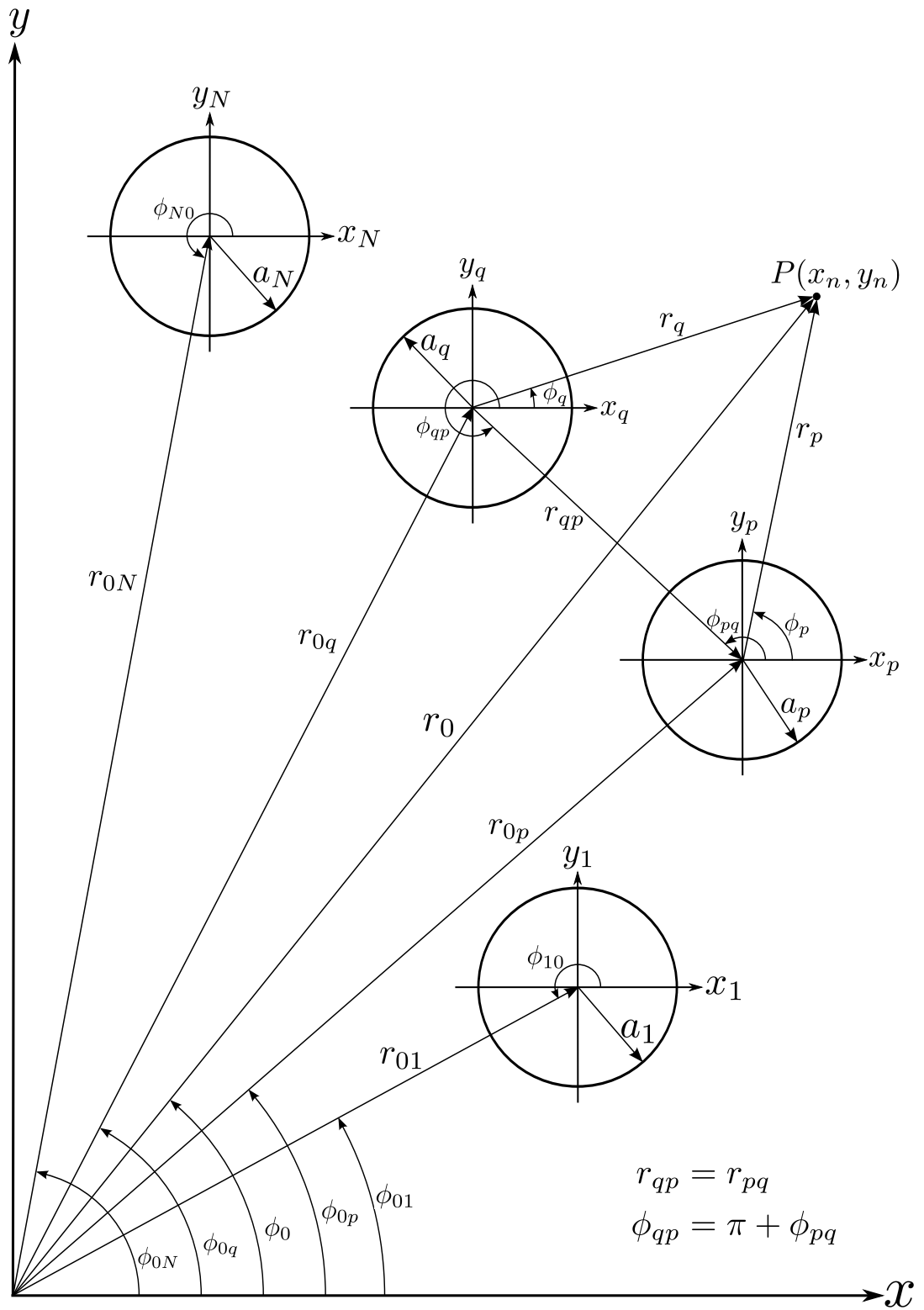


Figure 2.2.1: Geometry of N parallel cylinders arbitrarily located

cylinder the potential in (2.2.3) must be transformed to (r_p, ϕ_p) coordinates

$$u_{tot}^{(p)}(r_p, \phi_p) = u_0^{(p)}(r_p, \phi_p) + u_C^{(p)} + u_p(r_p, \phi_p) + \sum_{\substack{q=1 \\ q \neq p}}^N u_q^{(p)}(r_p, \phi_p), \quad r_p > a_p, \quad (2.2.4)$$

where $u_{tot}^{(p)}$, $u_0^{(p)}$ and $u_C^{(p)}$ are respectively u_{tot} , u_0 and u_C expressed in coordinates (r_p, ϕ_p) . The potential $u_q^{(p)}(r_p, \phi_p)$ is $u_q(r_q, \phi_q)$ expressed in terms of coordinates (r_p, ϕ_p) which will be obtained using the translations from the q^{th} to the p^{th} coordinate system.

2.3 Addition theorem for circular cylindrical scalar waves

The application of the translational addition theorems for cylindrical wave functions has been well documented. In [8] the translational addition theorems are applied to some elementary cylindrical waves. In [9] the translations are used for some acoustic or electromagnetic radiation scattering problems where an iterative method to the successive scattering by the cylinders of the primary field is used to obtain field quantities, and [6] employs a self-consistent method based on the known response of the isolated cylinders. It is this self-consistent method that will be applied to the problems here. The scalar Helmholtz wave equation used to describe time-harmonic scalar waves is

$$\nabla^2 \psi(\mathbf{r}_q) + k^2 \psi(\mathbf{r}_q) = 0, \quad (2.3.1)$$

where ψ is the wave function, k is the wave number and $\mathbf{r}_q \equiv \mathbf{r}$, that is, the position vector is in terms of the q^{th} coordinate system. The method of separation of variables in circular cylindrical coordinates for (2.3.1) with no z -dependence yields the cylindrical harmonics [10]

$$\psi_n(r_q, \phi_q) = Z_n(kr_q) e^{\pm jn\phi_q}, \quad (2.3.2)$$

where kr_q is the argument of the cylindrical Bessel functions when $k \neq 0$ with the integral orders of the functions represented by $n = 0, 1, 2, \dots$. Note for $k = 0$ the harmonic solution to (2.3.1) reduces to that of the Laplace equation solved earlier. The symbol $Z_n(kr_q)$ (referred to as *Cylindrical Bessel function*) represents either the Bessel function $J_n(kr_q)$, the Neumann function $Y_n(kr_q)$ or the linear combination of Bessel and Neumann functions known as Hankel functions $H_n(kr_q)$. To express the cylindrical wave in (2.3.2) in terms of a sum of cylindrical wave functions translated to the p^{th} coordinate system the Graf addition theorem [11] is used to obtain

$$Z_n(kr_q)e^{-jn\phi_q} = \sum_{m=-\infty}^{\infty} (-1)^m Z_{n+m}(kr_{qp})J_m(kr_p)e^{j[m\phi_p-(m+n)\phi_{qp}]}, \quad (2.3.3a)$$

$$Z_n(kr_q)e^{jn\phi_q} = \sum_{m=-\infty}^{\infty} (-1)^{m-n} Z_{m-n}(kr_{qp})J_m(kr_p)e^{j[m\phi_p-(m-n)\phi_{qp}]}, \quad (2.3.3b)$$

for $r_p < r_{qp}$, and

$$Z_n(kr_q)e^{jn\phi_q} = \sum_{m=-\infty}^{\infty} (-1)^m Z_{n+m}(kr_p)J_m(kr_{qp})e^{j[(m+n)\phi_p-m\phi_{qp}]}, \quad (2.3.4a)$$

$$Z_n(kr_q)e^{-jn\phi_q} = \sum_{m=-\infty}^{\infty} (-1)^{m-n} Z_{m-n}(kr_p)J_m(kr_{qp})e^{j[(m-n)\phi_p-m\phi_{qp}]}. \quad (2.3.4b)$$

for $r_p > r_{qp}$. The relationship between r_q , r_p and r_{qp} in (2.3.3) and (2.3.4) are given by

$$y_q = r_p \sin \phi_p + r_{qp} \sin \phi_{qp},$$

$$x_q = r_p \cos \phi_p + r_{qp} \cos \phi_{qp},$$

therefore,

$$\begin{aligned} r_q &= \sqrt{x_q^2 + y_q^2} \\ &= \sqrt{r_p^2 + r_{qp}^2 + 2r_p r_{qp} \cos(\phi_{qp} - \phi_p)}, \end{aligned} \quad (2.3.5)$$

and

$$\phi_q = \begin{cases} \tan^{-1}\left(\frac{y_q}{x_q}\right), & \text{when } y_q > 0 \text{ and } x_q > 0, \\ \pi + \tan^{-1}\left(\frac{y_q}{x_q}\right), & \text{when } x_q < 0, \\ 2\pi + \tan^{-1}\left(\frac{y_q}{x_q}\right), & \text{when } y_q < 0 \text{ and } x_q > 0. \end{cases} \quad (2.3.6)$$

Chapter 3

Translational addition theorems for static and stationary fields

To obtain an analytical solution to the problem proposed in Section 2.2 translations from the q^{th} to the p^{th} coordinate systems are first derived for the harmonic functions in (2.2.1) and (2.2.2). Instead of deriving these theorems directly using the cosine law in (2.3.5) and expanding into a series, we particularize the existing translational addition theorems for Cylindrical Bessel functions in (2.3.3) and (2.3.4) using the limiting case for a vanishing wave number, $k \rightarrow 0$.

3.1 Limiting forms of the Bessel and Neumann functions for small arguments

To obtain the addition theorems for the circular harmonics $\ln r_q$, $r_q^{-n} \cos n\phi_q$ and $r_q^{-n} \sin n\phi_q$ we derive them from (2.3.3) using the limiting forms of the Neumann functions, valid only for small arguments, obtained from Abramowitz [12] for integral orders

$$\lim_{k \rightarrow 0} Y_0(kr) = \lim_{k \rightarrow 0} \frac{2}{\pi} \ln kr, \quad n = 0, \quad (3.1.1a)$$

$$\lim_{k \rightarrow 0} Y_n(kr) = \lim_{k \rightarrow 0} -\frac{1}{\pi} (n-1)! \left(\frac{1}{2} kr \right)^{-n}, \quad n = 1, 2, \dots, \quad (3.1.1b)$$

where the substitution $\Gamma(n) \equiv (n-1)!$ is used and r is some finite distance in any of the coordinate systems. The limiting forms in (3.1.1) are valid approximations only for positive integral order Neumann functions; when negative orders appear

the following relation will be used

$$Y_{-n}(kr) = (-1)^n Y_n(kr), \quad n = 0, 1, 2, \dots, \quad (3.1.2)$$

to convert to Neumann functions of positive integer order.

The limiting form of the Bessel function will be used to obtain the addition theorems for the circular harmonics $r_q^n \cos n\phi_q$ and $r_q^n \sin n\phi_q$, which is

$$\lim_{k \rightarrow 0} J_n(kr) = \lim_{k \rightarrow 0} \frac{1}{n!} \left(\frac{1}{2} kr \right)^n, \quad n = 0, 1, 2, \dots, \quad (3.1.3)$$

where the substitution $\Gamma(n+1) \equiv n!$ is used. Again the limiting form of the Bessel function (3.1.3) is not valid for negative integral orders and the relation

$$J_{-n}(kr) = (-1)^n J_n(kr), \quad n = 0, 1, 2, \dots, \quad (3.1.4)$$

is used to convert to Bessel functions of positive order.

3.2 Derivation of the translational addition theorems for two-dimensional circular cylindrical Laplacian functions $r^{-n} \cos n\phi$ and $r^{-n} \sin n\phi$

To obtain expressions for the circular harmonic functions $r_q^{-n} \cos n\phi_q$ and $r_q^{-n} \sin n\phi_q$ the Neumann functions Y_n and Y_{n+m} are substituted for Z_n and Z_{n+m} , respectively in (2.3.3) and (2.3.4) because the asymptotic behaviours are the same as $r_q^{-n} \cos n\phi_q$ and $r_q^{-n} \sin n\phi_q$ functions. First, the addition theorem is derived when $r_p < r_{qp}$, thus (2.3.3a) is rewritten as

$$Y_n(kr_q) e^{-jn\phi_q} = \sum_{m=-\infty}^{\infty} (-1)^m Y_{n+m}(kr_{qp}) J_m(kr_p) e^{j[m\phi_p - (m+n)\phi_{qp}]}, \quad (3.2.1)$$

for $n = 1, 2, \dots$. The series is split up according to all the negative order combinations that functions $Y_{n+m}(kr_{qp})$ and $J_m(kr_p)$ make, and then all the series are

changed over positive indices giving

$$\begin{aligned}
Y_n(kr_q)e^{-jn\phi_q} &= \sum_{m=0}^{\infty} (-1)^m Y_{n+m}(kr_{qp}) J_m(kr_p) e^{j[m\phi_p - (m+n)\phi_{qp}]} \\
&\quad + \sum_{m=1}^{n-1} (-1)^m Y_{n-m}(kr_{qp}) J_{-m}(kr_p) e^{-j[m\phi_p + (n-m)\phi_{qp}]} \\
&\quad + (-1)^n Y_0(kr_{qp}) J_{-n}(kr_p) e^{-jn\phi_p} \\
&\quad + \sum_{m=n+1}^{\infty} (-1)^m Y_{n-m}(kr_{qp}) J_{-m}(kr_p) e^{-j[m\phi_p + (n-m)\phi_{qp}]}.
\end{aligned} \tag{3.2.2}$$

Replacing the negative integral ordered Neumann and Bessel functions in (3.2.2) with their positive integer equivalents and using the relations in (3.1.2) and (3.1.4) gives, after some algebraic simplification

$$\begin{aligned}
Y_n(kr_q)e^{-jn\phi_q} &= \sum_{m=0}^{\infty} (-1)^m Y_{n+m}(kr_{qp}) J_m(kr_p) e^{j[m\phi_p - (m+n)\phi_{qp}]} \\
&\quad + \sum_{m=1}^{n-1} Y_{n-m}(kr_{qp}) J_m(kr_p) e^{-j[m\phi_p + (n-m)\phi_{qp}]} \\
&\quad + Y_0(kr_{qp}) J_n(kr_p) e^{-jn\phi_p} \\
&\quad + \sum_{m=n+1}^{\infty} (-1)^{m-n} Y_{m-n}(kr_{qp}) J_m(kr_p) e^{-j[m\phi_p + (n-m)\phi_{qp}]}.
\end{aligned} \tag{3.2.3}$$

Now all the Neumann and Bessel functions in (3.2.3) are of positive integer order, thus for vanishing arguments kr_q , kr_{qp} and kr_p as $k \rightarrow 0$ the Neumann and Bessel

limiting forms (3.1.1) and (3.1.3) can be substituted in (3.2.3), which yields

$$\begin{aligned}
r_q^{-n} e^{-jn\phi_q} = & \\
\lim_{k \rightarrow 0} \left\{ \sum_{m=0}^{\infty} \frac{(-1)^m (n+m-1)!}{m!(n-1)!} \left(\frac{1}{r_{qp}}\right)^n \left(\frac{r_p}{r_{qp}}\right)^m e^{j[m\phi_p - (m+n)\phi_{qp}]} \right. & \\
+ \sum_{m=1}^{n-1} \frac{(n-m-1)!}{m!(n-1)!} \left(\frac{k}{2}\right)^{2m} r_p^m r_{qp}^{n-m} e^{-j[m\phi_p + (n-m)\phi_{qp}]} & \quad (3.2.4) \\
+ \sum_{m=n+1}^{\infty} \frac{(-1)^{m-n} (m-n-1)!}{m!(n-1)!} \left(\frac{k}{2}\right)^{2n} r_p^m r_{qp}^{n-m} e^{-j[m\phi_p + (n-m)\phi_{qp}]} & \\
\left. - \frac{2}{n!(n-1)!} \left[\left(\frac{k}{2}\right)^n r_p^n \ln r_{qp} e^{-jn\phi_p} + \ln k \left(\frac{k}{2}\right)^n r_p^n e^{-jn\phi_p} \right] \right\}. &
\end{aligned}$$

Taking the limit as $k \rightarrow 0$ reduces (3.2.4) to only the first term. Note, the limit for the last term in (3.2.4) is of indeterminate form but applying L'Hopital's rule

$$\begin{aligned}
\lim_{k \rightarrow 0} \frac{\ln k}{k^{-n}} &\equiv \lim_{k \rightarrow 0} \frac{\frac{d}{dk}(\ln k)}{\frac{d}{dk}(k^{-n})} \\
&\equiv \lim_{k \rightarrow 0} k^n = 0,
\end{aligned}$$

confirms it vanishes, therefore (3.2.4) reduces to

$$r_q^{-n} e^{-jn\phi_q} = \sum_{m=0}^{\infty} \frac{(-1)^m (n+m-1)!}{m!(n-1)!} \left(\frac{1}{r_{qp}}\right)^n \left(\frac{r_p}{r_{qp}}\right)^m e^{j[m\phi_p - (m+n)\phi_{qp}]}. \quad (3.2.5)$$

Taking the real and imaginary parts of (3.2.5) gives, respectively,

$$r_q^{-n} \cos n\phi_q = \sum_{m=0}^{\infty} \frac{(-1)^m (n+m-1)!}{m!(n-1)!} \left(\frac{1}{r_{qp}}\right)^n \left(\frac{r_p}{r_{qp}}\right)^m \cos [m\phi_p - (m+n)\phi_{qp}], \quad (3.2.6a)$$

$$r_q^{-n} \sin n\phi_q = - \sum_{m=0}^{\infty} \frac{(-1)^m (n+m-1)!}{m!(n-1)!} \left(\frac{1}{r_{qp}}\right)^n \left(\frac{r_p}{r_{qp}}\right)^m \sin [m\phi_p - (m+n)\phi_{qp}]. \quad (3.2.6b)$$

Now consider the case for $r_p > r_{qp}$ for which Y_n is substituted in for Z_n in (2.3.4) to give

$$Y_n(kr_q)e^{jn\phi_q} = \sum_{m=-\infty}^{\infty} (-1)^m Y_{n+m}(kr_p) J_m(kr_{qp}) e^{j[(m+n)\phi_p - m\phi_{qp}]}, \quad (3.2.7)$$

for $n = 1, 2, \dots$. Once again the series range in (3.2.7) is split up according to all the negative order combinations that the Cylindrical Bessel functions take. Using the relations to convert negative ordered Cylindrical Bessel functions to positive orders and converting all the series to positive indices, yields

$$\begin{aligned} Y_n(kr_q)e^{jn\phi_q} &= \sum_{m=0}^{\infty} (-1)^m Y_{n+m}(kr_p) J_m(kr_{qp}) e^{j[(m+n)\phi_p - m\phi_{qp}]} \\ &\quad + \sum_{m=1}^{n-1} Y_{n-m}(kr_p) J_m(kr_{qp}) e^{-j[(m-n)\phi_p - m\phi_{qp}]} \\ &\quad + Y_0(kr_p) J_n(kr_{qp}) e^{jn\phi_{qp}} \\ &\quad + \sum_{m=n+1}^{\infty} (-1)^{m-n} Y_{m-n}(kr_p) J_m(kr_{qp}) e^{-j[(m-n)\phi_p - m\phi_{qp}]}. \end{aligned} \quad (3.2.8)$$

For vanishing arguments kr_q , kr_{qp} and kr_p as $k \rightarrow 0$ the Cylindrical Bessel function limiting forms (3.1.1) and (3.1.3) are substituted in (3.2.8) to give

$$\begin{aligned} r_q^{-n} e^{jn\phi_q} &= \\ \lim_{k \rightarrow 0} &\left\{ \sum_{m=0}^{\infty} \frac{(-1)^m (n+m-1)!}{m!(n-1)!} \left(\frac{1}{r_p}\right)^n \left(\frac{r_{qp}}{r_p}\right)^m e^{j[(m+n)\phi_p - m\phi_{qp}]} \right. \\ &\quad + \sum_{m=1}^{n-1} \frac{(n-m-1)!}{m!(n-1)!} \left(\frac{k}{2}\right)^{2m} r_p^{m-n} r_{qp}^m e^{-j[(m-n)\phi_p - m\phi_{qp}]} \\ &\quad + \sum_{m=n+1}^{\infty} \frac{(-1)^{m-n} (m-n-1)!}{m!(n-1)!} \left(\frac{k}{2}\right)^{2n} r_p^{n-m} r_{qp}^m e^{-j[(m-n)\phi_p - m\phi_{qp}]} \\ &\quad \left. - \frac{2}{n!(n-1)!} \left[\left(\frac{k}{2}\right)^n r_{qp}^n \ln r_p e^{jn\phi_{qp}} + \ln k \left(\frac{k}{2}\right)^n r_{qp}^n e^{jn\phi_{qp}} \right] \right\}. \end{aligned} \quad (3.2.9)$$

Taking the limit as $k \rightarrow 0$ reduces (3.2.9) to

$$r_q^{-n} e^{jn\phi_q} = \sum_{m=0}^{\infty} \frac{(-1)^m (n+m-1)!}{m!(n-1)!} \left(\frac{1}{r_p}\right)^n \left(\frac{r_{qp}}{r_p}\right)^m e^{j[(m+n)\phi_p - m\phi_{qp}]}. \quad (3.2.10)$$

Taking the real and imaginary parts of (3.2.10) gives, respectively

$$r_q^{-n} \cos n\phi_q = \sum_{m=0}^{\infty} \frac{(-1)^m (n+m-1)!}{m!(n-1)!} \left(\frac{1}{r_p}\right)^n \left(\frac{r_{qp}}{r_p}\right)^m \cos [(m+n)\phi_p - m\phi_{qp}], \quad (3.2.11a)$$

$$r_q^{-n} \sin n\phi_q = \sum_{m=0}^{\infty} \frac{(-1)^m (n+m-1)!}{m!(n-1)!} \left(\frac{1}{r_p}\right)^n \left(\frac{r_{qp}}{r_p}\right)^m \sin [(m+n)\phi_p - m\phi_{qp}]. \quad (3.2.11b)$$

For completeness it can be shown using the same method as above that the Cylindrical Bessel function addition theorems for the opposite signed exponential arguments in (2.3.3) and (2.3.4) give

$$r_q^{-n} e^{jn\phi_q} = \sum_{m=0}^{\infty} \frac{(-1)^m (n+m-1)!}{m!(n-1)!} \left(\frac{1}{r_{qp}}\right)^n \left(\frac{r_p}{r_{qp}}\right)^m e^{-j[m\phi_p - (m+n)\phi_{qp}]}, \quad (3.2.12)$$

$$r_q^{-n} e^{-jn\phi_q} = \sum_{m=0}^{\infty} \frac{(-1)^m (n+m-1)!}{m!(n-1)!} \left(\frac{1}{r_p}\right)^n \left(\frac{r_{qp}}{r_p}\right)^m e^{-j[(m+n)\phi_p - m\phi_{qp}]}. \quad (3.2.13)$$

Taking the real and imaginary parts of (3.2.12) and (3.2.13) can be shown to be the exact addition theorem equations in (3.2.6) and (3.2.11), respectively.

3.3 Derivation of the translational addition theorems for two-dimensional circular cylindrical Laplacian functions $r^n \cos n\phi$ and $r^n \sin n\phi$

To obtain expressions for the circular harmonic functions $r_q^n \cos n\phi_q$ and $r_q^n \sin n\phi_q$, the Bessel functions J_n and J_{n+m} are substituted for Z_n and Z_{n+m} , respectively, in (2.3.4) since the limiting behaviours are similar to the functions $r_q^n \cos n\phi_q$ and $r_q^n \sin n\phi_q$. The addition theorems for $r_p < r_{qp}$ and $r_p > r_{qp}$ can therefore be written

as

$$J_n(kr_q)e^{-jn\phi_q} = \sum_{m=-\infty}^{\infty} (-1)^m J_{n+m}(kr_{qp})J_m(kr_p)e^{j[m\phi_p-(m+n)\phi_{qp}]}, \quad (3.3.1)$$

$$J_n(kr_q)e^{jn\phi_q} = \sum_{m=-\infty}^{\infty} (-1)^m J_{n+m}(kr_p)J_m(kr_{qp})e^{j[(m+n)\phi_p-m\phi_{qp}]}, \quad (3.3.2)$$

for the integral orders $n = 0, 1, 2, \dots$

When we compare (3.3.1) and (3.3.2) to each other we notice the arguments for the exponentials are of opposite sign and the arguments of the Bessel functions under the series summations are interchanged. This implies that the final forms will have exactly the same structure but with r_p and ϕ_p interchanged with r_{qp} and ϕ_{qp} , respectively, and the arguments of the exponentials will be of opposite sign. Therefore only (3.3.1) is used to derive the addition theorem for both $r_p < r_{qp}$ and $r_p > r_{qp}$ cases.

The series in (3.3.1) is split up according to all the negative order combinations that functions $J_{n+m}(kr_{qp})$ and $J_n(kr_p)$ make, then changing the series over positive integer indices gives

$$\begin{aligned} J_n(kr_q)e^{-jn\phi_q} &= \sum_{m=1}^{\infty} (-1)^m J_{n+m}(kr_{qp})J_m(kr_p)e^{j[m\phi_p-(m+n)\phi_{qp}]} \\ &+ \sum_{m=0}^n (-1)^m J_{n-m}(kr_{qp})J_{-m}(kr_p)e^{-j[m\phi_p+(n-m)\phi_{qp}]} \\ &+ \sum_{m=n+1}^{\infty} (-1)^m J_{n-m}(kr_{qp})J_{-m}(kr_p)e^{-j[m\phi_p+(n-m)\phi_{qp}]}. \end{aligned} \quad (3.3.3)$$

Replacing the negative integral ordered Bessel functions in (3.3.3) with their

positive order equivalents using the relation in (3.1.4) gives

$$\begin{aligned}
J_n(kr_q)e^{-jn\phi_q} &= \sum_{m=1}^{\infty} (-1)^m J_{n+m}(kr_{qp})J_m(kr_p)e^{j[m\phi_p-(m+n)\phi_{qp}]} \\
&+ \sum_{m=0}^n J_{n-m}(kr_{qp})J_m(kr_p)e^{-j[m\phi_p+(n-m)\phi_{qp}]} \\
&+ \sum_{m=n+1}^{\infty} (-1)^{m-n} J_{n-m}(kr_{qp})J_m(kr_p)e^{-j[m\phi_p+(n-m)\phi_{qp}]}.
\end{aligned} \tag{3.3.4}$$

For vanishing arguments kr_q , kr_{qp} and kr_p as $k \rightarrow 0$ the limiting forms of the Bessel functions (3.1.3) are substituted in (3.3.4) giving

$$\begin{aligned}
r_q^n e^{-jn\phi_q} &= \\
\lim_{k \rightarrow 0} &\left\{ \sum_{m=1}^{\infty} \frac{n!(-1)^m}{m!(n+m)!} \left(\frac{k}{2}\right)^{2m} r_{qp}^{m+n} r_p^m e^{j[m\phi_p-(m+n)\phi_{qp}]} \right. \\
&+ \sum_{m=0}^n \frac{n!}{m!(n-m)!} r_{qp}^n \left(\frac{r_p}{r_{qp}}\right)^m e^{-j[m\phi_p+(n-m)\phi_{qp}]} \\
&\left. + \sum_{m=n+1}^{\infty} \frac{n!(-1)^{m-n}}{m!(m-n)!} \left(\frac{k}{2}\right)^{2(m-n)} r_{qp}^{m-n} r_p^m e^{-j[m\phi_p+(n-m)\phi_{qp}]} \right\}.
\end{aligned} \tag{3.3.5}$$

Taking the limit as $k \rightarrow 0$ reduces (3.3.5) to

$$r_q^n e^{-jn\phi_q} = \sum_{\substack{m=0 \\ r_p < r_{qp}}}^n \frac{n!}{m!(n-m)!} r_{qp}^n \left(\frac{r_p}{r_{qp}}\right)^m e^{-j[m\phi_p+(n-m)\phi_{qp}]}. \tag{3.3.6}$$

Taking the real and imaginary parts of (3.3.6) gives, respectively

$$r_q^n \cos n\phi_q = \sum_{\substack{m=0 \\ r_p < r_{qp}}}^n \frac{n!}{m!(n-m)!} r_{qp}^n \left(\frac{r_p}{r_{qp}}\right)^m \cos [m\phi_p + (n-m)\phi_{qp}], \tag{3.3.7a}$$

$$r_q^n \sin n\phi_q = \sum_{\substack{m=0 \\ r_p < r_{qp}}}^n \frac{n!}{m!(n-m)!} r_{qp}^n \left(\frac{r_p}{r_{qp}}\right)^m \sin [m\phi_p + (n-m)\phi_{qp}]. \tag{3.3.7b}$$

Now for the case when $r_p > r_{qp}$, we interchange r_p with r_{qp} , ϕ_p with ϕ_{qp} and change the signs of the exponential arguments in (3.3.6) which gives

$$r_q^n e^{jn\phi_q} = \sum_{\substack{m=0 \\ r_p > r_{qp}}}^n \frac{n!}{m!(n-m)!} r_p^n \left(\frac{r_{qp}}{r_p}\right)^m e^{j[(n-m)\phi_p+m\phi_{qp}]} \tag{3.3.8}$$

and taking the real and imaginary parts of (3.3.8) gives, respectively,

$$r_q^n \cos n\phi_q = \sum_{m=0}^n \frac{n!}{m!(n-m)!} r_p^n \left(\frac{r_{qp}}{r_p}\right)^m \cos [(n-m)\phi_p + m\phi_{qp}], \quad (3.3.9a)$$

$$r_q^n \sin n\phi_q = \sum_{m=0}^n \frac{n!}{m!(n-m)!} r_p^n \left(\frac{r_{qp}}{r_p}\right)^m \sin [(n-m)\phi_p + m\phi_{qp}]. \quad (3.3.9b)$$

3.4 Derivation of the translational addition theorems for two-dimensional circular cylindrical Laplacian function $\ln r$

To obtain the addition theorem for the circular harmonic function $\ln r_q$ for the case when $r_p < r_{qp}$, the Neumann function of integral order $n = 0$ is substituted in (2.3.3) yielding

$$Y_0(kr_q) = \sum_{m=-\infty}^{\infty} (-1)^m Y_m(kr_p) J_m(kr_{qp}) e^{jm(\phi_p - \phi_{qp})}. \quad (3.4.1)$$

Converting all the negative order Cylindrical Bessel functions in (3.4.1) to positive order and rearranging the series gives

$$\begin{aligned} Y_0(kr_q) &= \sum_{m=1}^{\infty} (-1)^m Y_m(kr_{qp}) J_m(kr_p) e^{jm(\phi_p - \phi_{qp})} \\ &\quad + Y_0(kr_{qp}) J_0(kr_p) \\ &\quad + \sum_{m=1}^{\infty} (-1)^m Y_m(kr_{qp}) J_m(kr_p) e^{-jm(\phi_p - \phi_{qp})}, \end{aligned} \quad (3.4.2)$$

using the relation $e^{jm(\phi_p - \phi_{qp})} + e^{-jm(\phi_p - \phi_{qp})} = 2 \cos [m(\phi_p - \phi_{qp})]$ simplifies (3.4.2)

to

$$\begin{aligned} Y_0(kr_q) &= Y_0(kr_{qp}) J_0(kr_p) \\ &\quad + 2 \sum_{m=1}^{\infty} (-1)^m Y_m(kr_{qp}) J_m(kr_p) \cos m(\phi_p - \phi_{qp}). \end{aligned} \quad (3.4.3)$$

Using the limiting forms of the Cylindrical Bessel functions for vanishing arguments as $k \rightarrow 0$ gives

$$\begin{aligned} & \frac{2}{\pi} \lim_{k \rightarrow 0} (\ln k + \ln r_q) = \\ & \frac{2}{\pi} \lim_{k \rightarrow 0} \left(\ln k + \ln r_{qp} - \sum_{m=1}^{\infty} \frac{(-1)^m}{m} \left(\frac{r_p}{r_{qp}} \right)^m \cos [m(\phi_p - \phi_{qp})] \right). \end{aligned} \quad (3.4.4)$$

Taking the limit of (3.4.4) reduces it to

$$\ln r_q = \ln r_{qp} - \sum_{m=1}^{\infty} \frac{(-1)^m}{m} \left(\frac{r_p}{r_{qp}} \right)^m \cos [m(\phi_p - \phi_{qp})]. \quad (3.4.5)$$

For the case when $r_p > r_{qp}$ we use the Neumann function of order $n = 0$ and substitute in (2.3.4) which gives

$$Y_0(kr_q) = \sum_{m=-\infty}^{\infty} (-1)^m Y_m(kr_p) J_m(kr_{qp}) e^{jm(\phi_p - \phi_{qp})}. \quad (3.4.6)$$

Converting all the negative order Cylindrical Bessel functions in (3.4.6) and simplifying yields

$$\begin{aligned} Y_0(kr_q) &= Y_0(kr_p) J_0(kr_{qp}) \\ &+ 2 \sum_{m=1}^{\infty} (-1)^m Y_m(kr_p) J_m(kr_{qp}) \cos m(\phi_p - \phi_{qp}). \end{aligned} \quad (3.4.7)$$

Using the limiting forms of the Cylindrical Bessel functions gives

$$\begin{aligned} & \frac{2}{\pi} \lim_{k \rightarrow 0} (\ln k + \ln r_q) = \\ & \frac{2}{\pi} \lim_{k \rightarrow 0} \left(\ln k + \ln r_p - \sum_{m=1}^{\infty} \frac{(-1)^m}{m} \left(\frac{r_{qp}}{r_p} \right)^m \cos [m(\phi_p - \phi_{qp})] \right). \end{aligned} \quad (3.4.8)$$

Taking the limit of (3.4.8) reduces it to

$$\ln r_q = \ln r_p - \sum_{m=1}^{\infty} \frac{(-1)^m}{m} \left(\frac{r_{qp}}{r_p} \right)^m \cos [m(\phi_p - \phi_{qp})]. \quad (3.4.9)$$

The addition theorems (3.4.5) and (3.4.9) are also the recognizable harmonic expansions of a line charge found in [10] where

$$\ln R = \begin{cases} \ln r_0 - \sum_{n=1}^{\infty} \frac{1}{n} \left(\frac{r}{r_0}\right)^n \left[\cos n\theta_0 \cos \theta + \sin n\theta_0 \sin \theta \right], & r < r_0 \\ \ln r - \sum_{n=1}^{\infty} \frac{1}{n} \left(\frac{r_0}{r}\right)^n \left[\cos n\theta_0 \cos \theta + \sin n\theta_0 \sin \theta \right], & r > r_0 \end{cases} \quad (3.4.10)$$

If the following substitutions are made in (3.4.10) to relate the geometries of the variables $R \equiv r_q$, $r \equiv r_p$, $r_0 \equiv r_{qp}$, $\theta \equiv \phi_p$ and $\theta_0 \equiv \pi - \phi_{qp}$ and, after some trigonometric manipulation, the expansions are exactly those found in (3.4.5) and (3.4.9). Since the problems considered here are two-dimensional, the addition theorem for $\ln R$ can also be obtained by positioning the centres of the local systems q and p in the complex plane as in [10, 13] and, then, substituting with $z = re^{j\theta}$ and taking the real parts to yield the same expressions in (3.4.10).

3.5 Numerical analysis of the series expansions in the addition theorems

The convergence of the series involved in the translational addition theorems given in (3.2.6), (3.2.11), (3.3.7), (3.3.9), (3.4.5) and (3.4.9) can be tested for given n by using numerical values for the variables in both sides of the respective equations. The numerical testing for (3.2.6) is presented in detail to outline some convergence properties as variables are changed because of its extensive use in the next three chapters. The remaining addition theorems are tested only for a single case to verify that the series converge for a particular set of variables.

Consider Figure 3.5.1 where point P moves along a circle of constant radius r_p . In the figure, it is evident that $\phi_{qp} = 0$ when the x_q and x_p axes are aligned.

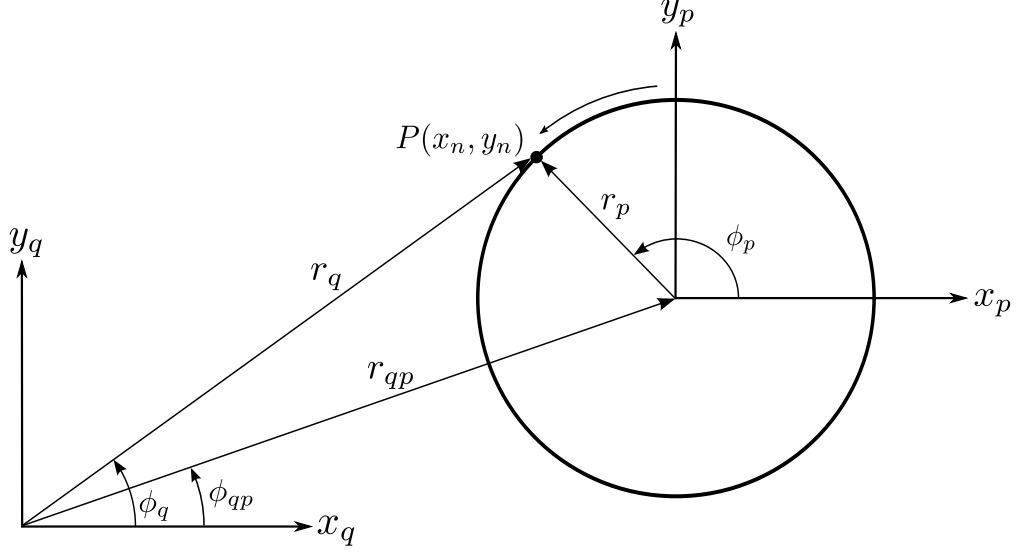


Figure 3.5.1: Point P along a circle of radius r_p when $r_p < r_{qp}$

3.5.1 Evaluation of the translational addition theorems for Laplacian functions $r^{-n} \cos n\phi$ and $r^{-n} \sin n\phi$

For Figure 3.5.1, where $r_p < r_{qp}$ and the point P moves along the circle of radius r_p , the addition theorems (3.2.6) must be used, which are normalized as

$$\underbrace{\left(\frac{r_{qp}}{r_q}\right)^n \cos n\phi_q}_{f_1(r_q, \phi_q)_{\cos}} = \underbrace{\sum_{m=0}^{\infty} \frac{(-1)^m (n+m-1)!}{m!(n-1)!} \left(\frac{r_p}{r_{qp}}\right)^m \cos [m\phi_p - (m+n)\phi_{qp}]}_{g_1(r_p, \phi_p)_{\cos}}, \quad (3.5.1a)$$

$$\underbrace{\left(\frac{r_{qp}}{r_q}\right)^n \sin n\phi_q}_{f_1(r_q, \phi_q)_{\sin}} = - \underbrace{\sum_{m=0}^{\infty} \frac{(-1)^m (n+m-1)!}{m!(n-1)!} \left(\frac{r_p}{r_{qp}}\right)^m \sin [m\phi_p - (m+n)\phi_{qp}]}_{g_1(r_p, \phi_p)_{\sin}}. \quad (3.5.1b)$$

The left hand sides of (3.5.1a) and (3.5.1b) are denoted as $f_1(r_q, \phi_q)_{\cos}$ and $f_1(r_q, \phi_q)_{\sin}$ and the right hand sides as $g_1(r_p, \phi_p)_{\cos}$ and $g_1(r_p, \phi_p)_{\sin}$, respectively. The numerical values of the functions f_1 and g_1 are calculated at several discrete locations on the circle. Theoretically, f_1 should yield the same results as g_1 if an infinite number of series terms are taken. In order to find results for g_1 , the infinite

series are truncated to a finite number of terms M .

Consider the situation where $r_{qp} = 75$ cm, $r_p = 37.5$ cm and $\phi_{qp} = 0$, then r_p , ϕ_p and ϕ_q vary as P moves along the circle. Test point locations are taken by varying ϕ_p from 0° to 180° . In the case of $n = 3$, M is truncated to 20 and the numerical results are shown in Table 3.5.1.

Table 3.5.1: Truncation errors of $g_1(r_p, \phi_p)_{\cos}$ and $g_1(r_p, \phi_p)_{\sin}$ for $n = 3$, $M = 20$, $\phi_{qp} = 0$ and $r_p/r_{qp} = 0.5$

Point	ϕ_p	r_{qp}/r_q	ϕ_q	$f_1(r_q, \phi_q)_{\cos}$	$g_1(r_p, \phi_p)_{\cos}$	% Error	$f_1(r_q, \phi_q)_{\sin}$	$g_1(r_p, \phi_p)_{\sin}$	% Error
1	0	0.6667	0	0.2963	0.2964	2.6333×10^{-2}	0.0000	0.0000	—
2	18	0.6740	5.98	0.2914	0.2914	2.6527×10^{-2}	0.0943	0.0943	-1.6908×10^{-2}
3	36	0.6969	11.82	0.2757	0.2758	2.7182×10^{-2}	0.1963	0.1963	-1.6547×10^{-2}
4	54	0.7377	17.36	0.2467	0.2467	2.8595×10^{-2}	0.3167	0.3166	-1.5883×10^{-2}
5	72	0.8009	22.39	0.1994	0.1995	3.1650×10^{-2}	0.4734	0.4734	-1.4818×10^{-2}
6	90	0.8944	26.57	0.1280	0.1281	3.9691×10^{-2}	0.7040	0.7039	-1.3208×10^{-2}
7	108	1.0309	29.35	0.0370	0.0370	8.0480×10^{-2}	1.0949	1.0948	-1.0921×10^{-2}
8	126	1.2289	29.81	0.0187	0.0187	-4.1808×10^{-2}	1.8556	1.8554	-8.0271×10^{-3}
9	144	1.5059	26.27	0.6631	0.6630	-1.1625×10^{-2}	3.3498	3.3497	-5.1046×10^{-3}
10	162	1.8290	16.41	3.9941	3.9939	-4.7191×10^{-3}	4.6345	4.6343	-3.0752×10^{-3}
11	180	2.0000	0	8.0000	7.9997	-3.3021×10^{-3}	0.0000	0.0000	—

For a first approximation the percentage errors are relatively high. By increasing the truncation to $M = 50$ terms the percentage errors are reduced as shown in Table 3.5.2.

Table 3.5.2: Truncation errors of $g_1(r_p, \phi_p)_{\cos}$ and $g_1(r_p, \phi_p)_{\sin}$ for $n = 3$, $M = 50$, $\phi_{qp} = 0$ and $r_p/r_{qp} = 0.5$

Point	ϕ_p	r_{qp}/r_q	ϕ_q	$f_1(r_q, \phi_q)_{\cos}$	$g_1(r_p, \phi_p)_{\cos}$	% Error	$f_1(r_q, \phi_q)_{\sin}$	$g_1(r_p, \phi_p)_{\sin}$	% Error
1	0	0.6667	0	0.2963	0.2963	1.3596×10^{-10}	0.0000	0.0000	—
2	18	0.6740	5.98	0.2914	0.2914	-1.3667×10^{-10}	0.0943	0.0943	8.8806×10^{-11}
3	36	0.6969	11.82	0.2757	0.2757	1.3969×10^{-10}	0.1963	0.1963	-8.6745×10^{-11}
4	54	0.7377	17.36	0.2467	0.2467	-1.4615×10^{-10}	0.3167	0.3167	8.3149×10^{-11}
5	72	0.8009	22.39	0.1994	0.1994	1.5980×10^{-10}	0.4734	0.4734	-7.7281×10^{-11}
6	90	0.8944	26.57	0.1280	0.1280	-1.9559×10^{-10}	0.7040	0.7040	6.8490×10^{-11}
7	108	1.0309	29.35	0.0370	0.0370	3.6767×10^{-10}	1.0949	1.0949	-5.6114×10^{-11}
8	126	1.2289	29.81	0.0187	0.0187	3.3601×10^{-10}	1.8556	1.8556	4.0470×10^{-11}
9	144	1.5059	26.27	0.6631	0.6631	-6.2502×10^{-11}	3.3498	3.3498	-2.4963×10^{-11}
10	162	1.8290	16.41	3.9941	3.9941	2.3472×10^{-11}	4.6345	4.6345	1.4508×10^{-11}
11	180	2.0000	0	8.0000	8.0000	-1.5898×10^{-11}	0.0000	0.0000	—

It is evident that for the same variable conditions simply by increasing the number of terms M used before truncating the series results in a better approximation. Table 3.5.3 shows the numerical results when the order n is increased to 9 and keeping the series truncation at $M = 50$.

Table 3.5.3: Truncation errors of $g_1(r_p, \phi_p)_{\cos}$ and $g_1(r_p, \phi_p)_{\sin}$ for $n = 9$, $M = 50$, $\phi_{qp} = 0$ and $r_p/r_{qp} = 0.5$

Point	ϕ_p	r_{qp}/r_q	ϕ_q	$f_1(r_q, \phi_q)_{\cos}$	$g_1(r_p, \phi_p)_{\cos}$	% Error	$f_1(r_q, \phi_q)_{\sin}$	$g_1(r_p, \phi_p)_{\sin}$	% Error
1	0	0.6667	0	0.0260	0.0260	2.3999×10^{-3}	0.0000	0.0000	—
2	18	0.6740	5.98	0.0170	0.0170	-3.6494×10^{-3}	0.0232	0.0232	5.3978×10^{-4}
3	36	0.6969	11.82	-0.0109	-0.0109	-5.5110×10^{-3}	0.0372	0.0372	-6.8592×10^{-4}
4	54	0.7377	17.36	-0.0592	-0.0592	9.6371×10^{-4}	0.0261	0.0261	1.5198×10^{-3}
5	72	0.8009	22.39	-0.1262	-0.1262	-4.0957×10^{-4}	-0.0496	-0.0496	1.1165×10^{-3}
6	90	0.8944	26.57	-0.1882	-0.1882	2.2675×10^{-4}	-0.3143	-0.3143	-2.3507×10^{-4}
7	108	1.0309	29.35	-0.1331	-0.1331	-2.0355×10^{-4}	-1.3081	-1.3081	7.3381×10^{-5}
8	126	1.2289	29.81	-0.1936	-0.1936	-8.4992×10^{-6}	-6.3871	-6.3871	-1.9078×10^{-5}
9	144	1.5059	26.27	-22.0307	-22.0307	2.6113×10^{-6}	-33.1705	-33.1705	4.3733×10^{-6}
10	162	1.8290	16.41	-193.6435	-193.6435	-8.0961×10^{-7}	122.2558	122.2558	1.0520×10^{-6}
11	180	2.0000	0	512.0000	512.0000	-4.5262×10^{-7}	0.0000	0.0000	—

The approximations of g_1 for f_1 are less accurate than that of Table 3.5.2, verifying that with increasing n the percentage error increases correspondingly for the same series truncation. Therefore, for increasing n more terms M need to be taken to keep the percentage error of the same order. To emphasize this, the series truncation is increased to $M = 80$ and the numerical results are shown in Table 3.5.4.

Table 3.5.4: Truncation errors of $g_1(r_p, \phi_p)_{\cos}$ and $g_1(r_p, \phi_p)_{\sin}$ for $n = 9$, $M = 80$, $\phi_{qp} = 0$ and $r_p/r_{qp} = 0.5$.

Point	ϕ_p	r_{qp}/r_q	ϕ_q	$f_1(r_q, \phi_q)_{\cos}$	$g_1(r_p, \phi_p)_{\cos}$	% Error	$f_1(r_q, \phi_q)_{\sin}$	$g_1(r_p, \phi_p)_{\sin}$	% Error
1	0	0.6667	0	0.0260	0.0260	7.2557×10^{-11}	0.0000	0.0000	—
2	18	0.6740	5.98	0.0170	0.0170	1.4812×10^{-10}	0.0232	0.0232	-2.0360×10^{-11}
3	36	0.6969	11.82	-0.0109	-0.0109	-1.4115×10^{-10}	0.0372	0.0372	-4.7320×10^{-11}
4	54	0.7377	17.36	-0.0592	-0.0592	-5.3377×10^{-11}	0.0261	0.0261	-3.7922×10^{-11}
5	72	0.8009	22.39	-0.1262	-0.1262	-1.0758×10^{-11}	-0.0496	-0.0496	2.7932×10^{-11}
6	90	0.8944	26.57	-0.1882	-0.1882	-9.6220×10^{-11}	-0.3143	-0.3143	9.1662×10^{-12}
7	108	1.0309	29.35	-0.1331	-0.1331	2.8743×10^{-11}	-1.3081	-1.3081	3.7174×10^{-12}
8	126	1.2289	29.81	-0.1936	-0.1936	2.0980×10^{-11}	-6.3871	-6.3871	3.4764×10^{-13}
9	144	1.5059	26.27	-22.0307	-22.0307	-4.8379×10^{-14}	-33.1705	-33.1705	0.0000
10	162	1.8290	16.41	-193.6435	-193.6435	1.7613×10^{-13}	122.2558	122.2558	5.8119×10^{-14}
11	180	2.0000	0	512.0000	512.0000	-3.3307×10^{-14}	0.0000	0.0000	—

The convergence of (3.5.1) is also sensitive to the ratio r_p/r_{qp} , valid for $r_p/r_{qp} < 1$. Table 3.5.5 shows how the percentage error changes for an observation point at $\phi_p = 72^\circ$ for increasing circle radii r_p for the ratios $r_p/r_{qp} = 0.5, 0.7$ and 0.9 each shown for series truncations of $M = 80, 200$, and 1000 . As the ratio approaches $r_p/r_{qp} \rightarrow 1$ the error increases and only with a greater number of series terms M will g_1 converge to f_1 .

Table 3.5.5: Truncation errors of $g_1(r_p, \phi_p)_{\cos}$ and $g_1(r_p, \phi_p)_{\sin}$ for $n = 9$, $\phi_p = 72^\circ$, $\phi_{qp} = 0$ and $r_p/r_{qp} = 0.5, 0.7, 0.9$

(a) for $r_p/r_{qp} = 0.5$, $\phi_q = 29.35^\circ$ and $r_{qp}/r_q = 1.0309$

M	$f_1(r_q, \phi_q)_{\cos}$	$g_1(r_p, \phi_p)_{\cos}$	% Error	$f_1(r_q, \phi_q)_{\sin}$	$g_1(r_p, \phi_p)_{\sin}$	% Error
80	-0.1331	-0.1331	2.7846×10^{-11}	-1.3081	-1.3081	3.7344×10^{-12}
200	-0.1331	-0.1331	3.3290×10^{-11}	-1.3081	-1.3081	1.5277×10^{-12}
1000	-0.1331	-0.1331	3.3290×10^{-11}	-1.3081	-1.3081	1.5277×10^{-12}

(b) for $r_p/r_{qp} = 0.7$, $\phi_q = 40.35^\circ$ and $r_{qp}/r_q = 0.9725$

M	$f_1(r_q, \phi_q)_{\cos}$	$g_1(r_p, \phi_p)_{\cos}$	% Error	$f_1(r_q, \phi_q)_{\sin}$	$g_1(r_p, \phi_p)_{\sin}$	% Error
80	0.7768	0.7851	1.0636	0.0425	0.0254	-40.233
200	0.7768	0.7768	-1.7719×10^{-9}	0.0425	0.0425	2.0964×10^{-8}
1000	0.7768	0.7768	-1.7719×10^{-9}	0.0425	0.0425	2.0964×10^{-8}

(c) for $r_p/r_{qp} = 0.9$, $\phi_q = 49.86^\circ$ and $r_{qp}/r_q = 0.8931$

M	$f_1(r_q, \phi_q)_{\cos}$	$g_1(r_p, \phi_p)_{\cos}$	% Error	$f_1(r_q, \phi_q)_{\sin}$	$g_1(r_p, \phi_p)_{\sin}$	% Error
80	0.0081	6913208.608	8.4962×10^{10}	0.3613	-9671242.259	-2.6765×10^9
200	0.0081	24188.768	2.9727×10^8	0.3613	-36702.5849	-1.0158×10^7
1000	0.0081	0.0081	3.1280×10^{-3}	0.3613	0.3613	1.0244×10^{-4}

Now consider the situation where $\phi_{qp} \neq 0$. Table 3.5.6 shows that the series in the addition theorems still converge for arbitrarily located cylinders.

Table 3.5.6: Truncation errors of $g_1(r_p, \phi_p)_{\cos}$ and $g_1(r_p, \phi_p)_{\sin}$ for $n = 9$, $M = 80$, $\phi_{qp} = \pi/3$ and $r_p/r_{qp} = 0.5$

Point	ϕ_p	r_{qp}/r_q	ϕ_q	$f_1(r_q, \phi_q)_{\cos}$	$g_1(r_p, \phi_p)_{\cos}$	% Error	$f_1(r_q, \phi_q)_{\sin}$	$g_1(r_p, \phi_p)_{\sin}$	% Error
1	0	0.7559	40.89	0.0798	0.0798	-1.0228×10^{-10}	0.0113	0.0113	-1.3088×10^{-9}
2	18	0.7083	46.29	0.0247	0.0247	5.2616×10^{-10}	0.0375	0.0375	-1.9967×10^{-10}
3	36	0.6799	52.05	-0.0098	-0.0098	7.5911×10^{-10}	0.0294	0.0294	-3.7486×10^{-10}
4	54	0.6675	58	-0.0250	-0.0250	3.1762×10^{-10}	0.0081	0.0081	1.2177×10^{-9}
5	72	0.6699	63.99	-0.0220	-0.0220	-5.5748×10^{-10}	-0.0160	-0.0160	4.6539×10^{-12}
6	90	0.6874	69.90	-0.0006	-0.0006	8.7604×10^{-9}	-0.0343	-0.0343	4.3451×10^{-10}
7	108	0.7219	75.56	0.0408	0.0408	1.4142×10^{-10}	-0.0342	-0.0342	-3.7855×10^{-10}
8	126	0.7769	80.79	0.1023	0.1023	-1.4192×10^{-10}	0.0127	0.0127	-2.3110×10^{-9}
9	144	0.8592	85.29	0.1720	0.1720	4.5305×10^{-11}	0.1886	0.1886	2.6252×10^{-11}
10	162	0.9796	88.63	0.1778	0.1778	7.9327×10^{-11}	0.8114	0.8114	1.1274×10^{-11}
11	180	1.1547	90	0.0000	0.0000	—	3.6494	3.6494	2.1539×10^{-12}

For the case where $r_p > r_{qp}$ as shown in Figure 3.5.2 the addition theorems in (3.2.11) are used, the equations are normalized to give

$$\underbrace{\left(\frac{r_p}{r_q}\right)^n \cos n\phi_q}_{f_2(r_q, \phi_q)_{\cos}} = \underbrace{\sum_{m=0}^{\infty} \frac{(-1)^m (n+m-1)!}{m!(n-1)!} \left(\frac{r_{qp}}{r_p}\right)^m \cos [m\phi_p - (m+n)\phi_{qp}]}_{g_2(r_p, \phi_p)_{\cos}}, \quad (3.5.2a)$$

$$\underbrace{\left(\frac{r_p}{r_q}\right)^n \sin n\phi_q}_{f_2(r_q, \phi_q)_{\sin}} = - \underbrace{\sum_{m=0}^{\infty} \frac{(-1)^m (n+m-1)!}{m!(n-1)!} \left(\frac{r_{qp}}{r_p}\right)^m \sin [m\phi_p - (m+n)\phi_{qp}]}_{g_2(r_p, \phi_p)_{\sin}}, \quad (3.5.2b)$$

Let us denote the left hand sides of (3.5.2a) and (3.5.2b) as $f_2(r_q, \phi_q)_{\cos}$ and $f_2(r_q, \phi_q)_{\sin}$, and the right hand sides as $g_2(r_p, \phi_p)_{\cos}$ and $g_2(r_p, \phi_p)_{\sin}$, respectively.

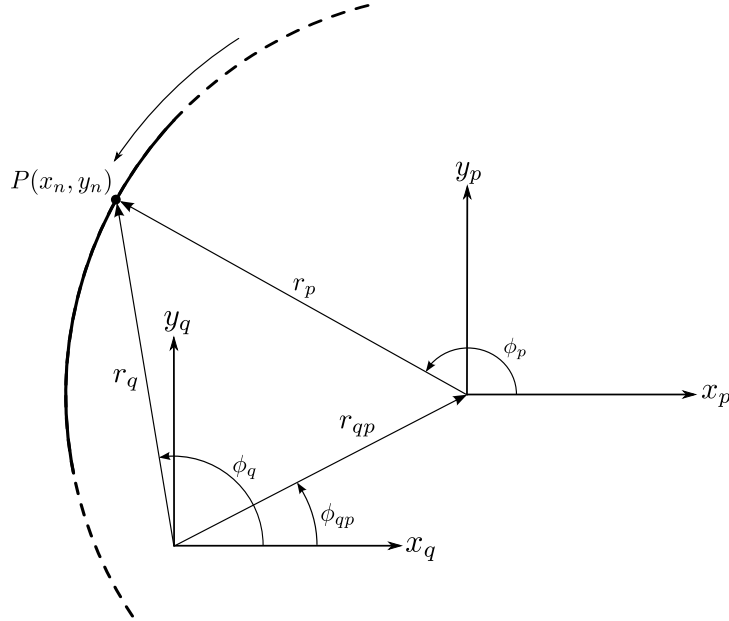


Figure 3.5.2: Point P along a circle of radius r_p when $r_p > r_{qp}$

Now consider the situation where $r_{qp} = 75$ cm, $r_p = 125$ cm and $\phi_{qp} = \pi/3$, then r_q , ϕ_p and ϕ_q vary when P moves along the circle. Test point locations are taken by varying ϕ_p from 0° to 180° . If $n = 6$ and M is truncated to 80 terms the numerical results in Table 3.5.7 show good convergence of the series.

Table 3.5.7: Truncation errors of $g_2(r_p, \phi_p)_{\cos}$ and $g_2(r_p, \phi_p)_{\sin}$ for $n = 6$, $M = 80$, $\phi_{qp} = \pi/3$ and $r_{qp}/r_p = 0.6$

Point	ϕ_p	r_p/r_q	ϕ_q	$f_2(r_q, \phi_q)_{\cos}$	$g_2(r_p, \phi_p)_{\cos}$	% Error	$f_2(r_q, \phi_q)_{\sin}$	$g_2(r_p, \phi_p)_{\sin}$	% Error
1	0	0.7143	21.79	-0.0866	-0.0866	2.7820×10^{-8}	0.1007	0.1007	-1.0054×10^{-8}
2	18	0.6664	33.52	-0.0817	-0.0817	-2.3486×10^{-8}	-0.0315	-0.0315	4.7350×10^{-8}
3	36	0.6381	44.96	-0.0003	-0.0003	-1.1904×10^{-6}	-0.0675	-0.0675	-3.4181×10^{-8}
4	54	0.6258	56.25	0.0555	0.0555	-3.8572×10^{-8}	-0.0230	-0.0230	3.4471×10^{-8}
5	72	0.6282	67.51	0.0434	0.0434	3.9995×10^{-8}	0.0435	0.0435	-3.4342×10^{-8}
6	90	0.6456	78.83	-0.0283	-0.0283	-1.6686×10^{-8}	0.0667	0.0667	3.4610×10^{-8}
7	108	0.6799	90.35	-0.0988	-0.0988	2.4061×10^{-8}	-0.0036	-0.0036	2.0507×10^{-7}
8	126	0.7356	102.22	-0.0454	-0.0454	-4.3477×10^{-8}	-0.1518	-0.1518	1.1982×10^{-8}
9	144	0.8205	114.69	0.2591	0.2591	2.5325×10^{-9}	-0.1612	-0.1612	-1.8195×10^{-8}
10	162	0.9489	128.16	0.4796	0.4796	-6.9465×10^{-9}	0.5506	0.5506	1.9834×10^{-9}
11	180	1.1471	143.41	-1.7573	-1.7573	-1.9000×10^{-9}	1.4496	1.4496	-1.8519×10^{-9}

3.5.2 Evaluation of the translational addition theorems for Laplacian functions $r^n \cos n\phi$ and $r^n \sin n\phi$

Consider again Figure 3.5.1 where $r_p < r_{qp}$ for the addition theorem (3.3.7) when normalized gives

$$\underbrace{\left(\frac{r_q}{r_{qp}}\right)^n \cos n\phi_q}_{f_3(r_q, \phi_q)_{\cos}} = \sum_{m=0}^n \frac{n!}{m!(n-m)!} \underbrace{\left(\frac{r_p}{r_{qp}}\right)^m \cos [m\phi_p + (n-m)\phi_{qp}]}_{g_3(r_p, \phi_p)_{\cos}}, \quad (3.5.3a)$$

$$\underbrace{\left(\frac{r_q}{r_{qp}}\right)^n \sin n\phi_q}_{f_3(r_q, \phi_q)_{\sin}} = \sum_{m=0}^n \frac{n!}{m!(n-m)!} \underbrace{\left(\frac{r_p}{r_{qp}}\right)^m \sin [m\phi_p + (n-m)\phi_{qp}]}_{g_3(r_p, \phi_p)_{\sin}}, \quad (3.5.3b)$$

Let the left hand sides of (3.5.3a) and (3.5.3b) be referred to as $f_3(r_q, \phi_q)_{\cos}$ and $f_3(r_q, \phi_q)_{\sin}$ and the right hand sides as $g_3(r_p, \phi_p)_{\cos}$ and $g_3(r_p, \phi_p)_{\sin}$, respectively. Now consider the situation where $r_{qp} = 75$ cm, $r_p = 67.5$ cm and $\phi_{qp} = \pi/3$. The results are given for the case when $n = 20$ in Table 3.5.8, verifying the series converges well for high order n and for ratios approaching $r_p/r_{qp} \rightarrow 1$.

Table 3.5.8: Truncation errors of $g_3(r_p, \phi_p)_{\cos}$ and $g_3(r_p, \phi_p)_{\sin}$ for $n = 20$, $\phi_{qp} = \pi/3$ and $r_p/r_{qp} = 0.9$

Point	ϕ_p	r_q/r_{qp}	ϕ_q	$f_3(r_q, \phi_q)_{\cos}$	$g_3(r_p, \phi_p)_{\cos}$	% Error	$f_3(r_q, \phi_q)_{\sin}$	$g_3(r_p, \phi_p)_{\sin}$	% Error
1	0	1.6462	31.74	1.7915×10^3	1.7915×10^3	-4.6960×10^{-12}	-2.1289×10^4	-2.1289×10^4	-2.0506×10^{-13}
2	18	1.7742	40.16	1.1390×10^4	1.1390×10^4	3.0982×10^{-12}	9.4791×10^4	9.4791×10^4	-3.8379×10^{-13}
3	36	1.8586	48.64	-7.1466×10^4	-7.1466×10^4	6.1086×10^{-13}	-2.3114×10^5	-2.3114×10^5	-1.6369×10^{-13}
4	54	1.8974	57.16	1.6514×10^5	1.6514×10^5	6.6972×10^{-13}	3.2636×10^5	3.2636×10^5	-2.6753×10^{-13}
5	72	1.8896	65.68	-1.9963×10^5	-1.9963×10^5	1.4579×10^{-13}	-2.7138×10^5	-2.7138×10^5	3.0029×10^{-13}
6	90	1.8354	74.19	1.3580×10^5	1.3580×10^5	1.9288×10^{-13}	1.3042×10^5	1.3042×10^5	-2.1201×10^{-13}
7	108	1.7362	82.66	-5.1868×10^4	-5.1868×10^4	4.9098×10^{-13}	-3.3880×10^4	-3.3880×10^4	-2.3623×10^{-13}
8	126	1.5944	91.04	1.0533×10^4	1.0533×10^4	-1.7096×10^{-12}	4.0114×10^3	4.0114×10^3	-6.5751×10^{-12}
9	144	1.4136	99.29	-1.0095×10^3	-1.0095×10^3	-7.3202×10^{-13}	-101.4018	-101.4018	3.2659×10^{-10}
10	162	1.1982	107.28	36.0581	36.0581	5.5378×10^{-10}	-9.2405	-9.2405	-1.0569×10^{-9}
11	180	0.9539	114.79	-0.2793	-0.2793	-3.2789×10^{-8}	0.2714	0.2714	-5.0121×10^{-8}

When $r_p > r_{qp}$ as shown in Figure 3.5.2 the addition theorem (3.3.9) when normalized gives

$$\underbrace{\left(\frac{r_q}{r_p}\right)^n \cos n\phi_q}_{f_4(r_q, \phi_q)_{\cos}} = \sum_{m=0}^n \frac{n!}{m!(n-m)!} \underbrace{\left(\frac{r_{qp}}{r_p}\right)^m \cos [(n-m)\phi_p + m\phi_{qp}]}_{g_4(r_p, \phi_p)_{\cos}}, \quad (3.5.4a)$$

$$\underbrace{\left(\frac{r_q}{r_p}\right)^n \sin n\phi_q}_{f_4(r_q, \phi_q)_{\sin}} = \sum_{m=0}^n \frac{n!}{m!(n-m)!} \underbrace{\left(\frac{r_{qp}}{r_p}\right)^m \sin [(n-m)\phi_p + m\phi_{qp}]}_{g_4(r_p, \phi_p)_{\sin}}, \quad (3.5.4b)$$

Let the left hand sides of (3.5.4a) and (3.5.4b) be referred to as $f_4(r_q, \phi_q)_{\cos}$ and $f_4(r_q, \phi_q)_{\sin}$ and the right hand sides as $g_4(r_p, \phi_p)_{\cos}$ and $g_4(r_p, \phi_p)_{\sin}$, respectively. Now consider the situation where $r_{qp} = 75$ cm, $r_p = 80$ cm and $\phi_{qp} = \pi/3$. The numerical results are given for the case when $n = 20$ in Table 3.5.9, showing good convergence of the series at various points.

Table 3.5.9: Truncation errors of $g_4(r_p, \phi_p)_{\cos}$ and $g_4(r_p, \phi_p)_{\sin}$ for $n = 20$, $\phi_{qp} = \pi/3$ and $r_{qp}/r_p = 0.9$

Point	ϕ_p	r_q/r_{qp}	ϕ_q	$f_4(r_q, \phi_q)_{\cos}$	$g_4(r_p, \phi_p)_{\cos}$	% Error	$f_4(r_q, \phi_q)_{\sin}$	$g_4(r_p, \phi_p)_{\sin}$	% Error
1	0	1.6782	28.93	-2.4520×10^4	-2.4520×10^4	1.7804×10^{-13}	-1.9617×10^4	-1.9617×10^4	-5.5636×10^{-13}
2	18	1.8090	38.29	9.8126×10^4	9.8126×10^4	5.1905×10^{-13}	1.0094×10^5	1.0094×10^5	-6.7754×10^{-13}
3	36	1.8952	47.61	-2.1932×10^5	-2.1932×10^5	5.3080×10^{-14}	-2.8216×10^5	-2.8216×10^5	-3.0943×10^{-13}
4	54	1.9348	56.90	2.8601×10^5	2.8601×10^5	8.7512×10^{-13}	4.5883×10^5	4.5883×10^5	-2.2835×10^{-13}
5	72	1.9269	66.19	-2.1918×10^5	-2.1918×10^5	9.0295×10^{-13}	-4.4710×10^5	-4.4710×10^5	-9.1132×10^{-14}
6	90	1.8716	75.50	9.5515×10^4	9.5515×10^4	1.2188×10^{-13}	2.6107×10^5	2.6107×10^5	-2.0066×10^{-13}
7	108	1.7702	84.82	-2.1374×10^4	-2.1374×10^4	2.0765×10^{-12}	-8.8733×10^4	-8.8733×10^4	2.6239×10^{-13}
8	126	1.6253	94.20	1.7285×10^3	1.7285×10^3	-3.1781×10^{-11}	1.6451×10^4	1.6451×10^4	-1.7249×10^{-12}
9	144	1.4405	103.66	84.4692	84.4692	1.1923×10^{-10}	-1.4766×10^3	-1.4766×10^3	3.9005×10^{-11}
10	162	1.2203	113.28	-14.4353	-14.4353	-1.3391×10^{-9}	51.6185	51.6185	2.0311×10^{-10}
11	180	0.9703	123.20	0.3054	0.3054	4.9050×10^{-8}	-0.4535	-0.4535	7.1061×10^{-8}

3.5.3 Evaluation of the translational addition theorems for Laplacian function $\ln r$

Consider again Figure 3.5.1 where $r_p < r_{qp}$ for the addition theorem (3.4.5) when normalized gives

$$\underbrace{\ln \left(\frac{r_{qp}}{r_p} \right)}_{f_5(r_q, \phi_q)} = \underbrace{\sum_{m=1}^{\infty} \frac{(-1)^m}{m} \left(\frac{r_p}{r_{qp}} \right)^m \cos [m(\phi_p - \phi_{qp})]}_{g_5(r_q, \phi_q)}, \quad r_p < r_{qp}. \quad (3.5.5)$$

Let us denote the left hand side of (3.5.5) as $f_5(r_q, \phi_q)$ and the right hand side as $g_5(r_q, \phi_q)$, respectively. For the situation where $r_{qp} = 75$ cm, $r_p = 37.5$ cm and $\phi_{qp} = 2\pi/3$, then r_q and ϕ_p vary when P moves along the circle. Test point locations are taken by varying ϕ_p over 0 to 180° . Numerical results are presented in Table 3.5.10 for the series truncations $M = 10$ and 30. As expected with greater values of M the better the convergence of the series.

Table 3.5.10: Truncation errors of $g_5(r_p, \phi_p)$ for $\phi_{qp} = 2\pi/3$, $r_p/r_{qp} = 0.5$, and $M = 10$ and 30

Point	ϕ_p	r_{qp}/r_q	$f_5(r_q, \phi_q)$	$g_5(r_p, \phi_p)_{M=10}$	% Error $_{M=10}$	$f_5(r_q, \phi_q)$	$g_5(r_p, \phi_p)_{M=30}$	% Error $_{M=30}$
1	0	1.1547	0.1438	0.1438	-2.9882×10^{-2}	0.1438	0.1438	-2.1712×10^{-10}
2	18	0.9796	-0.0206	-0.0206	-2.0507×10^{-1}	-0.0206	-0.0206	1.9487×10^{-8}
3	36	0.8592	-0.1517	-0.1518	2.5584×10^{-2}	-0.1517	-0.1517	-4.3629×10^{-9}
4	54	0.7769	-0.2524	-0.2524	-1.3596×10^{-2}	-0.2524	-0.2524	3.2555×10^{-9}
5	72	0.7219	-0.3259	-0.3260	9.0235×10^{-3}	-0.3259	-0.3259	-2.8234×10^{-9}
6	90	0.6874	-0.3748	-0.3747	-6.4796×10^{-3}	-0.3748	-0.3748	2.6104×10^{-9}
7	108	0.6699	-0.4006	-0.4006	4.7295×10^{-3}	-0.4006	-0.4006	-2.5134×10^{-9}
8	126	0.6675	-0.4042	-0.4042	-3.2927×10^{-3}	-0.4042	-0.4042	2.5004×10^{-9}
9	144	0.6799	-0.3859	-0.3859	1.8727×10^{-3}	-0.3859	-0.3859	-2.5676×10^{-9}
10	162	0.7083	-0.3449	-0.3449	-1.3819×10^{-4}	-0.3449	-0.3449	2.7357×10^{-9}
11	180	0.7559	-0.2798	-0.2798	-2.5863×10^{-3}	-0.2798	-0.2798	-3.0740×10^{-9}

When $r_p > r_{qp}$ as shown in Figure 3.5.2 the addition theorem (3.4.9) is normalized to give

$$\underbrace{\ln \left(\frac{r_p}{r_q} \right)}_{f_6(r_q, \phi_q)} = \underbrace{\sum_{m=1}^{\infty} \frac{(-1)^m}{m} \left(\frac{r_{qp}}{r_p} \right)^m \cos [m(\phi_p - \phi_{qp})]}_{g_6(r_p, \phi_p)}, \quad r_p > r_{qp}. \quad (3.5.6)$$

Let us denote the left hand side of (3.5.6) as $f_6(r_q, \phi_q)$ and the right hand side as

$g_6(r_p, \phi_p)$, respectively. Now consider the situation where $r_{qp} = 75$ cm, $r_p = 125$ cm and $\phi_{qp} = 2\pi/3$, the numerical results are shown in Table 3.5.11 for the series truncations $M = 10$ and 30, verifying the series converge.

Table 3.5.11: Truncation errors of $g_6(r_p, \phi_p)$ for $\phi_{qp} = 2\pi/3$, $r_{qp}/r_p = 0.6$, and $M = 10$ and 30

Point	ϕ_p	r_{qp}/r_p	$f_6(r_q, \phi_q)$	$g_6(r_p, \phi_p)_{M=10}$	% Error $_{M=10}$	$f_6(r_q, \phi_q)$	$g_6(r_p, \phi_p)_{M=30}$	% Error $_{M=30}$
1	0	1.1471	0.1372	0.1369	-0.2468	0.1372	0.1372	3.3449×10^{-7}
2	18	0.9489	-0.0524	-0.0521	-0.5956	-0.0524	-0.0524	2.7787×10^{-6}
3	36	0.8205	-0.1979	-0.1981	0.1397	-0.1979	-0.1979	-1.0159×10^{-6}
4	54	0.7356	-0.3071	-0.3068	-0.0779	-0.3071	-0.3071	7.6019×10^{-7}
5	72	0.6799	-0.3857	-0.3859	0.0526	-0.3857	-0.3857	-6.5556×10^{-7}
6	90	0.6456	-0.4376	-0.4374	-0.0382	-0.4376	-0.4376	6.0366×10^{-7}
7	108	0.6282	-0.4649	-0.4650	0.0282	-0.4649	-0.4649	-5.8004×10^{-7}
8	126	0.6258	-0.4687	-0.4686	-0.0200	-0.4687	-0.4687	5.7686×10^{-7}
9	144	0.6381	-0.4493	-0.4494	0.0121	-0.4493	-0.4493	-5.9322×10^{-7}
10	162	0.6664	-0.4059	-0.4058	-0.0025	-0.4059	-0.4059	6.3418×10^{-7}
11	180	0.7143	-0.3365	-0.3364	-0.0120	-0.3365	-0.3365	-7.1641×10^{-7}

Chapter 4

Application of the addition theorems to the solution of electrostatic fields in systems of parallel circular cylinders with coplanar axes

In this chapter the derived addition theorems from Sections 3.2 and 3.4 will be applied to the problem discussed in Section 2.2 for some simplified geometries. All the boundary problems solved for in this chapter apply to either Dirichlet or Neumann type.

For problems with all the cylinder axes coplanar on the x -axis the circular harmonic solution of Laplace's equation (2.2.1) can be simplified to

$$u_q(r_q, \phi_q) = C_A + A_0 \ln r_q + \sum_{n=1}^{\infty} A_n \left(\frac{1}{r_q}\right)^n \cos n\phi_q, \quad (4.0.1)$$

where the sin function is excluded and the constants are renamed.

4.1 Conducting cylinder parallel with a line charge

A straight line charge with linear charge density $+\rho_l$ is placed parallel to and a distance d away from the axis of a conducting cylinder of radius a_1 held at fixed voltage such that the potential vanishes at infinity, as shown in Figure 4.1.1. The medium outside the cylinder is linear and homogeneous, with permittivity ϵ . The

potential at any point outside the cylinder, expressed in (r_1, ϕ_1) coordinates, is found.

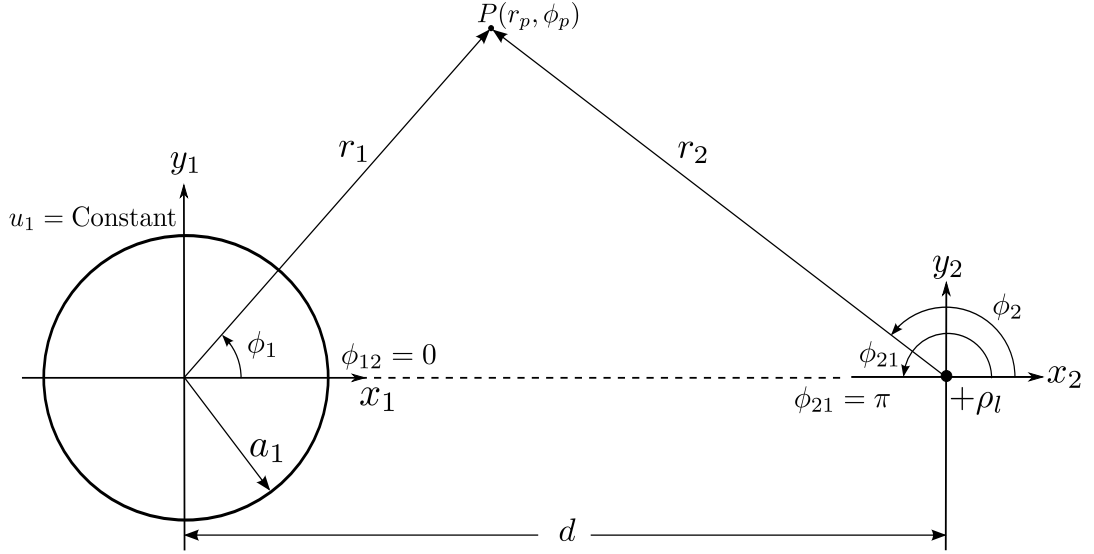


Figure 4.1.1: Conducting cylinder near a parallel line charge

The potential due to the presence of the conducting cylinder is expressed in (r_1, ϕ_1) coordinates as

$$u_1(r_1, \phi_1) = C_A + A_0 \ln r_1 + \sum_{n=1}^{\infty} A_n \left(\frac{1}{r_1} \right)^n \cos n\phi_1, \quad r_1 > a_1, \quad (4.1.1)$$

while the potential due to the line charge in (r_2, ϕ_2) coordinates is

$$u_2(r_2, \phi_2) = -\frac{\rho_l}{2\pi\epsilon} \ln r_2 + C_\beta = \beta \ln r_2 + C_\beta, \quad \text{where } \beta \equiv -\frac{\rho_l}{2\pi\epsilon} \quad (4.1.2)$$

and C_β is a reference constant.

The potential $u_2(r_2, \phi_2)$ is translated using the addition theorems of Section 3.4 into the coordinate system (r_1, ϕ_1) and the boundary condition that the potential at infinity vanish is imposed. To express $u_2(r_2, \phi_2)$ using (3.4.5) and (3.4.9) with the following substitutions $r_q \equiv r_2$, $\phi_q \equiv \phi_2$, $r_p \equiv r_1$, $\phi_p \equiv \phi_1$, $r_{qp} \equiv d$, $\phi_{qp} \equiv \phi_{21} = \pi$, changing the series index $m = n$, and making use of the trigonometric equation

$\cos(\alpha - \psi) = \cos \alpha \cos \psi + \sin \alpha \sin \psi$, gives

$$u_2^{(1)}(r_1, \phi_1) = C_\beta + \beta \ln d - \beta \sum_{n=1}^{\infty} \frac{1}{n} \left(\frac{r_1}{d}\right)^n \cos n\phi_1, \quad r_1 < d, \quad (4.1.3a)$$

$$u_2^{(1)}(r_1, \phi_1) = C_\beta + \beta \ln r_1 - \beta \sum_{n=1}^{\infty} \frac{1}{n} \left(\frac{d}{r_1}\right)^n \cos n\phi_1, \quad r_1 > d, \quad (4.1.3b)$$

The total potential $u_{tot}^{(1)}(r_1, \phi_1)$ at any point outside the cylinder is then expressed as

$$u_{tot}^{(1)}(r_1, \phi_1) = u_1(r_1, \phi_1) + u_2^{(1)}(r_1, \phi_1) + C, \quad (4.1.4)$$

where $C \equiv C_A + C_\beta$ is an arbitrary constant defined by the reference potential. Equation (4.1.4) is in the coordinates of the cylinder system and therefore the boundary conditions at infinity and at the surface of the cylinder can be imposed to solve for the constants of integration, C , A_0 and A_n . First imposing the boundary condition that the potential vanish at infinity using (4.1.3b) for $u_2^{(1)}$ gives

$$\begin{aligned} 0 &= \lim_{r_1 \rightarrow \infty} u_{tot}^{(1)}(r_1, \phi_1) \\ &= \lim_{r_1 \rightarrow \infty} \left\{ A_0 \ln r_1 + \beta \ln r_1 + C + \sum_{n=1}^{\infty} \left[A_n \left(\frac{1}{r_1}\right)^n - \beta \frac{1}{n} \left(\frac{d}{r_1}\right)^n \right] \cos n\phi_1 \right\} \\ &= \lim_{r_1 \rightarrow \infty} \{ A_0 \ln r_1 + \beta \ln r_1 + C \}. \end{aligned}$$

This expression is only valid if the constants are set to $A_0 = -\beta$ and $C = 0$. Now solving for the potential on the surface of the cylinder $r_1 = a_1$ using (4.1.4) with (4.1.3a) since $r_1 < d$ and substituting for the solved values gives

$$u_{tot}^{(1)}(a_1, \phi_1) = \beta \ln \left(\frac{d}{a_1}\right) + \sum_{n=1}^{\infty} \left[A_n \left(\frac{1}{a_1}\right)^n - \beta \frac{1}{n} \left(\frac{d}{a_1}\right)^n \right] \cos n\phi_1, \quad (4.1.5)$$

which after equating like terms since the potential on the cylinder is a constant,

yields

$$0 = A_n \left(\frac{1}{a_1} \right)^n - \beta \frac{1}{n} \left(\frac{d}{a_1} \right)^n$$

$$A_n = \beta \frac{1}{n} \left(\frac{a_1^2}{d} \right)^n .$$

Substituting all the constants A_0 , A_n and β into (4.1.4) and simplifying, for $a_1 \leq r_1 \leq d$ gives

$$u_{tot}^{(1)}(r_1, \phi_1) = -\frac{\rho_l}{2\pi\epsilon} \left\{ \ln \left(\frac{d}{r_1} \right) + \sum_{n=1}^{\infty} \frac{1}{n} \left(\frac{r_1}{d} \right)^n \left[\left(\frac{a_1}{r_1} \right)^{2n} - 1 \right] \cos n\phi_1 \right\}, \quad (4.1.6)$$

and for $r_1 \geq d$ we get

$$u_{tot}^{(1)}(r_1, \phi_1) = -\frac{\rho_l}{2\pi\epsilon} \sum_{n=1}^{\infty} \frac{1}{n} \left(\frac{d}{r_1} \right)^n \left[\left(\frac{a_1}{d} \right)^{2n} - 1 \right] \cos n\phi_1. \quad (4.1.7)$$

Note, using (4.1.6) the total potential on the cylinder is calculated as

$$u_{tot}^{(1)}(a_1, \phi_1) = -\frac{\rho_l}{2\pi\epsilon} \ln \left(\frac{d}{a_1} \right).$$

Potential distribution using image method

Alternatively, the potential solution for this elementary problem can be obtained using the image method. The equipotential surfaces of two parallel straight lines are circular cylinders described by [1]

$$u_{tot}^{im}(r_2, r_3) = \frac{\rho_l}{2\pi\epsilon} \ln \left(\frac{r_3}{r_2} \right) + u_0, \quad (4.1.8)$$

where u_0 is an arbitrary constant defined by the reference potential. The potential distribution given by (4.1.8) must also describe the potential between a finite cylinder of radius a_1 and a line charge $+\rho_l$, as shown in Figure 4.1.2.

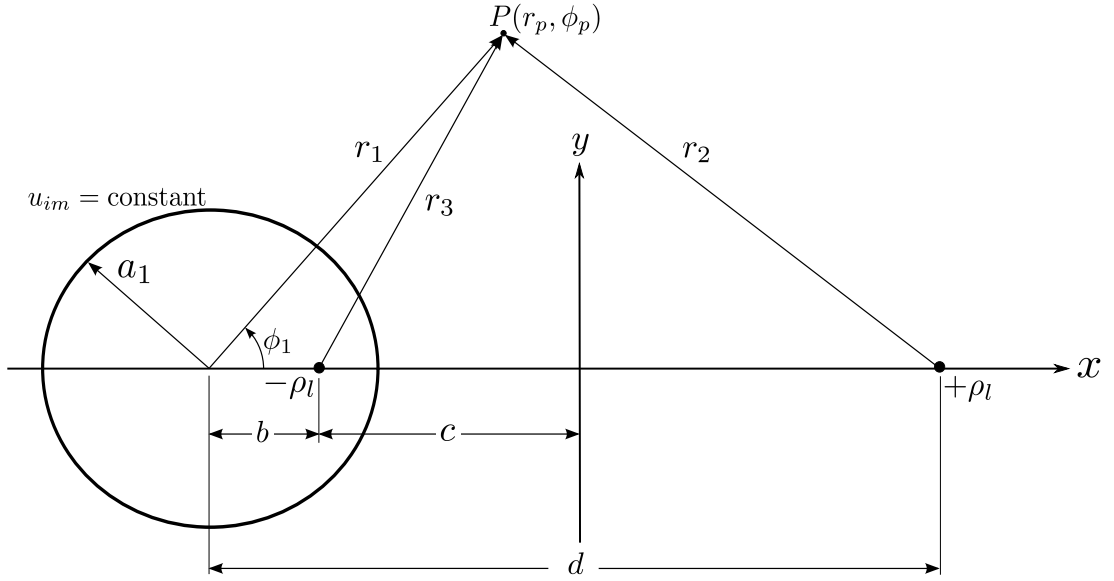


Figure 4.1.2: Two straight line charges of equal and opposite sign

The cylinder will carry the total charge per unit length $-\rho_l$ and will have a potential defined by the radial distances r_2 and r_3 along its surface. The radial distances can be expressed in terms of (r_1, ϕ_1) coordinates using the law of cosines relationship giving $r_2 = \sqrt{r_1^2 + d^2 - 2r_1d \cos \phi_1}$ and $r_3 = \sqrt{r_1^2 + b^2 - 2r_1b \cos \phi_1}$. Imposing the boundary condition that the potential vanish at infinity sets $u_0 = 0$ thus, the total potential is

$$u_{tot}^{im}(r_1, \phi_1) = \frac{\rho_l}{2\pi\epsilon} \left\{ \ln \left(\sqrt{r_1^2 + b^2 - 2r_1b \cos \phi_1} \right) - \ln \left(\sqrt{r_1^2 + d^2 - 2r_1d \cos \phi_1} \right) \right\}. \quad (4.1.9)$$

But using the harmonic expansions of a line charge [10]

$$\ln \left(\sqrt{r_1^2 + d^2 - 2r_1d \cos \phi_1} \right) = \begin{cases} \ln d - \sum_{n=1}^{\infty} \frac{1}{n} \left(\frac{r_1}{d} \right)^n \cos n\phi_1, & r_1 < d, \\ \ln r_1 - \sum_{n=1}^{\infty} \frac{1}{n} \left(\frac{d}{r_1} \right)^n \cos n\phi_1, & r_1 > d, \end{cases} \quad (4.1.10)$$

and from the geometry in Figure 4.1.2 it can be shown that $b = a_1^2/d$ and thus,

$$\ln \left(\sqrt{r_1^2 + b^2 - 2r_1 b \cos \phi_1} \right) = \begin{cases} \ln \left(\frac{a_1^2}{d} \right) - \sum_{n=1}^{\infty} \frac{1}{n} \left(\frac{r_1 d}{a_1^2} \right)^n \cos n\phi_1, & r_1 < a_1^2/d, \\ \ln r_1 - \sum_{n=1}^{\infty} \frac{1}{n} \left(\frac{a_1^2}{r_1 d} \right)^n \cos n\phi_1, & r_1 > a_1^2/d, \end{cases} \quad (4.1.11)$$

Using the expansions given in (4.1.10) and (4.1.11) the potential (4.1.9) can be reduced to the same expressions (4.1.6) and (4.1.7) for regions $a_1 \leq r_1 \leq d$ and $r_1 \geq d$, respectively.

Calculation of charge per unit length on the cylinder

The total charge on the cylinder can be found by integrating the surface charge density over the surface of the cylinder, i.e.,

$$Q_{tot} = \oint_S \rho_S dS. \quad (4.1.12)$$

Since the cylinder surface outward normal is only radial the charge density is obtained from

$$\rho_S = -\varepsilon \left. \frac{\partial u_{tot}^{(1)}}{\partial r_1} \right|_{r_1=a_1} \quad (4.1.13)$$

$$= -\frac{\rho_l}{2\pi} \left\{ \frac{1}{r_1} - \sum_{n=1}^{\infty} \frac{r_1^{n-1}}{d^n} \left[\left(\frac{a_1}{r_1} \right)^{2n} - 1 \right] \cos n\phi_1 \right\}_{r_1=a_1}. \quad (4.1.14)$$

The total charge for the length l of the cylinder can be calculated as

$$Q_{tot} = \int_0^l \int_0^{2\pi} \rho_S(a_1, \phi_1) a_1 d\phi_1 dz_1 \quad (4.1.15)$$

$$= l \int_0^{2\pi} -\frac{\rho_l}{2\pi} \left\{ \frac{1}{a_1} - \sum_{n=1}^{\infty} \frac{r_1^{n-1}}{d^n} \left[\left(\frac{a_1}{a_1} \right)^{2n} - 1 \right] \cos n\phi_1 \right\} a_1 d\phi_1 dz_1 \quad (4.1.16)$$

$$= -\rho_l l \quad (4.1.17)$$

and the charge per unit length is $Q_{tot}/l = -\rho_l$ which is the image line charge $-\rho_l$ given by the image method.

4.2 Two-cylinder system

Two conducting cylinders of radii a_1 and a_2 are placed parallel to each other with a separation distance d between their axes, as shown in the Figure 4.2.1. Charges per unit length of $-q$ and q are placed on cylinder 1 and 2, respectively, i.e., a complete system, with the requirement that the potential vanish at infinity. The medium outside the cylinders being homogeneous, with permittivity ε .

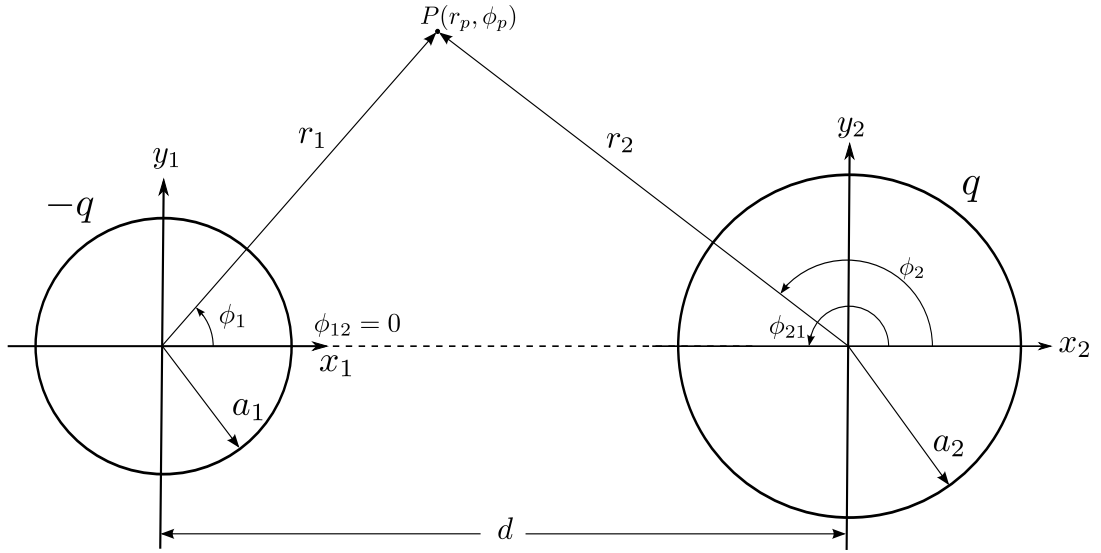


Figure 4.2.1: System of two conducting cylinders

The harmonic potentials of cylinders 1 and 2 are expressed in their respective coordinate systems as

$$u_1(r_1, \phi_1) = C_A + A_0 \ln r_1 + \sum_{n=1}^{\infty} A_n \left(\frac{a_1}{r_1}\right)^n \cos n\phi_1, \quad r_1 > a_1, \quad (4.2.1)$$

$$u_2(r_2, \phi_2) = C_B + B_0 \ln r_2 + \sum_{n=1}^{\infty} B_n \left(\frac{a_2}{r_2}\right)^n \cos n\phi_2, \quad r_2 > a_2, \quad (4.2.2)$$

where C_A and C_B are reference constants and the harmonics in the series expansions have been normalized to the radii a_1 and a_2 , respectively. Note, this has no effect on the potential distribution only the magnitudes of the constant change.

Then $u_2(r_2, \phi_2)$ is translated into the coordinate system (r_1, ϕ_1) allowing the boundary condition at the surface of cylinder $r_1 = a_1$ to be imposed. Using (3.2.6a) and (3.4.5) with the following substitutions $r_q \equiv r_2$, $\phi_q \equiv \phi_2$, $r_p \equiv r_1$, $\phi_p \equiv \phi_1$, $r_{qp} \equiv d$ and $\phi_{qp} = \pi$, the addition theorems reduce to

$$\ln r_2 = \ln d - \sum_{n=1}^{\infty} \frac{1}{n} \left(\frac{r_1}{d}\right)^n \cos n\phi_1, \quad (4.2.3)$$

$$\left(\frac{1}{r_2}\right)^n \cos n\phi_2 = \sum_{m=0}^{\infty} \frac{(-1)^n (n+m-1)!}{m!(n-1)!} \left(\frac{1}{d}\right)^n \left(\frac{r_1}{d}\right)^m \cos m\phi_1. \quad (4.2.4)$$

Therefore the translated potential $u_2^{(1)}(r_1, \phi_1)$ expressed in the coordinates of cylinder 1 is

$$\begin{aligned} u_2^{(1)}(r_1, \phi_1) = & C_B + B_0 \left\{ \ln d - \sum_{n=1}^{\infty} \frac{1}{n} \left(\frac{r_1}{d}\right)^n \cos n\phi_1 \right\} \\ & + \sum_{n=1}^{\infty} \sum_{m=0}^{\infty} B_n \frac{(-1)^n (n+m-1)!}{m!(n-1)!} \left(\frac{a_2}{d}\right)^n \left(\frac{r_1}{d}\right)^m \cos m\phi_1. \end{aligned} \quad (4.2.5)$$

For convenience let us denote

$$\tau_B(m, n, r_1, a_2, d) = \frac{(-1)^n (n+m-1)!}{m!(n-1)!} \left(\frac{a_2}{d}\right)^n \left(\frac{r_1}{d}\right)^m, \quad (4.2.6a)$$

$$\gamma_B(n, r_1, d) = -\frac{1}{n} \left(\frac{r_1}{d}\right)^n, \quad (4.2.6b)$$

so (4.2.5) can be rewritten as,

$$\begin{aligned} u_2^{(1)}(r_1, \phi_1) = & C_B + B_0 \left\{ \ln d + \sum_{n=1}^{\infty} \gamma_B(n, r_1, d) \cos n\phi_1 \right\} \\ & + \sum_{n=1}^{\infty} \sum_{m=0}^{\infty} B_n \tau_B(m, n, r_1, a_2, d) \cos m\phi_1. \end{aligned} \quad (4.2.7)$$

The total potential expressed in (r_1, ϕ_1) coordinates at any point $P(r_1, \phi_1)$ is then

$$\begin{aligned}
u_{tot}^{(1)}(r_1, \phi_1) &= u_1(r_1, \phi_1) + u_2^{(1)}(r_1, \phi_1) \\
&= C + A_0 \ln r_1 + B_0 \ln d + \sum_{n=1}^{\infty} \left[A_n \left(\frac{a_1}{r_1} \right)^n + B_0 \gamma_B(n, r_1, d) \right] \cos n\phi_1 \\
&\quad + \sum_{n=1}^{\infty} \sum_{m=0}^{\infty} B_n \tau_B(m, n, r_1, a_2, d) \cos m\phi_1,
\end{aligned} \tag{4.2.8}$$

where $C \equiv C_A + C_B$. Now applying the boundary condition at $r_1 = a_1$, that is,

$u_{tot}^{(1)}(r_1 = a_1, \phi_1) = V_1$ reduces (4.2.8) to

$$\begin{aligned}
V_1 &= C + A_0 \ln a_1 + B_0 \ln d + \sum_{n=1}^{\infty} [A_n + B_0 \gamma_B(n, a_1, d)] \cos n\phi_1 \\
&\quad + \sum_{n=1}^{\infty} \sum_{m=0}^{\infty} B_n \tau_B(m, n, a_1, a_2, d) \cos m\phi_1.
\end{aligned} \tag{4.2.9}$$

Making use of the orthogonal properties of trigonometric functions, which are

$$\int_0^{2\pi} \cos n\phi \cos m\phi d\phi = \begin{cases} \pi \delta_{n,m} & n \neq 0 \\ 2\pi & n = m = 0 \end{cases} \tag{4.2.10a}$$

$$\int_0^{2\pi} \sin n\phi \sin m\phi d\phi = \begin{cases} \pi \delta_{n,m} & n \neq 0 \\ 2\pi & n = m = 0 \end{cases} \tag{4.2.10b}$$

$$\int_0^{2\pi} \cos n\phi \sin m\phi d\phi = 0 \quad n, m \text{ all integral values} \tag{4.2.10c}$$

where $\delta_{n,m}$ is the Kronecker delta¹. Therefore multiply (4.2.9) by $\cos m\phi_1$ and integrating in ϕ_1 from 0 to 2π , for all positive integral values of m , gives the infinite

¹The Kronecker delta symbol is $\delta_{n,m} = \begin{cases} 1 & n = m \\ 0 & n \neq m \end{cases}$.

set of equations

$$V_1 - C = A_0 \ln a_1 + B_0 \ln d + \sum_{n=1}^{\infty} B_n \tau_B(0, n, a_1, d), \quad m = 0, \quad (4.2.11)$$

$$0 = A_m + B_0 \gamma_B(m, a_1) + \sum_{n=1}^{\infty} B_n \tau_B(m, n, a_1, a_2, d), \quad m = 1, 2, \dots \quad (4.2.12)$$

The same steps taken to apply the boundary conditions at cylinder 1, are followed for cylinder 2. Now $u_1(r_1, \phi_1)$ is translated into the coordinate system (r_2, ϕ_2) and the boundary conditions at $r_2 = a_2$, that is, $u_{tot}^{(2)}(r_2 = a_2, \phi_2) = V_2$ gives the infinite set of equations

$$V_2 - C = B_0 \ln a_2 + A_0 \ln d + \sum_{n=1}^{\infty} A_n \tau_A(0, n, a_2, d), \quad m = 0, \quad (4.2.13)$$

$$0 = B_m + A_0 \gamma_A(m, a_2) + \sum_{n=1}^{\infty} A_n \tau_A(m, n, a_2, a_1, d), \quad m = 1, 2, \dots \quad (4.2.14)$$

where

$$\tau_A(m, n, r_2, a_1, d) = \frac{(-1)^m (n + m - 1)!}{m! (n - 1)!} \left(\frac{a_1}{d}\right)^n \left(\frac{r_2}{d}\right)^m, \quad (4.2.15a)$$

$$\gamma_A(n, r_2, d) = -\frac{(-1)^n}{n} \left(\frac{r_2}{d}\right)^n, \quad (4.2.15b)$$

The known boundary conditions are given in terms of the charges per unit length on the cylinders, therefore, we need to find the charges in terms of the constants of integration. The total charge on the p^{th} cylinder is given by

$$Q_{tot}^{(p)} = \oint_S \rho_S^{(p)} dS$$

and the charge per unit length ($q = Q/l$) is calculated with

$$q_{tot}^{(p)} = \int_0^{2\pi} \rho_S^{(p)} r_p d\phi_p \Big|_{r_p=a_p}, \quad (4.2.16)$$

where the surface charge density on cylinder p is

$$\rho_S^{(p)}(r_p = a_p, \phi_p) = -\varepsilon \left. \frac{\partial u_{tot}^{(p)}}{\partial r_p} \right|_{r_p=a_p}. \quad (4.2.17)$$

Solving for the charge density on cylinder 1, that is $\rho_S^{(1)}(r_1, \phi_1)$, and substituting into (4.2.16) gives

$$\begin{aligned} q_{tot}^{(1)}(r_1, \phi_1) = -\varepsilon \int_0^{2\pi} \left\{ \frac{A_0}{r_1} + \sum_{n=1}^{\infty} \frac{n}{r_1} \left[B_0 \gamma_B(n, r_1, d) - A_n \left(\frac{a_1}{r_1} \right)^n \right] \cos n\phi_1 \right. \\ \left. + \sum_{n=1}^{\infty} \sum_{m=0}^{\infty} B_n \frac{m}{r_1} \tau_B(m, n, r_1, a_2, d) \cos m\phi_1 \right\} r_1 d\phi_1, \end{aligned} \quad (4.2.18)$$

where the derivatives of $\tau_B(m, n, r_1, a_2, d)$ and $\gamma_B(n, r_1, d)$ are given by

$$\begin{aligned} \frac{\partial}{\partial r_1} \left[\tau_B(m, n, r_1, a_2, d) \right] &= \frac{m}{r_1} \tau_B(m, n, r_1, a_2, d), \\ \frac{\partial}{\partial r_1} \left[\gamma_B(n, r_1, d) \right] &= \frac{n}{r_1} \gamma_B(n, r_1, d). \end{aligned}$$

Evaluating (4.2.18) at the surface of cylinder 1, reduces it to

$$q_{tot}^{(1)}(a_1, \phi_1) = -2\pi\varepsilon A_0. \quad (4.2.19)$$

Similarly, the charge per unit length of cylinder 2 can be found to be

$$q_{tot}^{(2)}(a_2, \phi_2) = -2\pi\varepsilon B_0. \quad (4.2.20)$$

This shows that the total charges per unit length $q_{tot}^{(1)}$ and $q_{tot}^{(2)}$ on cylinders 1 and 2 are proportional to the constants of integration A_0 and B_0 , respectively, by the factor $-2\pi\varepsilon$. However, for the potential at infinity to vanish we require the logarithms vanish in the potential distribution. For the potential $u_{tot}^{(1)}(r_1, \phi_1)$ when $r_1 > d$ we use addition theorems (3.3.9a) and (3.4.9) to translate $u_2(r_2, \phi_2)$ to

(r_1, ϕ_1) coordinates giving

$$\begin{aligned}
u_{tot}^{(1)}(r_1, \phi_1) = & C + A_0 \ln r_1 + B_0 \ln r_1 + \sum_{n=1}^{\infty} \left[A_n \left(\frac{a_1}{r_1} \right)^n - B_0 \frac{1}{n} \left(\frac{d}{r_1} \right)^n \right] \cos n\phi_1 \\
& + \sum_{n=1}^{\infty} \sum_{m=0}^{\infty} B_n \frac{(-1)^n (n+m-1)!}{m!(n-1)!} \left(\frac{a_2}{a_1} \right)^n \left(\frac{d}{r_1} \right)^m \cos m\phi_1,
\end{aligned} \tag{4.2.21}$$

The potential as $r_1 \rightarrow \infty$, reduces to

$$\lim_{r_1 \rightarrow \infty} u_{tot}^{(1)}(r_1, \phi_1) = \lim_{r_1 \rightarrow \infty} [C + A_0 \ln r_1 + B_0 \ln r_1] = 0, \tag{4.2.22}$$

The only way to satisfy that the logarithmic potential at infinity vanish is for $A_0 + B_0 = 0$, i.e., the sum of the charges on all the conductors is equal to zero. The uniqueness theorem states that C can be set to any value because it makes no contribution to the electric field intensity, since the addition of a constant makes no difference to the gradient, thus, we choose $C = 0$ for the potential to vanish at infinity.

The equations (4.2.11) to (4.2.14), (4.2.19), (4.2.20) and with $C = 0$, form a complete system that constitute an infinite set of coupled linear equations which solved simultaneously determine the unknown constants of integration. To obtain numerical results, the infinite series must be truncated to a finite number of terms $n = m = M$. The truncated system can be written in matrix and vector form, $Ax = b$, where we use the abbreviations for $\tau_B(m, n, a_1, a_2, d) \equiv \tau_B(m, n)$, $\tau_A(m, n, a_2, a_1, d) \equiv \tau_A(m, n)$, $\gamma_B(n, a_1, d) \equiv \gamma_B(n)$ and $\gamma_A(n, a_2, d) \equiv \gamma_A(n)$ to give

$$\begin{bmatrix}
-1 & 0 & 0 & \tau_B(0, 1) & \dots & 0 & \tau_B(0, M) \\
0 & -1 & \tau_A(0, 1) & 0 & \dots & \tau_A(0, M) & 0 \\
0 & 0 & 1 & \tau_B(1, 1) & \dots & 0 & \tau_B(1, M) \\
0 & 0 & \tau_A(1, 1) & 1 & \dots & \tau_A(1, M) & 0 \\
\vdots & \vdots & \vdots & \vdots & \ddots & \vdots & \vdots \\
0 & 0 & 0 & \tau_B(M, 1) & \dots & 1 & \tau_B(M, M) \\
0 & 0 & \tau_A(M, 1) & 0 & \dots & \tau_A(M, M) & 1
\end{bmatrix}
\begin{bmatrix}
V_1 \\
V_2 \\
A_1 \\
B_1 \\
\vdots \\
A_M \\
B_M
\end{bmatrix}
=
\begin{bmatrix}
-A_0 \ln a_1 - B_0 \ln d \\
-A_0 \ln d - B_0 \ln a_2 \\
-B_0 \gamma_B(1) \\
-A_0 \gamma_A(1) \\
\vdots \\
-B_0 \gamma_B(M) \\
-A_0 \gamma_A(M)
\end{bmatrix}$$

Once the constants of integration $A_1, \dots, A_M, B_1, \dots, B_M$, along with potentials V_1 and V_2 are numerically calculated, substitution back into the equation for the potential distribution gives

$$u_{tot}(r_1, \phi_1 | r_2, \phi_2) = A_0 \ln r_1 + B_0 \ln r_2 + \sum_{n=1}^{\infty} \left\{ A_n \left(\frac{a_1}{r_1} \right)^n \cos n\phi_1 + B_n \left(\frac{a_2}{r_2} \right)^n \cos n\phi_2 \right\}, \quad (4.2.23)$$

where the location of the observation point $P(r_1, \phi_1 | r_2, \phi_2)$ must be expressed in terms of both (r_1, ϕ_1) and (r_2, ϕ_2) coordinates which can be done using the relations in (2.3.5) and (2.3.6).

Planar bipolar coordinate solution to the two cylinder system

The two cylinder system can naturally be described in the planar (or two-dimensional) bipolar coordinate system (η, ξ) where [14]

$$x = a \frac{\sinh \eta}{\cosh \eta - \cos \xi}, \quad y = a \frac{\sin \xi}{\cosh \eta - \cos \xi}, \quad (4.2.24)$$

where $\eta = \text{constant}$ are Apollonian circles and $\xi = \text{constant}$ are sections of circles orthogonal to $\eta = \text{constant}$ (see Figure 4.2.2).

Eliminating η from (4.2.24) gives $x^2 + (y - a \cot \xi)^2 = a^2 \csc^2 \xi$, which defines the coordinate surface $\xi = \text{constant}$ for $0 \leq \xi \leq 2\pi$ as circular cylinders centred at $(0, a \cot \xi)$ with radius $a|\csc \xi|$. In the same way, eliminating ξ from (4.2.24) gives $(x - a \coth \eta)^2 + y^2 = a^2 \text{csch}^2 \eta$, which defines the coordinate surface $\eta = \text{constant}$ for $-\infty < \eta < \infty$ as circular cylinders centred at $(a \coth \eta, 0)$ with radius $a|\text{csch} \eta|$. As $\eta \rightarrow \pm\infty$ the circles degenerate to the focal points $(\pm a, 0)$.

Consider again, in bipolar coordinates, the case of two cylinders of radii a_1 and a_2 positioned parallel to each other in a homogeneous medium of permittivity ε ,

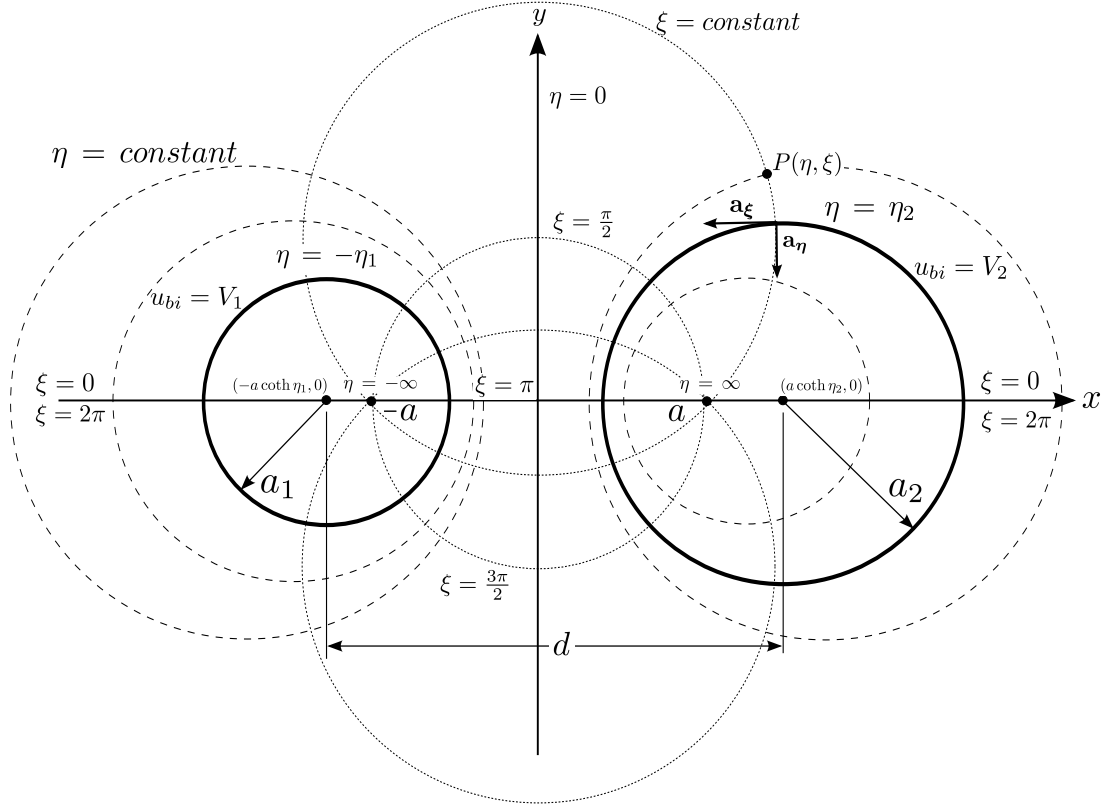


Figure 4.2.2: Two conducting cylinders in bipolar coordinates (η, ξ)

as shown in Figure 4.2.2. Charges of $-q$ and q are placed on cylinders 1 and 2, respectively, with the potential vanishing at infinity. The total potential distribution is governed by Laplace's equation

$$\nabla^2 u_{bi}(\eta, \xi) = \left(\frac{\cosh \eta - \cos \xi}{a} \right)^2 \left[\frac{\partial^2 u_{bi}}{\partial \eta^2} + \frac{\partial^2 u_{bi}}{\partial \xi^2} \right] = 0. \quad (4.2.25)$$

The general harmonic solution of the Laplace equation for the configuration in Figure 4.2.2 [15] is [see Appendix B]

$$u_{bi}(\eta, \xi) = A_0 + B_0 \eta + \sum_{n=1}^{\infty} (A_n e^{n\eta} + B_n e^{-n\eta}) \cos n\xi. \quad (4.2.26)$$

The potential distribution at a point near infinity, that is, $(\eta \rightarrow 0, \xi = 0)$, gives

$$u_{bi}(\eta \rightarrow 0, \xi = 0) \approx A_0 + \sum_{n=1}^{\infty} (A_n + B_n). \quad (4.2.27)$$

For the potential to vanish near infinity $A_0 = 0$ and $A_n = -B_n$, but since we require the potentials on the cylinders to be fixed values, the constants $A_n = B_n = 0$. Therefore, the potential distribution reduces to

$$u_{bi}(\eta, \xi) = B_0\eta. \quad (4.2.28)$$

To solve for the constant B_0 in (4.2.28) we find the charge per unit length in terms of the potential distribution. For cylinder 1, the charge density is

$$\rho_{S_{bi}}(\eta = \eta_1, \xi) = -\varepsilon \frac{1}{h_\eta} \frac{\partial u_{bi}}{\partial \eta} = -\varepsilon \frac{1}{h_\eta} B_0. \quad (4.2.29)$$

The charge per unit length is

$$q_{tot}^{(1)} = \int_0^{2\pi} \rho_{S_{bi}} h_\xi d\xi = -\varepsilon B_0 \int_0^{2\pi} \frac{h_\xi}{h_\eta} d\xi, \quad (4.2.30)$$

since the scale factors $h_\xi = h_\eta$, we obtain $q_{tot}^{(1)} = -2\pi\varepsilon B_0$. In the same way the charge per unit length on cylinder 2 can be found to be $q_{tot}^{(2)} = 2\pi\varepsilon B_0$. Therefore, we see, using the bipolar method the charge on the cylinders must always be equal and opposite. The cylinder surfaces in bipolar coordinates are given by

$$\eta_1 = \operatorname{csch}^{-1} \left(\frac{a_1}{a} \right), \quad \eta_2 = \operatorname{csch}^{-1} \left(\frac{a_2}{a} \right), \quad (4.2.31)$$

$$a = \frac{\sqrt{(d + a_1 + a_2)(d + a_1 - a_2)(d - a_1 + a_2)(d - a_1 - a_2)}}{2d}. \quad (4.2.32)$$

Numerical results of the two cylinder system

Tables 4.2.1 and 4.2.2 for $a_1 = 1$ cm, $a_2 = 2$ cm, $d = 5$ cm, $q_{tot}^{(1)} = -1$ nC/m and $q_{tot}^{(2)} = 1$ nC/m show the percentage error between the potentials from the translational and bipolar methods at various points for truncations of $M = 5$ and 15, respectively. The points are chosen along circles of radii 0.25 cm, 5 cm and 10 cm taken with respect to the global coordinates (x, y) , where the origin of the system can be easily seen in Figure 4.2.2.

Table 4.2.1: Percentage error between the potential values of the translational and bipolar boundary value methods for $a_1 = 1$ cm, $a_2 = 2$ cm, $d = 5$ cm, $q_{tot}^{(1)} = -1$ nC/m, $q_{tot}^{(2)} = 1$ nC/m, and $M = 5$

Point	r [cm]	ϕ [°]	r_1 [cm]	ϕ_1 [°]	r_2 [cm]	ϕ_2 [°]	η	ξ	u_{tot} [V]	u_{bi} [V]	% Error
1	0.25	0	2.4500	0.00	2.5500	0.00	0.2566	-3.14	4.606248	4.611570	-1.1540×10^{-1}
2	0.25	72	2.2896	5.96	2.7331	175.01	0.0777	2.90	1.394524	1.397398	-2.0566×10^{-1}
3	0.25	144	2.0031	4.21	3.0058	177.20	-0.2060	2.99	-3.704300	-3.702575	4.6571×10^{-2}
4	0.25	216	2.0031	355.79	3.0058	182.80	-0.2060	-2.99	-3.704300	-3.702575	4.6571×10^{-2}
5	0.25	288	2.2896	354.04	2.7331	184.99	0.0777	-2.90	1.394524	1.397398	-2.0566×10^{-1}
6	5	0	7.2000	0.00	2.2000	0.00	0.8281	0.00	14.878705	14.885705	-4.7028×10^{-2}
7	5	72	6.0530	51.78	4.9181	104.78	0.2131	0.72	3.831194	3.831172	5.7578×10^{-4}
8	5	144	3.4701	122.12	7.4493	156.76	-0.6180	0.50	-11.107827	-11.107813	1.2691×10^{-4}
9	5	216	3.4701	237.88	7.4493	203.24	-0.6180	-0.50	-11.107827	-11.107813	1.2691×10^{-4}
10	5	288	6.0530	308.22	4.9181	255.22	0.2131	-0.72	3.831194	3.831172	5.7578×10^{-4}
11	10	0	12.2000	0.00	7.2000	0.00	0.3971	0.00	7.137087	7.137083	6.0578×10^{-5}
12	10	72	10.8829	60.92	9.5150	88.25	0.1172	0.37	2.106041	2.106035	2.7153×10^{-4}
13	10	144	8.3213	135.06	12.3752	151.64	-0.3154	0.24	-5.669392	-5.669382	1.6997×10^{-4}
14	10	216	8.3213	224.94	12.3752	208.36	-0.3154	-0.24	-5.669392	-5.669382	1.6997×10^{-4}
15	10	288	10.8829	299.08	9.5150	271.75	0.1172	-0.37	2.106041	2.106035	2.7153×10^{-4}

The potentials for the translational method with truncations of $M = 5$ give relatively good results compared with the bipolar method. It is evident that at greater distances from the two cylinders the potential distribution has better convergence, as points 11 to 15 show decreased errors. For the exact same conditions but with the truncation increased to $M = 15$ the error between the two methods is substantially decreased.

Table 4.2.2: Percentage error between the potential values of the translational and bipolar boundary value methods for $a_1 = 1$ cm, $a_2 = 2$ cm, $d = 5$ cm, $q_{tot}^{(1)} = -1$ nC/m, $q_{tot}^{(2)} = 1$ nC/m, and $M = 15$

Point	r [cm]	ϕ [°]	r_1 [cm]	ϕ_1 [°]	r_2 [cm]	ϕ_2 [°]	η	ξ	u_{tot} [V]	u_{bi} [V]	% Error
1	0.25	0	2.4500	0.00	2.5500	0.00	0.2566	-3.14	4.611570	4.611570	-6.8462×10^{-7}
2	0.25	72	2.2896	5.96	2.7331	175.01	0.0777	2.90	1.397398	1.397398	-1.0175×10^{-7}
3	0.25	144	2.0031	4.21	3.0058	177.20	-0.2060	2.99	-3.702575	-3.702575	3.9939×10^{-8}
4	0.25	216	2.0031	355.79	3.0058	182.80	-0.2060	-2.99	-3.702575	-3.702575	3.9939×10^{-8}
5	0.25	288	2.2896	354.04	2.7331	184.99	0.0777	-2.90	1.397398	1.397398	-1.0174×10^{-7}
6	5	0	7.2000	0.00	2.2000	0.00	0.8281	0.00	14.885705	14.885705	-1.1418×10^{-6}
7	5	72	6.0530	51.78	4.9181	104.78	0.2131	0.72	3.831172	3.831172	1.4536×10^{-11}
8	5	144	3.4701	122.12	7.4493	156.76	-0.6180	0.50	-11.107813	-11.107813	3.5182×10^{-12}
9	5	216	3.4701	237.88	7.4493	203.24	-0.6180	-0.50	-11.107813	-11.107813	3.4383×10^{-12}
10	5	288	6.0530	308.22	4.9181	255.22	0.2131	-0.72	3.831172	3.831172	1.4617×10^{-11}
11	10	0	12.2000	0.00	7.2000	0.00	0.3971	0.00	7.137083	7.137083	3.1858×10^{-12}
12	10	72	10.8829	60.92	9.5150	88.25	0.1172	0.37	2.106035	2.106035	3.4371×10^{-12}
13	10	144	8.3213	135.06	12.3752	151.64	-0.3154	0.24	-5.669382	-5.669382	3.4466×10^{-12}
14	10	216	8.3213	224.94	12.3752	208.36	-0.3154	-0.24	-5.669382	-5.669382	3.2742×10^{-12}
15	10	288	10.8829	299.08	9.5150	271.75	0.1172	-0.37	2.106035	2.106035	3.5214×10^{-12}

4.3 Two-cylinder system in external electric field

Consider the same system in Section 4.2 but placed in an external electric field oriented along the common x -axis of the cylinders, $\mathbf{E}_0 = E_0 \mathbf{a}_x$, as shown in Figure 4.3.1. Here again, consider a complete system with the external electric field being the only contribution to the potential at infinity.

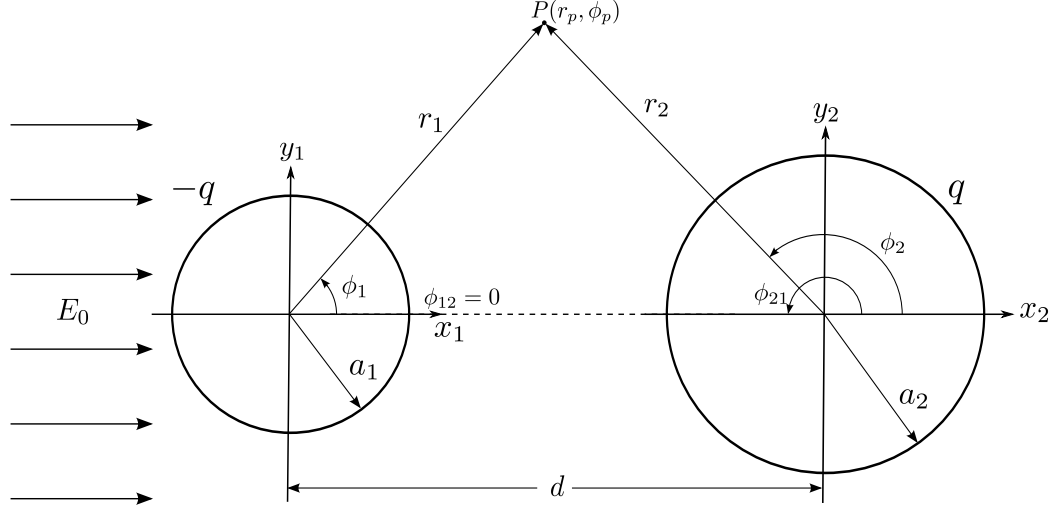


Figure 4.3.1: Two conducting cylinders in an external electric field, $\mathbf{E}_0 = E_0 \mathbf{a}_x$

The potential due to the external field, expressed in the local coordinates of each cylinder are

$$u_{ex}^{(1)} = -E_0 x_1 + C_{ex}^{(1)} = -E_0 r_1 \cos \phi_1 + C_{ex}^{(1)}, \quad (4.3.1)$$

$$u_{ex}^{(2)} = -E_0 x_2 + C_{ex}^{(2)} = -E_0 r_2 \cos \phi_2 + C_{ex}^{(2)}, \quad (4.3.2)$$

where $C_{ex}^{(1)}$ and $C_{ex}^{(2)}$ are constants of reference. Lets consider the potential produced by the external field to be C_{ex} at the origin of the global coordinate system (x, y) , see Figure 4.2.2, that is, in terms of the coordinates attached to cylinder 1 or 2 as $(r_1 = a \coth \eta_1, \phi_1 = 0)$ or $(r_2 = a \coth \eta_2, \phi_2 = \pi)$, respectively, where a , η_1 and η_2 are defined in the previous section. Note $(-a \coth \eta_1, 0)$ and $(a \coth \eta_2, 0)$ are the locations of the axes of cylinders 1 and 2, respectively, in the global coordinates. Therefore (4.3.1) and (4.3.2) yield values for the constants $C_{ex}^{(1)} = E_0 a \coth \eta_1 + C_{ex}$

and $u_C^{(2)} = -E_0 a \coth \eta_2 + C_{ex}$ giving

$$u_{ex}^{(1)}(r_1, \phi_1) = -E_0 r_1 \cos \phi_1 + E_0 a \coth \eta_1 + C_{ex}, \quad (4.3.3)$$

$$u_{ex}^{(2)}(r_2, \phi_2) = -E_0 r_2 \cos \phi_2 - E_0 a \coth \eta_2 + C_{ex}, \quad (4.3.4)$$

To apply the boundary conditions at cylinder 1 the total potential distribution must be expressed in terms of the attached coordinate system. We use the translational addition theorems to express the potential $u_2(r_2, \phi_2)$ in terms of the coordinates (r_1, ϕ_1) and the external potential $u_{ex}^{(1)}(r_1, \phi_1)$ to give

$$\begin{aligned} u_{tot}^{(1)}(r_1, \phi_1) &= u_{ex}^{(1)}(r_1, \phi_1) + u_1(r_1, \phi_1) + u_2^{(1)}(r_1, \phi_1) \\ &= -E_0 r_1 \cos \phi_1 + E_0 a \coth \eta_1 + C + A_0 \ln r_1 + B_0 \ln d \\ &+ \sum_{n=1}^{\infty} \left[A_n \left(\frac{a_1}{r_1} \right)^n + B_0 \gamma_B(n, r_1, d) \right] \cos n\phi_1 + \sum_{n=1}^{\infty} \sum_{m=0}^{\infty} B_n \tau_B(m, n, r_1, a_2, d) \cos m\phi_1. \end{aligned} \quad (4.3.5)$$

where $\gamma_B(n, r_1, d)$ and $\tau_B(m, n, r_1, d)$ are defined in (4.2.6) and $C \equiv C_A + C_B + C_{ex}$.

Applying the boundary condition $u_{tot}^{(1)}(r_1 = a_1, \phi_1) = V_1$ to (4.3.5) gives

$$\begin{aligned} V_1 &= -E_0 a_1 \cos \phi_1 + E_0 a \coth \eta_1 + C + A_0 \ln a_1 + B_0 \ln d \\ &+ \sum_{n=1}^{\infty} [A_n + B_0 \gamma_B(n, a_1, d)] \cos n\phi_1 + \sum_{n=1}^{\infty} \sum_{m=0}^{\infty} B_n \tau_B(m, n, a_1, a_2, d) \cos m\phi_1. \end{aligned} \quad (4.3.6)$$

Multiplying (4.3.6) by $\cos m\phi_1$ and integrating in ϕ_1 from 0 to 2π over all positive integral values of m gives

$$\begin{aligned} -V_1 + \sum_{n=1}^{\infty} B_n \tau_B(0, n, a_1, a_2, d) &= -C - A_0 \ln a_1 - B_0 \ln d - E_0 a \coth \eta_1, \\ A_1 + \sum_{n=1}^{\infty} B_n \tau_B(1, n, a_1, a_2, d) &= E_0 a_1 - B_0 \gamma_B(1, a_1, d), \\ A_m + \sum_{n=1}^{\infty} B_n \tau_B(m, n, a_1, a_2, d) &= -B_0 \gamma_B(m, a_1, d), \quad m = 2, 3, \dots \end{aligned} \quad (4.3.7)$$

In the same way when the total potential is expressed in terms of (r_2, ϕ_2) coordinates and the boundary condition $u_{tot}^{(2)}(r_2 = a_2, \phi_2) = V_2$ is applied at the surface of cylinder 2 yields the set of equations

$$\begin{aligned}
-V_2 + \sum_{n=1}^{\infty} A_n \tau_A(0, n, a_2, a_1, d) &= -C - B_0 \ln a_2 - A_0 \ln d + E_0 a \coth \eta_2, \\
B_1 + \sum_{n=1}^{\infty} A_n \tau_A(1, n, a_2, a_1, d) &= E_0 a_2 - A_0 \gamma_A(1, a_2, d), \\
B_m + \sum_{n=1}^{\infty} A_n \tau_A(m, n, a_2, a_1, d) &= -A_0 \gamma_A(m, a_2, d), \quad m = 2, 3, \dots,
\end{aligned} \tag{4.3.8}$$

where $\gamma_A(n, r_2, d)$ and $\tau_A(m, n, r_2, a_1, d)$ are defined in (4.2.15).

The boundary conditions, given as the charge per unit length on the conductors are then used to solve for constants A_0 and B_0 from $q_{tot}^{(1)} = -2\pi\epsilon A_0$ and $q_{tot}^{(2)} = -2\pi\epsilon B_0$, respectively. As long as the charges are equal and opposite the logarithmic potentials vanish at infinity and with $C = 0$ the only contribution to the potential at infinity will be due to the external field. Then, the constants of integration in the infinite set of equations (4.3.7) and (4.3.8), with $C = 0$, are solved for after truncating the series to a finite number $n = m = M$.

Planar bipolar coordinate solution

The two cylinder system in an external field is analyzed using the two-dimensional bipolar coordinates for comparison. The reference potential is zero at $x = 0$, i.e., the origin of the global coordinate system, thus the potential of the external field is $u_{bi}^{ex}(x, y) = -E_0 x$. The coordinate x can be expressed in (η, ξ) coordinates using the series expansion [15]

$$u_{bi}^{ex}(\eta, \xi) = \begin{cases} -E_0 a - E_0 a \sum_{n=1}^{\infty} e^{-n\eta} \cos n\xi, & \eta > 0, \\ E_0 a + E_0 a \sum_{n=1}^{\infty} e^{n\eta} \cos n\xi, & \eta < 0. \end{cases} \tag{4.3.9}$$

Note that the series expansions are not valid at $\eta = 0$ and as $\eta \rightarrow 0$ greater numbers of terms must be taken in the series for it to converge. The total potential distribution outside the two cylinders is given by

$$u_{bi}(\eta, \xi) = u_{bi}^{ex}(\eta, \xi) + B_0\eta + \sum_{n=1}^{\infty} B_n \sinh n\eta \cos n\xi, \quad (4.3.10)$$

where we set $A_0 = 0$ and $B_n = -A_n$ in (4.2.26) for the contribution to the potential from the cylinders to vanish at infinity. Solving for the constants in (4.3.10) yields the potential distribution

$$u_{bi}(\eta, \xi)_{\eta < 0} = E_0a + 2E_0a \sum_{n=1}^{\infty} e^{-n\eta} \cos n\xi - \frac{q_{tot}^{(1)}}{2\pi\epsilon} \eta + 2E_0a \sum_{n=1}^{\infty} \frac{e^{-n\eta_1}}{\sinh n\eta_1} \sinh n\eta \cos n\xi, \quad (4.3.11)$$

for $\eta < 0$ and

$$u_{bi}(\eta, \xi)_{\eta > 0} = -E_0a - 2E_0a \sum_{n=1}^{\infty} e^{n\eta} \cos n\xi + \frac{q_{tot}^{(2)}}{2\pi\epsilon} \eta + 2E_0a \sum_{n=1}^{\infty} \frac{e^{-n\eta_2}}{\sinh n\eta_2} \sinh n\eta \cos n\xi, \quad (4.3.12)$$

for $\eta > 0$.

Numerical results

Table 4.3.1 for $a_1 = 1$ cm, $a_2 = 2$ cm, $d = 5$ cm, $q_{tot}^{(1)} = -1$ nC/m, $q_{tot}^{(2)} = 1$ nC/m and $E_0 = 10$ V/m show the percentage error between the potentials from the translational and bipolar methods at various points for truncation of $M = 25$. The points are chosen along circles of radii 0.25 cm, 5 cm and 10 cm taken with respect to the global coordinates (x, y) .

The results show that the potentials calculated from the two methods are in relatively good agreement. Note that the potentials obtained from the bipolar method for points approaching the $\eta = 0$ axis begin to diverge because our series expansion for the uniform field diverges as $\eta \rightarrow \infty$, as can be seen for points 3, 4, 8, 9, 13, 14, 18, 19, 23, 24, 28 and 29 which all have higher percentage errors. For these points the calculated potentials from the translational method are better

approximations.

Table 4.3.1: Percentage error between the potential values of the translational and bipolar boundary value methods for $a_1 = 1$ cm, $a_2 = 2$ cm, $d = 5$ cm, $q_{tot}^{(1)} = -1$ nC/m, $q_{tot}^{(2)} = 1$ nC/m, $E_0 = 10$ V/m and $M = 25$

Point	r [cm]	ϕ [°]	r_1 [cm]	ϕ_1 [°]	r_2 [cm]	ϕ_2 [°]	η	ξ	u_{tot} [V]	u_{bi} [V]	% Error
1	0.25	0	2.4500	0.00	2.5500	180.00	0.2566	-3.14	4.467250	4.553559	-1.8954
2	0.25	36	2.4067	3.50	2.6019	176.76	0.2060	2.99	3.567551	3.655995	-2.4191
3	0.25	72	2.2896	5.96	2.7331	175.01	0.0777	2.90	1.285695	1.379815	-6.8212
4	0.25	108	2.1360	6.39	2.8871	175.28	-0.0777	2.90	-1.481503	-1.386378	6.8614
5	0.25	144	2.0031	4.21	3.0058	177.20	-0.2060	2.99	-3.764624	-3.673469	2.4814
6	0.25	180	1.9500	0.00	3.0500	180.00	-0.2566	3.14	-4.665113	-4.575388	1.9610
7	0.25	216	2.0031	355.79	3.0058	182.80	-0.2060	3.29	-3.764624	-3.673469	2.4814
8	0.25	252	2.1360	353.61	2.8871	184.72	-0.0777	3.38	-1.481503	-1.386378	6.8614
9	0.25	288	2.2896	354.04	2.7331	184.99	0.0777	3.38	1.285695	1.379815	-6.8212
10	0.25	324	2.4067	356.50	2.6019	183.24	0.2060	3.29	3.567551	3.655995	-2.4191
11	5	0	7.2000	0.00	2.2000	0.00	0.8281	0.00	14.590165	14.648429	-0.3977
12	5	36	6.9021	25.20	3.1918	67.04	0.6180	0.50	10.770614	10.819361	-0.4505
13	5	72	6.0530	51.78	4.9181	104.78	0.2131	0.72	3.667479	3.702615	-0.9490
14	5	108	4.8002	82.16	6.4415	132.42	-0.2131	0.72	-3.717281	-3.684491	0.8899
15	5	144	3.4701	122.12	7.4493	156.76	-0.6180	0.50	-10.773232	-10.733350	0.3716
16	5	180	2.8000	180.00	7.8000	180.00	-0.8281	0.00	-14.481101	-14.437904	0.2992
17	5	216	3.4701	237.88	7.4493	203.24	-0.6180	5.78	-10.773232	-10.733350	0.3716
18	5	252	4.8002	277.84	6.4415	227.58	-0.2131	5.56	-3.717281	-3.684491	0.8899
19	5	288	6.0530	308.22	4.9181	255.22	0.2131	5.56	3.667479	3.702615	-0.9490
20	5	324	6.9021	334.80	3.1918	292.96	0.6180	5.78	10.770614	10.819361	-0.4505
21	10	0	12.2000	0.00	7.2000	0.00	0.3971	0.00	6.204628	6.236714	-0.5145
22	10	36	11.8506	29.74	7.9079	48.01	0.3154	0.24	4.904407	4.932395	-0.5674
23	10	72	10.8829	60.92	9.5150	88.25	0.1172	0.37	1.803740	1.820518	-0.9216
24	10	108	9.5521	95.35	11.1868	121.77	-0.1172	0.37	-1.817853	-1.802766	0.8369
25	10	144	8.3213	135.06	12.3752	151.64	-0.3154	0.24	-4.900172	-4.877071	0.4737
26	10	180	7.8000	180.00	12.8000	180.00	-0.3971	0.00	-6.184869	-6.159240	0.4161
27	10	216	8.3213	224.94	12.3752	208.36	-0.3154	6.05	-4.900172	-4.877071	0.4737
28	10	252	9.5521	264.65	11.1868	238.23	-0.1172	5.91	-1.817853	-1.802766	0.8369
29	10	288	10.8829	299.08	9.5150	271.75	0.1172	5.91	1.803740	1.820518	-0.9216
30	10	324	11.8506	330.26	7.9079	311.99	0.3154	6.05	4.904407	4.932395	-0.5674

4.4 Three-cylinder system

Consider three conducting cylinders of radii a_1 , a_2 and a_3 with charges per unit length of $q_{tot}^{(1)}$, $q_{tot}^{(2)}$ and $q_{tot}^{(3)}$, respectively, placed on them. The separation distances between the axes of the cylinders, d_{12} , d_{13} and d_{23} , are identified in the Figure 4.4.1. The medium outside the cylinders is homogeneous, with permittivity ε . The potential is found for a complete system, such that the potential vanishes at infinity.

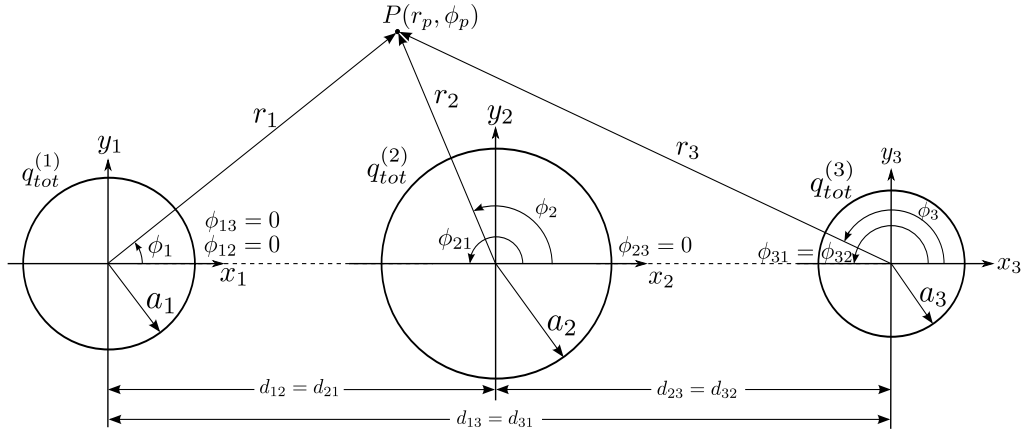


Figure 4.4.1: Three conducting cylinder system with given charges

The harmonic potentials of the three cylinders can be expressed in their attached coordinate systems as

$$u_1(r_1, \phi_1) = C_A + A_0 \ln r_1 + \sum_{n=1}^{\infty} A_n \left(\frac{a_1}{r_1} \right)^n \cos n\phi_1, \quad r_1 > a_1, \quad (4.4.1)$$

$$u_2(r_2, \phi_2) = C_B + B_0 \ln r_2 + \sum_{n=1}^{\infty} B_n \left(\frac{a_2}{r_2} \right)^n \cos n\phi_2, \quad r_2 > a_2, \quad (4.4.2)$$

$$u_3(r_3, \phi_3) = C_C + C_0 \ln r_3 + \sum_{n=1}^{\infty} C_n \left(\frac{a_3}{r_3} \right)^n \cos n\phi_3, \quad r_3 > a_3, \quad (4.4.3)$$

For the complete system, the sum of the charge per unit length of all the conductors must equal zero, i.e., $q_{tot}^{(1)} + q_{tot}^{(2)} + q_{tot}^{(3)} = 0$. The total charge per unit length on each of the cylinders is (see Section 4.5)

$$q_{tot}^{(1)} = -2\pi\epsilon A_0, \quad q_{tot}^{(2)} = -2\pi\epsilon B_0, \quad q_{tot}^{(3)} = -2\pi\epsilon C_0. \quad (4.4.4)$$

Therefore $A_0 + B_0 + C_0 = 0$ and, as long as, the condition is satisfied this ensures the logarithmic potentials disappear at infinity. Note as the radial distance $r \rightarrow \infty$ the coordinates are effectively equivalent $r_1 \equiv r_2 \equiv r_3 \equiv r$, therefore for the potential to vanish at infinity, we have

$$\begin{aligned} \lim_{r \rightarrow \infty} u_{tot}(r, \phi) &= \lim_{r \rightarrow \infty} \{u_1(r, \phi) + u_2(r, \phi) + u_3(r, \phi)\} = 0 \\ &= \lim_{r \rightarrow \infty} \{C + (A_0 + B_0 + C_0) \ln r\} = 0, \end{aligned}$$

where the constant is set to $C \equiv C_A + C_B + C_C = 0$. As shown in detail for the two cylinder case, using the applicable translational addition theorems for (4.4.1), (4.4.2) and (4.4.3) and imposing the boundary conditions at each of the three cylinders, i.e., the fixed charges on cylinders 1, 2 and 3 results in the following sets of linear equations. For cylinder 1

$$-A_0 \ln a_1 - B_0 \ln d_{21} - C_0 \ln d_{31} = -V_1 \quad (4.4.5)$$

$$+ \sum_{n=1}^{\infty} \left[B_n \tau_B^{(1)}(0, n, a_1, a_2, d_{21}) + C_n \tau_C^{(1)}(0, n, a_1, a_3, d_{31}) \right], \quad m = 0,$$

$$-B_0 \gamma_B^{(1)}(m, a_1, d_{21}) - C_0 \gamma_C^{(1)}(m, a_1, d_{31}) = A_m \quad (4.4.6)$$

$$+ \sum_{n=1}^{\infty} \left[B_n \tau_B^{(1)}(m, n, a_1, a_2, d_{21}) + C_n \tau_C^{(1)}(m, n, a_1, a_3, d_{31}) \right], \quad m = 1, 2, \dots,$$

where

$$\tau_B^{(1)}(m, n, r_1, a_2, d_{21}) = \frac{(-1)^n (n+m-1)!}{m!(n-1)!} \left(\frac{a_2}{d_{21}} \right)^n \left(\frac{r_1}{d_{21}} \right)^m, \quad (4.4.7a)$$

$$\tau_C^{(1)}(m, n, r_1, a_3, d_{31}) = \frac{(-1)^n (n+m-1)!}{m!(n-1)!} \left(\frac{a_3}{d_{31}} \right)^n \left(\frac{r_1}{d_{31}} \right)^m, \quad (4.4.7b)$$

$$\gamma_B^{(1)}(n, r_1, d_{21}) = -\frac{1}{n} \left(\frac{r_1}{d_{21}} \right)^n, \quad (4.4.7c)$$

$$\gamma_C^{(1)}(n, r_1, d_{31}) = -\frac{1}{n} \left(\frac{r_1}{d_{31}} \right)^n. \quad (4.4.7d)$$

For cylinder 2, the infinite set of equations are

$$-A_0 \ln d_{12} - B_0 \ln a_2 - C_0 \ln d_{32} = -V_2 \quad (4.4.8)$$

$$+ \sum_{n=1}^{\infty} \left[A_n \tau_A^{(2)}(0, n, a_2, a_1, d_{12}) + C_n \tau_C^{(2)}(0, n, a_2, a_3, d_{32}) \right], \quad m = 0,$$

$$-A_0 \gamma_A^{(2)}(m, a_2, d_{12}) - C_0 \gamma_C^{(2)}(m, a_2, d_{32}) = B_m \quad (4.4.9)$$

$$+ \sum_{n=1}^{\infty} \left[A_n \tau_A^{(2)}(m, n, a_2, a_1, d_{12}) + C_n \tau_C^{(2)}(m, n, a_2, a_3, d_{32}) \right], \quad m = 1, 2, \dots,$$

where

$$\tau_A^{(2)}(m, n, r_2, a_1, d_{12}) = \frac{(-1)^m (n+m-1)!}{m!(n-1)!} \left(\frac{a_1}{d_{12}}\right)^n \left(\frac{r_2}{d_{12}}\right)^m, \quad (4.4.10a)$$

$$\tau_C^{(2)}(m, n, r_2, a_3, d_{32}) = \frac{(-1)^n (n+m-1)!}{m!(n-1)!} \left(\frac{a_3}{d_{32}}\right)^n \left(\frac{r_2}{d_{32}}\right)^m, \quad (4.4.10b)$$

$$\gamma_A^{(2)}(n, r_2, d_{12}) = -\frac{(-1)^n}{n} \left(\frac{r_2}{d_{12}}\right)^n, \quad (4.4.10c)$$

$$\gamma_C^{(2)}(n, r_2, d_{32}) = -\frac{1}{n} \left(\frac{r_2}{d_{32}}\right)^n. \quad (4.4.10d)$$

For cylinder 3, we have

$$-A_0 \ln d_{13} - B_0 \ln d_{23} - C_0 \ln a_3 = -V_3 \quad (4.4.11)$$

$$+ \sum_{n=1}^{\infty} \left[A_n \tau_A^{(3)}(0, n, a_3, a_1, d_{13}) + B_n \tau_B^{(3)}(0, n, a_3, a_2, d_{23}) \right], \quad m = 0,$$

$$-A_0 \gamma_A^{(3)}(m, a_3, d_{13}) - B_0 \gamma_B^{(3)}(m, a_3, d_{23}) = C_m \quad (4.4.12)$$

$$+ \sum_{n=1}^{\infty} \left[A_n \tau_A^{(3)}(m, n, a_3, a_1, d_{13}) + B_n \tau_B^{(3)}(m, n, a_3, a_2, d_{23}) \right], \quad m = 1, 2, \dots,$$

where

$$\tau_A^{(3)}(m, n, r_3, a_1, d_{13}) = \frac{(-1)^m (n+m-1)!}{m!(n-1)!} \left(\frac{a_1}{d_{13}}\right)^n \left(\frac{r_3}{d_{13}}\right)^m, \quad (4.4.13a)$$

$$\tau_B^{(3)}(m, n, r_3, a_2, d_{23}) = \frac{(-1)^m (n+m-1)!}{m!(n-1)!} \left(\frac{a_2}{d_{23}}\right)^n \left(\frac{r_3}{d_{23}}\right)^m, \quad (4.4.13b)$$

$$\gamma_A^{(3)}(n, r_3, d_{13}) = -\frac{(-1)^n}{n} \left(\frac{r_3}{d_{13}}\right)^n, \quad (4.4.13c)$$

$$\gamma_B^{(3)}(n, r_3, d_{23}) = -\frac{(-1)^n}{n} \left(\frac{r_3}{d_{23}}\right)^n. \quad (4.4.13d)$$

Equations (4.4.5), (4.4.6), (4.4.8), (4.4.9), (4.4.11), (4.4.12) and (4.4.4) constitute the set of infinite equations which are solved for simultaneously using Gaussian elimination for the constants of integration $A_1, B_1, C_1, A_2, B_2, C_2, \dots$, and the unknown potentials V_1, V_2 and V_3 . To obtain numerical results the infinite series are truncated to a finite number of terms $n = m = M$.

Numerical results are plotted for the case $a_1 = 1$ cm, $a_2 = 2$ cm, $a_3 = 3$ cm, $d_{12} = 5$

cm, $d_{23} = 7$ cm, $d_{13} = 12$ cm, $q_{tot}^{(1)} = -2$ nC/m, $q_{tot}^{(2)} = 1$ nC/m, $q_{tot}^{(3)} = 1$ nC/m, and truncation of $M = 15$ in Figure 4.4.2. The plots show how the potential varies radially with respect to coordinate r_1 over the range $0 < r_1 < 80$ cm along the lines defined by the angles $\phi_1 = 0, \pi/6, \pi/4, \pi/3$ and $\pi/2$. The results are as expected the potential starts to decrease as $r_1 \rightarrow \infty$ and the calculated potentials on the cylinders are $V_1 = -63.9160$ V, $V_2 = 10.7380$ V and $V_3 = 28.2765$ V.

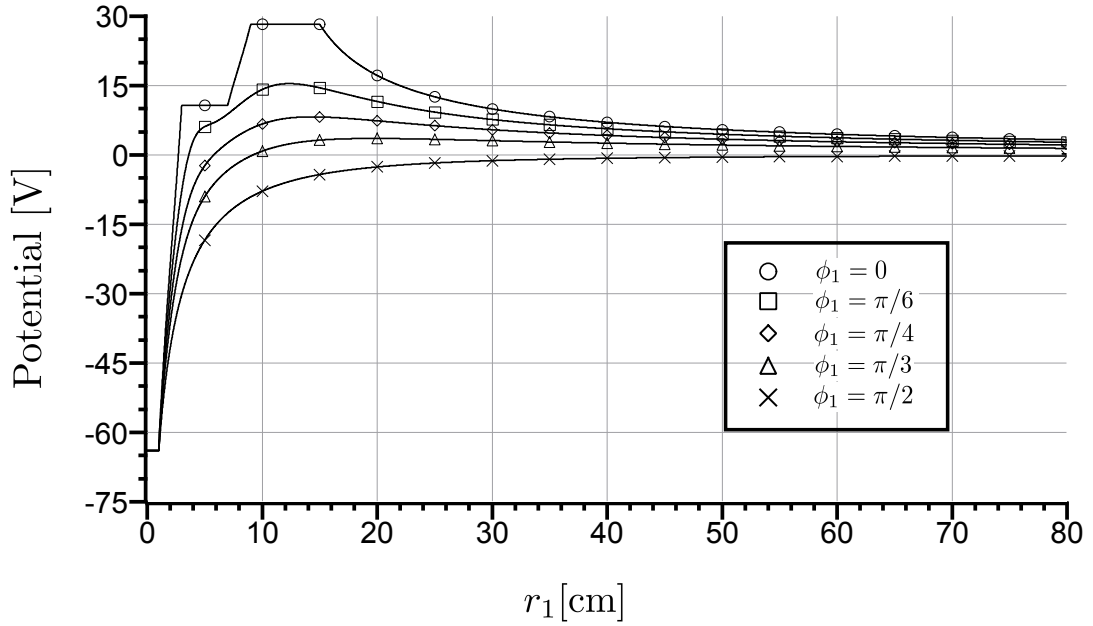


Figure 4.4.2: Potential distribution with respect to r_1 for angles $\phi_1 = 0, \pi/6, \pi/4, \pi/3$ and $\pi/2$, when $a_1 = 1$ cm, $a_2 = 2$ cm, $a_3 = 3$ cm, $d_{12} = 5$ cm, $d_{23} = 7$ cm, $d_{13} = 12$ cm, $q_{tot}^{(1)} = -2$ nC/m, $q_{tot}^{(2)} = 1$ nC/m, $q_{tot}^{(3)} = 1$ nC/m and $M = 15$

4.5 Three-cylinder system in external electric field

Consider the three-cylinder system in Figure 4.5.1 placed in an external electric field oriented along the common x -axis, $\mathbf{E}_0 = E_0 \mathbf{a}_x$, with the potentials on the surfaces of the cylinders as unknowns. The electric field is determined when the total charge per unit length of each of the cylinders is forced to be zero, that is $q_{tot}^{(1)} = q_{tot}^{(2)} = q_{tot}^{(3)} = 0$, with only the external electric field remaining at infinity. The surrounding medium is homogeneous, with permittivity ϵ .

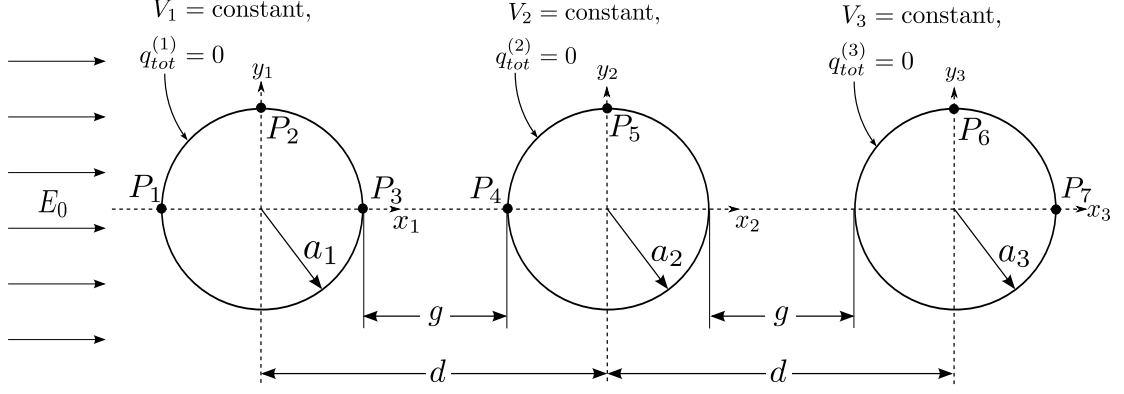


Figure 4.5.1: Three conducting cylinders in an external field, $\mathbf{E}_0 = E_0 \mathbf{a}_x$

The total charge per unit length on the first cylinder is calculated by

$$q_{tot}^{(1)} = -\varepsilon \int_0^{2\pi} \frac{\partial u_{tot}^{(1)}}{\partial r_1} r_1 d\phi_1 \Big|_{r_1=a_1} \quad (4.5.1)$$

where $u_{tot}^{(1)}(r_1, \phi_1)$ is, after performing the translations of $u_2(r_2, \phi_2)$ and $u_3(r_3, \phi_3)$ to the coordinates (r_1, ϕ_1) ,

$$\begin{aligned} u_{tot}^{(1)}(r_1, \phi_1) &= u_{ex}^{(1)}(r_1, \phi_1) + u_1(r_1, \phi_1) + u_2^{(1)}(r_1, \phi_1) + u_3^{(1)}(r_1, \phi_1) \\ u_{tot}^{(1)}(r_1, \phi_1) &= -E_0 r_1 \cos \phi_1 + C + A_0 \ln r_1 + B_0 \ln d_{21} + C_0 \ln d_{31} \\ &+ \sum_{n=1}^{\infty} \left[A_n \left(\frac{a_1}{r_1} \right)^n + B_0 \gamma_B^{(1)}(n, r_1, d_{21}) + C_0 \gamma_C^{(1)}(n, r_1, d_{31}) \right] \cos n\phi_1 \\ &+ \sum_{n=1}^{\infty} \sum_{m=0}^{\infty} \left[B_n \tau_B^{(1)}(m, n, r_1, a_2, d_{21}) + C_n \tau_C^{(1)}(m, n, r_1, a_3, d_{31}) \right] \cos m\phi_1, \end{aligned} \quad (4.5.2)$$

with $\gamma_B^{(1)}(n, r_1, d_{21})$, $\gamma_C^{(1)}(n, r_1, d_{31})$, $\tau_B^{(1)}(m, n, r_1, a_2, d_{21})$ and $\tau_C^{(1)}(m, n, r_1, a_3, d_{31})$ defined in (4.4.7) and $C \equiv C_A + C_B + C_C + C_{ex} = 0$. Taking the derivative $\frac{\partial u_{tot}^{(1)}}{\partial r_1}$ and substituting back into (4.5.1) gives

$$q_{tot}^{(1)} = -2\pi\varepsilon A_0.$$

Applying the boundary condition, $q_{tot}^{(1)} = 0$, at the surface of cylinder 1 yields $A_0 = 0$. Similarly, the charge per unit length on cylinders 2 and 3 are $q_{tot}^{(2)} = -2\pi\varepsilon B_0$ and

$q_{tot}^{(3)} = -2\pi\epsilon C_0$, which yield $B_0 = 0$ and $C_0 = 0$, respectively.

Using the orthogonal properties of the trigonometric functions at the surface of cylinder 1, $r_1 = a_1$ gives the set of infinite linear equations

$$0 = -V_1 + \sum_{n=1}^{\infty} \left[B_n \tau_B^{(1)}(0, n, a_1, a_2, d_{21}) + C_n \tau_C^{(1)}(0, n, a_1, a_3, d_{31}) \right], \quad (4.5.3)$$

$$E_0 a_1 = A_1 + \sum_{n=1}^{\infty} \left[B_n \tau_B^{(1)}(1, n, a_1, a_2, d_{21}) + C_n \tau_C^{(1)}(1, n, a_1, a_3, d_{31}) \right], \quad (4.5.4)$$

$$0 = A_m + \sum_{n=1}^{\infty} \left[B_n \tau_B^{(1)}(m, n, a_1, a_2, d_{21}) + C_n \tau_C^{(1)}(m, n, a_1, a_3, d_{31}) \right], \quad (4.5.5)$$

where $m = 2, 3, \dots$. Similarly, the set of infinite equations that result from cylinders 2 and 3 are

$$E_0 d_{12} = -V_2 + \sum_{n=1}^{\infty} \left[A_n \tau_A^{(2)}(0, n, a_2, a_1, d_{12}) + C_n \tau_C^{(2)}(0, n, a_2, a_3, d_{32}) \right], \quad (4.5.6)$$

$$E_0 a_2 = B_1 + \sum_{n=1}^{\infty} \left[A_n \tau_A^{(2)}(1, n, a_2, a_1, d_{12}) + C_n \tau_C^{(2)}(1, n, a_2, a_3, d_{32}) \right], \quad (4.5.7)$$

$$0 = B_m + \sum_{n=1}^{\infty} \left[A_n \tau_A^{(2)}(m, n, a_2, a_1, d_{12}) + C_n \tau_C^{(2)}(m, n, a_2, a_3, d_{32}) \right], \quad (4.5.8)$$

$$E_0 d_{13} = -V_3 + \sum_{n=1}^{\infty} \left[A_n \tau_A^{(3)}(0, n, a_3, a_1, d_{13}) + C_n \tau_B^{(3)}(0, n, a_3, a_2, d_{23}) \right], \quad (4.5.9)$$

$$E_0 a_3 = C_1 + \sum_{n=1}^{\infty} \left[A_n \tau_A^{(3)}(1, n, a_3, a_1, d_{13}) + C_n \tau_B^{(3)}(1, n, a_3, a_2, d_{23}) \right], \quad (4.5.10)$$

$$0 = C_m + \sum_{n=1}^{\infty} \left[A_n \tau_A^{(3)}(m, n, a_3, a_1, d_{13}) + C_n \tau_B^{(3)}(m, n, a_3, a_2, d_{23}) \right], \quad (4.5.11)$$

where the notations $\tau_A^{(2)}(m, n, r_2, a_1, d_{12})$, $\tau_C^{(2)}(m, n, r_2, a_3, d_{32})$, $\tau_A^{(3)}(m, n, r_3, a_1, d_{13})$ and $\tau_B^{(3)}(m, n, r_3, a_2, d_{23})$ are defined in (4.4.10) and (4.4.13).

Like before, the constants of integration are determined by truncating the infinite set of linear equations to $n = m = M$ and then using Gaussian elimination to solve the truncated system. Once the constants are determined the electric field is

found from

$$\begin{aligned}\mathbf{E} &= -\nabla u_{tot}(r_1, \phi_1 | r_2, \phi_2 | r_3, \phi_3) \\ &= E_0 \mathbf{a}_x - \left[\nabla_1 u_1(r_1, \phi_1) + \nabla_2 u_2(r_2, \phi_2) + \nabla_3 u_3(r_3, \phi_3) \right],\end{aligned}$$

where the subscripts the ∇ operator indicate that the gradient is taken with respect to the respective coordinate system. The electric field components are found to be

$$\begin{aligned}E_x &= E_0 + \sum_{n=1}^{\infty} \left[A_n \left(\frac{n}{r_1} \right) \left(\frac{a_1}{r_1} \right)^n \cos(n+1)\phi_1 + B_n \left(\frac{n}{r_2} \right) \left(\frac{a_2}{r_2} \right)^n \cos(n+1)\phi_2 \right. \\ &\quad \left. + C_n \left(\frac{n}{r_3} \right) \left(\frac{a_3}{r_3} \right)^n \cos(n+1)\phi_3 \right], \\ E_y &= \sum_{n=1}^{\infty} \left[A_n \left(\frac{n}{r_1} \right) \left(\frac{a_1}{r_1} \right)^n \sin(n+1)\phi_1 + B_n \left(\frac{n}{r_2} \right) \left(\frac{a_2}{r_2} \right)^n \sin(n+1)\phi_2 \right. \\ &\quad \left. + C_n \left(\frac{n}{r_3} \right) \left(\frac{a_3}{r_3} \right)^n \sin(n+1)\phi_3 \right].\end{aligned}$$

Numerical results are generated for the relative values of the electric field components at various points, shown in Figure 4.5.1, for the three cylinder systems with $a_1 = a_2 = a_3 \equiv a$, $d_{12} = d_{23} = 2a + g$ and $d_{13} = 2d_{23}$ for some different g/a ratios, that is, for different gap distances, in Table 4.5.1.

Table 4.5.1: Relative electric field components at selected points on the cylinders in Figure 4.5.1 for different relative gaps g/a , when $\mathbf{E}_0 = E_0 \mathbf{a}_x$ and zero total charge of the cylinders

Point	Fields	Gap ratios (g/a)						
		1.0	0.5	0.1	0.05	0.01	0.005	0.001
P_1	E_x/E_0	2.2082	2.3140	2.5448	2.6196	2.7152	2.7238	2.7179
	E_y/E_0	0.0000	0.0000	0.0000	0.0000	0.0000	0.0000	0.0000
P_2	E_x/E_0	0.0000	0.0000	0.0000	-0.0007	-0.0224	-0.0445	-0.0875
	E_y/E_0	-0.1754	0.3256	-0.6980	-0.8241	-1.0352	-1.1030	-1.1978
P_3	E_x/E_0	2.7436	3.5679	7.7208	11.0076	23.8160	30.5329	41.2069
	E_y/E_0	0.0000	0.0000	0.0000	0.0000	0.0000	0.0000	0.0000
P_4	E_x/E_0	2.7734	3.5802	7.7208	11.0072	23.8114	30.5280	41.2048
	E_y/E_0	0.0000	0.0000	0.0000	0.0000	0.0000	0.0000	0.0000
P_5	E_x/E_0	0.0000	0.0000	-0.0001	-0.0014	-0.0455	-0.0904	-0.1781
	E_y/E_0	0.0000	0.0000	0.0000	0.0000	0.0000	0.0000	0.0000
P_6	E_x/E_0	0.0000	0.0000	0.0000	-0.0007	-0.0224	-0.0445	-0.0875
	E_y/E_0	0.1754	0.3256	0.6980	0.8241	1.0352	1.1030	1.1978
P_7	E_x/E_0	2.2082	2.3140	2.5448	2.6196	2.7152	2.7238	2.7179
	E_y/E_0	0.0000	0.0000	0.0000	0.0000	0.0000	0.0000	0.0000

The potentials on each of the cylinders changes depending on the gap size as shown in Table 4.5.2.

Table 4.5.2: Potential on each cylinder in Figure 4.5.1 for different relative gaps g/a , when $\mathbf{E}_0 = E_0 \mathbf{a}_x$ and zero total charge of the cylinders

Cylinder Potential [V]	Gap ratios (g/a)						
	1.0	0.5	0.1	0.05	0.01	0.005	0.001
V_1	-0.1556	-0.2121	-0.3351	-0.3759	-0.4395	-0.4558	-0.4750
V_2	-0.7500	-0.6250	-0.5250	-0.5125	-0.5025	-0.5013	-0.5003
V_3	-1.3444	-1.0379	-0.7149	-0.6491	-0.5655	-0.5467	-0.5255

Let now the direction of the electric field be oriented in the y -direction, $\mathbf{E}_0 = E_0 \mathbf{a}_y$, for the same geometry in Figure 4.5.1. The harmonic potential of each cylinder expressed in its attached coordinate system are, then

$$u_1(r_1, \phi_1) = C_A + \sum_{n=1}^{\infty} A_n \left(\frac{a_1}{r_1} \right)^n \sin n\phi_1, \quad r_1 > a_1, \quad (4.5.12)$$

$$u_2(r_2, \phi_2) = C_B + \sum_{n=1}^{\infty} B_n \left(\frac{a_2}{r_2} \right)^n \sin n\phi_2, \quad r_2 > a_2, \quad (4.5.13)$$

$$u_3(r_3, \phi_3) = C_C + \sum_{n=1}^{\infty} C_n \left(\frac{a_3}{r_3} \right)^n \sin n\phi_3, \quad r_3 > a_3. \quad (4.5.14)$$

The $\cos n\phi_p$ functions can be excluded from the solution because the field is directed only in the y -direction and, since $A_0 = B_0 = C_0 = 0$, the $\cos n\phi_p$ terms from the translations of the $\ln r_p$ function disappear. Thus the set of linear equations that is to be solved for, with a zero potential at infinity, is

$$0 = -V_1 - \sum_{n=1}^{\infty} \left[B_n \tau_B^{(1)}(0, n, a_1, a_2, d_{21}) + C_n \tau_C^{(1)}(0, n, a_1, a_3, d_{31}) \right], \quad (4.5.15)$$

$$E_0 a_1 = A_1 - \sum_{n=1}^{\infty} \left[B_n \tau_B^{(1)}(1, n, a_1, a_2, d_{21}) + C_n \tau_C^{(1)}(1, n, a_1, a_3, d_{31}) \right], \quad (4.5.16)$$

$$0 = A_m - \sum_{n=1}^{\infty} \left[B_n \tau_B^{(1)}(m, n, a_1, a_2, d_{21}) + C_n \tau_C^{(1)}(m, n, a_1, a_3, d_{31}) \right], \quad (4.5.17)$$

$$0 = -V_2 - \sum_{n=1}^{\infty} \left[A_n \tau_A^{(2)}(0, n, a_2, a_1, d_{12}) + C_n \tau_C^{(2)}(0, n, a_2, a_3, d_{32}) \right], \quad (4.5.18)$$

$$E_0 a_2 = B_1 - \sum_{n=1}^{\infty} \left[A_n \tau_A^{(2)}(1, n, a_2, a_1, d_{12}) + C_n \tau_C^{(2)}(1, n, a_2, a_3, d_{32}) \right], \quad (4.5.19)$$

$$0 = B_m - \sum_{n=1}^{\infty} \left[A_n \tau_A^{(2)}(m, n, a_2, a_1, d_{12}) + C_n \tau_C^{(2)}(m, n, a_2, a_3, d_{32}) \right], \quad (4.5.20)$$

$$0 = -V_3 - \sum_{n=1}^{\infty} \left[A_n \tau_A^{(3)}(0, n, a_3, a_1, d_{13}) + B_n \tau_B^{(3)}(0, n, a_3, a_2, d_{23}) \right], \quad (4.5.21)$$

$$E_0 a_3 = C_1 - \sum_{n=1}^{\infty} \left[A_n \tau_A^{(3)}(1, n, a_3, a_1, d_{13}) + B_n \tau_B^{(3)}(1, n, a_3, a_2, d_{23}) \right], \quad (4.5.22)$$

$$0 = C_m - \sum_{n=1}^{\infty} \left[A_n \tau_A^{(3)}(m, n, a_3, a_1, d_{13}) + B_n \tau_B^{(3)}(m, n, a_3, a_2, d_{23}) \right]. \quad (4.5.23)$$

The constants of integration and the potentials V_1 , V_2 and V_3 are solved for by first truncating the infinite set of equations and, then, using Gaussian elimination to solve the system. The electric field components are found to be

$$\begin{aligned} E_x &= \sum_{n=1}^{\infty} \left[A_n \left(\frac{n}{r_1} \right) \left(\frac{a_1}{r_1} \right)^n \sin(n+1)\phi_1 + B_n \left(\frac{n}{r_2} \right) \left(\frac{a_2}{r_2} \right)^n \sin(n+1)\phi_2 \right. \\ &\quad \left. + C_n \left(\frac{n}{r_3} \right) \left(\frac{a_3}{r_3} \right)^n \sin(n+1)\phi_3 \right], \\ E_y &= E_0 - \sum_{n=1}^{\infty} \left[A_n \left(\frac{n}{r_1} \right) \left(\frac{a_1}{r_1} \right)^n \cos(n+1)\phi_1 + B_n \left(\frac{n}{r_2} \right) \left(\frac{a_2}{r_2} \right)^n \cos(n+1)\phi_2 \right. \\ &\quad \left. + C_n \left(\frac{n}{r_3} \right) \left(\frac{a_3}{r_3} \right)^n \cos(n+1)\phi_3 \right]. \end{aligned}$$

Numerical results are generated for the relative values of the electric field components, for the different gap distances, at the same points, but only P_2 , P_5 and P_6 are shown in Table 4.5.3 because the fields at the other points are zero.

Table 4.5.3: Relative electric field components at selected points on the cylinders in Figure 4.5.1 for different gap ratios g/a , when $\mathbf{E}_0 = E_0\mathbf{a}_y$ and no charge on the cylinders

Point	Fields	Gap ratios (g/a)						
		1.0	0.5	0.1	0.05	0.01	0.005	0.001
P_2	E_x/E_0	0.0000	0.0000	0.0000	0.0000	0.0000	0.0000	0.0000
	E_y/E_0	1.8262	1.7924	1.7650	1.7617	1.7590	1.7587	1.7584
P_5	E_x/E_0	0.0000	0.0000	0.0000	0.0000	0.0000	0.0000	0.0000
	E_y/E_0	1.7214	1.6688	1.6276	1.6227	1.6189	1.6184	1.6180
P_6	E_x/E_0	0.0000	0.0000	0.0000	0.0000	0.0000	0.0000	0.0000
	E_y/E_0	1.8262	1.7924	1.7650	1.7617	1.7590	1.7587	1.7584

The potential on each of the cylinders for the different gap sizes is shown in Table 4.5.4.

Table 4.5.4: Induced potential on each cylinder in Figure 4.5.1 for different relative gaps g/a , when $\mathbf{E}_0 = E_0\mathbf{a}_y$ and zero total charge of the cylinders

Cylinder Potential [V]	Gap ratios (g/a)						
	1.0	0.5	0.1	0.05	0.01	0.005	0.001
V_1	0.1039	0.1158	0.1260	0.1272	0.1283	0.1284	0.1285
V_2	0.0000	0.0000	0.0000	0.0000	0.0000	0.0000	0.0000
V_3	-0.1039	-0.1158	-0.1260	-0.1272	-0.1283	-0.1284	-0.1285

Chapter 5

Application of the addition theorems to the solution of electrostatic fields in systems of parallel cylinders with arbitrary axis locations

In the previous chapter, applications of the translational addition theorems have been illustrated for systems of parallel cylinders with axes in the same plane, which simplified the expressions for the potential distributions. For problems that do not exhibit any symmetry about the axes, the general solution of Laplace's equation for each cylinder expressed in its attached coordinate system, normalized to its respective radius a_q , becomes

$$u_q(r_q, \phi_q) = C_A + A_0 \ln r_q + \sum_{n=1}^{\infty} \left[A_n^C \left(\frac{a_q}{r_q} \right)^n \cos n\phi_q + A_n^S \left(\frac{a_q}{r_q} \right)^n \sin n\phi_q \right]. \quad (5.0.1)$$

5.1 Two-cylinder system arbitrarily located in the system of coordinates

Two circular cylinders outside each other, of radii a_1 and a_2 are charged to $-q$ and q , respectively. The separation distance between the centres of the two cylinders is $d_{12} = d_{21}$, as shown in Figure 5.1.1. The system of cylinders being complete, let the potential vanish at infinity. Consider the surrounding medium to be homogeneous,

with permittivity ε . The expressions for the total potential distribution is found, in what follows.

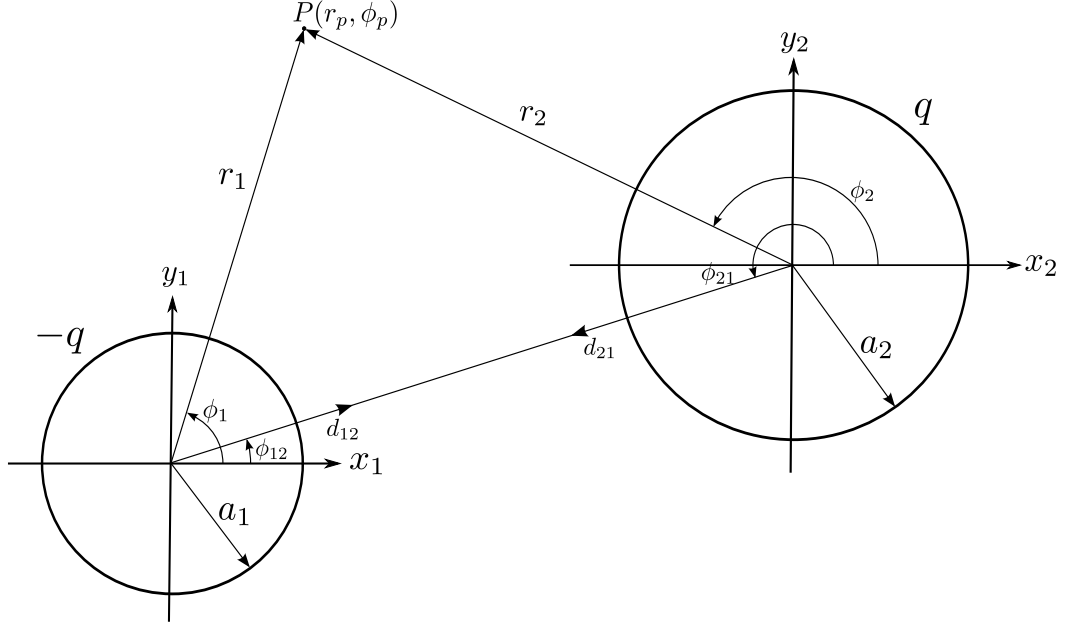


Figure 5.1.1: Two conducting cylinders arbitrarily located in space

The individual potential from each of the two cylinders, in their respective coordinate systems, are

$$u_1(r_1, \phi_1) = C_A + A_0 \ln r_1 + \sum_{n=1}^{\infty} \left[A_n^C \left(\frac{a_1}{r_1} \right)^n \cos n\phi_1 + A_n^S \left(\frac{a_1}{r_1} \right)^n \sin n\phi_1 \right], \quad (5.1.1)$$

$$u_2(r_2, \phi_2) = C_B + B_0 \ln r_2 + \sum_{n=1}^{\infty} \left[B_n^C \left(\frac{a_2}{r_2} \right)^n \cos n\phi_2 + B_n^S \left(\frac{a_2}{r_2} \right)^n \sin n\phi_2 \right]. \quad (5.1.2)$$

The translated potential $u_2^{(1)}(r_1, \phi_1)$ is obtained by applying the addition theorems (3.2.6) and (3.4.5), with the following substitutions $r_q \equiv r_2$, $\phi_q \equiv \phi_2$, $r_p \equiv r_1$,

$\phi_p \equiv \phi_1$, $r_{qp} \equiv d_{21}$ and $\phi_{qp} = \phi_{21}$. This gives

$$\begin{aligned}
u_2^{(1)}(r_1, \phi_1) = & C_B + B_0 \left\{ \ln d_{21} - \sum_{n=1}^{\infty} \frac{(-1)^n}{n} \left(\frac{r_1}{d_{21}} \right)^n \cos(n\phi_1 - n\phi_{21}) \right\} \\
& + \sum_{n=1}^{\infty} \sum_{m=0}^{\infty} \frac{(-1)^m (n+m-1)!}{m!(n-1)!} \left(\frac{a_2}{d_{21}} \right)^n \left(\frac{r_1}{d_{21}} \right)^m \times \\
& \left[B_n^C \cos(m\phi_1 - (m+n)\phi_{21}) - B_n^S \sin(m\phi_1 - (m+n)\phi_{21}) \right]. \tag{5.1.3}
\end{aligned}$$

For convenience, let us denote the functions

$$\tau_{21}^{C/S}(m, n, r_1) = \frac{(-1)^m (n+m-1)!}{m!(n-1)!} \left(\frac{a_2}{d_{21}} \right)^n \left(\frac{r_1}{d_{21}} \right)^m \frac{\cos[(n+m)\phi_{21}]}{\sin[(n+m)\phi_{21}]}, \tag{5.1.4a}$$

$$\gamma_{21}^{C/S}(n, r_1) = -\frac{(-1)^n}{n} \left(\frac{r_1}{d_{21}} \right)^n \frac{\cos n\phi_{21}}{\sin n\phi_{21}}, \tag{5.1.4b}$$

for which the abbreviated notation $\tau_{21}^{C/S}(m, n, r_1)$ and $\gamma_{21}^{C/S}(n, r_1)$ is understood to be $\tau_{21}^{C/S}(m, n, r_1, a_2, d_{21}, \phi_{21})$ and $\gamma_{21}^{C/S}(n, r_1, d_{21}, \phi_{21})$, respectively. Using the trigonometric relationships

$$\cos(\alpha - \beta) = \cos \alpha \cos \beta + \sin \alpha \sin \beta,$$

$$\sin(\alpha - \beta) = \sin \alpha \cos \beta - \cos \alpha \sin \beta,$$

allows the total potential $u_{tot}^{(1)}(r_1 = a_1, \phi_1) = u_1(a_1, \phi_1) + u_2^{(1)}(a_1, \phi_1)$, at the surface of cylinder 1, to be expressed as

$$\begin{aligned}
V_1 = & C + A_0 \ln r_1 + B_0 \ln d_{21} \\
& + \sum_{n=1}^{\infty} \left\{ [A_n^C + B_0 \gamma_{21}^C(n, a_1)] \cos n\phi_1 + [A_n^S + B_0 \gamma_{21}^S(n, a_1)] \sin n\phi_1 \right\} \\
& + \sum_{n=1}^{\infty} \sum_{m=0}^{\infty} \left\{ [B_n^C \tau_{21}^C(m, n, a_1) + B_n^S \tau_{21}^S(m, n, a_1)] \cos m\phi_1 \right. \\
& \quad \left. + [B_n^C \tau_{21}^S(m, n, a_1) - B_n^S \tau_{21}^C(m, n, a_1)] \sin m\phi_1 \right\}, \tag{5.1.5}
\end{aligned}$$

where $C \equiv C_A + C_B$. Multiplying (5.1.5) by $\cos m\phi_1$ for all positive integral values of m and integrating in ϕ_1 from 0 to 2π gives the following infinite set of linear

equations

$$\begin{aligned}
-V_1 + \sum_{n=1}^{\infty} \left[B_n^C \tau_{21}^C(0, n, a_1) + B_n^S \tau_{21}^S(0, n, a_1) \right] &= -A_0 \ln a_1 - B_0 \ln d_{21} - C, \\
A_m^C + \sum_{n=1}^{\infty} \left[B_n^C \tau_{21}^C(m, n, a_1) + B_n^S \tau_{21}^S(m, n, a_1) \right] &= -B_0 \gamma_{21}^C(m, a_1), \\
A_m^S + \sum_{n=1}^{\infty} \left[B_n^C \tau_{21}^S(m, n, a_1) - B_n^S \tau_{21}^C(m, n, a_1) \right] &= -B_0 \gamma_{21}^S(m, a_1).
\end{aligned} \tag{5.1.6}$$

Likewise, after translating $u_1(r_1, \phi_1)$ to (r_2, ϕ_2) coordinates and applying the boundary condition at the surface of cylinder 2, that is, $u_{tot}^{(2)}(r_2 = a_2, \phi_2) = V_2$ gives the infinite set of equations

$$\begin{aligned}
-V_2 + \sum_{n=1}^{\infty} \left[A_n^C \tau_{12}^C(0, n, a_2) + A_n^S \tau_{12}^S(0, n, a_2) \right] &= -B_0 \ln a_2 - A_0 \ln d_{12} - C, \\
B_m^C + \sum_{n=1}^{\infty} \left[A_n^C \tau_{12}^C(m, n, a_2) + A_n^S \tau_{12}^S(m, n, a_2) \right] &= -A_0 \gamma_{12}^C(m, a_2), \\
B_m^S + \sum_{n=1}^{\infty} \left[A_n^C \tau_{12}^S(m, n, a_2) - A_n^S \tau_{12}^C(m, n, a_2) \right] &= -A_0 \gamma_{12}^S(m, a_2),
\end{aligned} \tag{5.1.7}$$

where,

$$\tau_{12}^{C/S}(m, n, r_2) = \frac{(-1)^m (n+m-1)!}{m!(n-1)!} \left(\frac{a_1}{d_{12}} \right)^n \left(\frac{r_2}{d_{12}} \right)^m \frac{\cos}{\sin} [(n+m)\phi_{12}], \tag{5.1.8a}$$

$$\gamma_{12}^{C/S}(n, r_2) = -\frac{(-1)^n}{n} \left(\frac{r_2}{d_{12}} \right)^n \frac{\cos}{\sin} n\phi_{12}. \tag{5.1.8b}$$

where again the abbreviated notation $\tau_{12}^{C/S}(m, n, r_2)$ and $\gamma_{12}^{C/S}(n, r_2)$ is understood to be $\tau_{12}^{C/S}(m, n, r_2, a_1, d_{12}, \phi_{12})$ and $\gamma_{12}^{C/S}(n, r_2, d_{12}, \phi_{12})$, respectively.

Here again the charge per unit length must be found in terms of the constants of integration to impose the known boundary conditions on the cylinders. The charge

density on cylinder 1 was found to be $\rho_S^{(1)}(r_1, \phi_1) = -\varepsilon \frac{\partial u_{tot}^{(1)}}{\partial r_1}$, which gives

$$\begin{aligned} \rho_S^{(1)}(r_1, \phi_1) = & -\varepsilon \left\{ \frac{A_0}{r_1} + \sum_{n=1}^{\infty} \frac{n}{r_1} \left\{ \left[B_0 \gamma_{21}^C(n, r_1) - A_n^C \left(\frac{a_1}{r_1} \right)^n \right] \cos n\phi_1 \right. \right. \\ & + \left. \left[B_0 \gamma_{21}^S(n, r_1) - A_n^S \left(\frac{a_1}{r_1} \right)^n \right] \sin n\phi_1 \right\} \\ & + \sum_{n=1}^{\infty} \sum_{m=0}^{\infty} \frac{m}{r_1} \left\{ \left[B_n^C \tau_{21}^C(m, n, r_1) + B_n^S \tau_{21}^S(m, n, r_1) \right] \cos m\phi_1 \right. \\ & \left. \left. - \left[B_n^C \tau_{21}^S(m, n, r_1) + B_n^S \tau_{21}^C(m, n, r_1) \right] \sin m\phi_1 \right\} \right\}, \quad (5.1.9) \end{aligned}$$

since

$$\frac{\partial}{\partial r_1} \left[\tau_{21}^{C/S}(m, n, r_1) \right] = \frac{m}{r_1} \tau_{21}^{C/S}(m, n, r_1) \quad \text{and} \quad \frac{\partial}{\partial r_1} \left[\gamma_{21}^{C/S}(n, r_1) \right] = \frac{n}{r_1} \gamma_{21}^{C/S}(n, r_1).$$

Therefore the total charge per unit length on cylinder 1, $q_{tot}^{(1)} = \int_0^{2\pi} \rho_S^{(1)}(a_1, \phi_1) a_1 d\phi_1$, is, as before,

$$q_{tot}^{(1)} = -2\pi\varepsilon A_0.$$

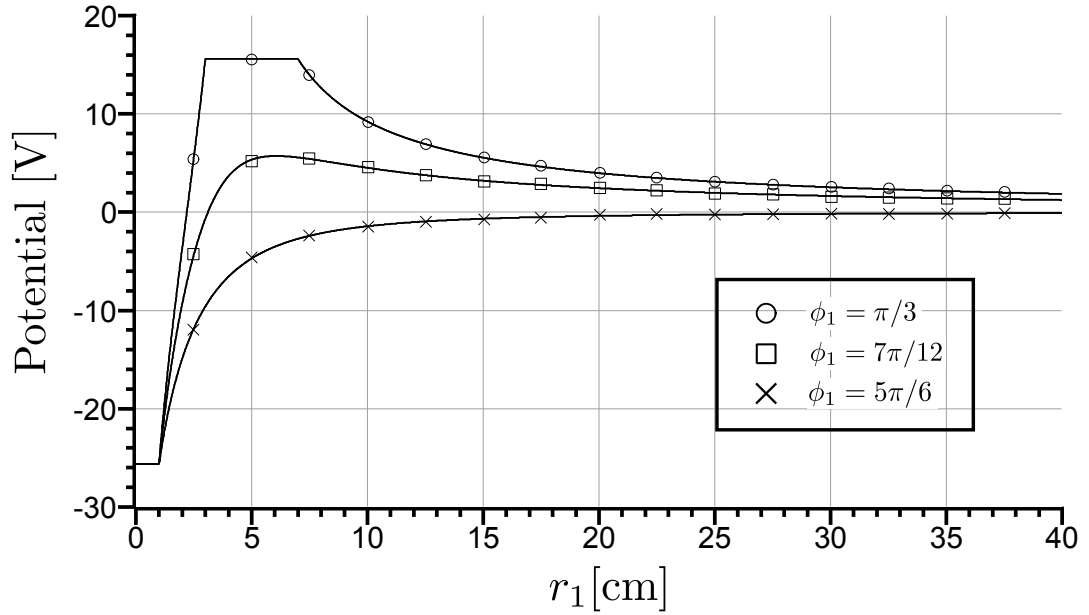
Similarly, the total charge per unit length on the second cylinder is

$$q_{tot}^{(2)} = -2\pi\varepsilon B_0.$$

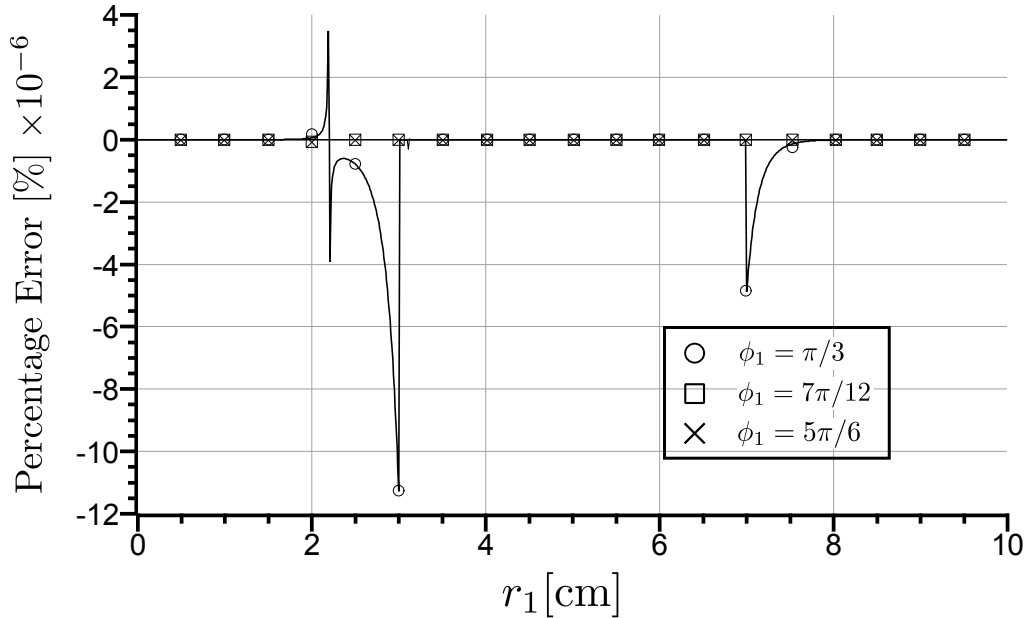
Like before for the potential to vanish at infinity, we require the total charges per unit length on the cylinders be equal and opposite, i.e., $-q_{tot}^{(1)} = q_{tot}^{(2)} = q$ and the reference constant set to $C = 0$. The series are truncated to $n = m = M$ in the sets of linear equations (5.1.6) and (5.1.7), then, using Gaussian elimination we solve the system to find the constants of integration.

Numerical results of the potential are obtained for the case $a_1 = 1$ cm, $a_2 = 2$ cm, $d_{12} = d_{21} = 5$ cm, $\phi_{12} = \pi/3$ and $\phi_{21} = 4\pi/3$ and plotted in Figure 5.1.2. The charges, per unit length, placed on cylinders 1 and 2 are $q_{tot}^{(1)} = -1$ nC/m and $q_{tot}^{(2)} = 1$ nC/m, respectively. Note, apart from the rotational shift of cylinder 2,

the geometry and charges of the cylinders are the same numerical values used in Section 4.2. Since the cylinders are of the same radii and separation distance, the potential distribution for the arbitrarily located parallel cylinders along the lines for $\phi_1 = \pi/3, 7\pi/12$ and $5\pi/6$ correspond, in the case of the coplanar symmetric cylinder problem, to lines along $\phi_1 = 0, \pi/4$ and $\pi/2$, respectively.



(a) Potentials distribution for $\phi_1 = \pi/3, 7\pi/12$ and $5\pi/6$ over $0 < r_1 < 40$ cm



(b) Percentage Error for $\phi_1 = \pi/3, 7\pi/12$ and $5\pi/6$ over $0 < r_1 < 10$ cm

Figure 5.1.2: Potential distribution and errors between translational and bipolar methods for $a_1 = 1$ cm, $a_2 = 2$ cm, $d_{12} = d_{21} = 5$ cm, $\phi_{12} = \pi/3$, $\phi_{21} = 4\pi/3$, $q_{tot}^{(1)} = -1$ nC/m, $q_{tot}^{(2)} = 1$ nC/m and $M = 25$

Figure 5.1.2a compares the potential distribution between the translational and bipolar methods for $\phi_1 = \pi/3, 7\pi/12$ and $5\pi/6$ with respect to r_1 over the interval $0 < r_1 < 40$ cm. To emphasize that the percentage error between the two methods is small the results are graphed in Figure 5.1.2b over the shorter range of $0 < r_1 < 10$ cm, since for distances greater than 10 cm the percentage error is of order 10^{-10} or less.

5.2 System with N arbitrarily located cylinders

For the case with $N = 2$ cylinders a recognizable pattern emerges to the sets of coupled linear equations obtained when applying the boundary conditions at the cylinders. Therefore the linear equations found for the two cylinder case can be generalized to N number of cylinders as shown in Figure 2.2.1. The potential distribution for the p^{th} cylinder represented in its attached coordinate system is

$$u_p(r_p, \phi_p) = C_A^{(p)} + A_0^{(p)} \ln r_p + \sum_{n=1}^{\infty} \left[A_n^{(p)C} \left(\frac{a_p}{r_p} \right)^n \cos n\phi_p + A_n^{(p)S} \left(\frac{a_p}{r_p} \right)^n \sin n\phi_p \right], \quad (5.2.1)$$

where $p = 1, 2, \dots, N$, for all the cylinders. Translating all the potentials to (r_p, ϕ_p) coordinates and applying the boundary condition at the p^{th} cylinder, that is, $u_{tot}^{(p)}(r_p = a_p, \phi_p) = V_p$, generates the set of linear equations

$$\begin{aligned} V_p - C_A &= A_0^{(p)} \ln a_p + \sum_{\substack{q=1 \\ q \neq p}}^N \left\{ A_0^{(q)} \ln d_{qp} + \sum_{n=1}^{\infty} [A_n^{(q)C} \tau_{qp}^C(0, n, a_p) + A_n^{(q)S} \tau_{qp}^S(0, n, a_p)] \right\}, \\ 0 &= A_m^{(p)C} + \sum_{\substack{q=1 \\ q \neq p}}^N \left\{ A_0^{(q)} \gamma_{qp}^C(m, a_p) + \sum_{n=1}^{\infty} [A_n^{(q)C} \tau_{qp}^C(m, n, a_p) + A_n^{(q)S} \tau_{qp}^S(m, n, a_p)] \right\}, \\ 0 &= A_m^{(p)S} + \sum_{\substack{q=1 \\ q \neq p}}^N \left\{ A_0^{(q)} \gamma_{qp}^S(m, a_p) + \sum_{n=1}^{\infty} [A_n^{(q)C} \tau_{qp}^S(m, n, a_p) - A_n^{(q)S} \tau_{qp}^C(m, n, a_p)] \right\}, \end{aligned} \quad (5.2.2)$$

for all positive integral values of $m = 0, 1, 2, \dots$, with $C_A = \sum_{p=1}^N C_A^{(p)}$ and the notation

$$\tau_{qp}^{C/S}(m, n, r_p) = \frac{(-1)^m (n + m - 1)!}{m!(n - 1)!} \left(\frac{a_q}{d_{qp}} \right)^n \left(\frac{r_p}{d_{qp}} \right)^m \frac{\cos(m + n)\phi_{qp}}{\sin(m + n)\phi_{qp}}, \quad (5.2.3a)$$

$$\gamma_{qp}^{C/S}(n, r_p) = -\frac{(-1)^n}{n} \left(\frac{a_p}{d_{qp}} \right)^n \frac{\cos n\phi_{qp}}{\sin n\phi_{qp}}. \quad (5.2.3b)$$

If the infinite set of equations and series are truncated $n = m = M$, every cylinder generates $(2M + 1)$ linear equations. For a system of N cylinders the resultant number of constants of integration to solve for becomes $N(2M + 1)$.

As an example, let us take the case for $N = 3$ conducting cylinders with radii a_1 , a_2 and a_3 with placed charges, per unit length, of $q_{tot}^{(1)}$, $q_{tot}^{(2)}$ and $q_{tot}^{(3)}$, respectively. The distances between the centres of the cylinders are d_{12} , d_{13} and d_{23} with the surrounding medium being homogeneous with permittivity ε , as shown in Figure 5.2.1. Consider a complete system with the potential vanishing at infinity.

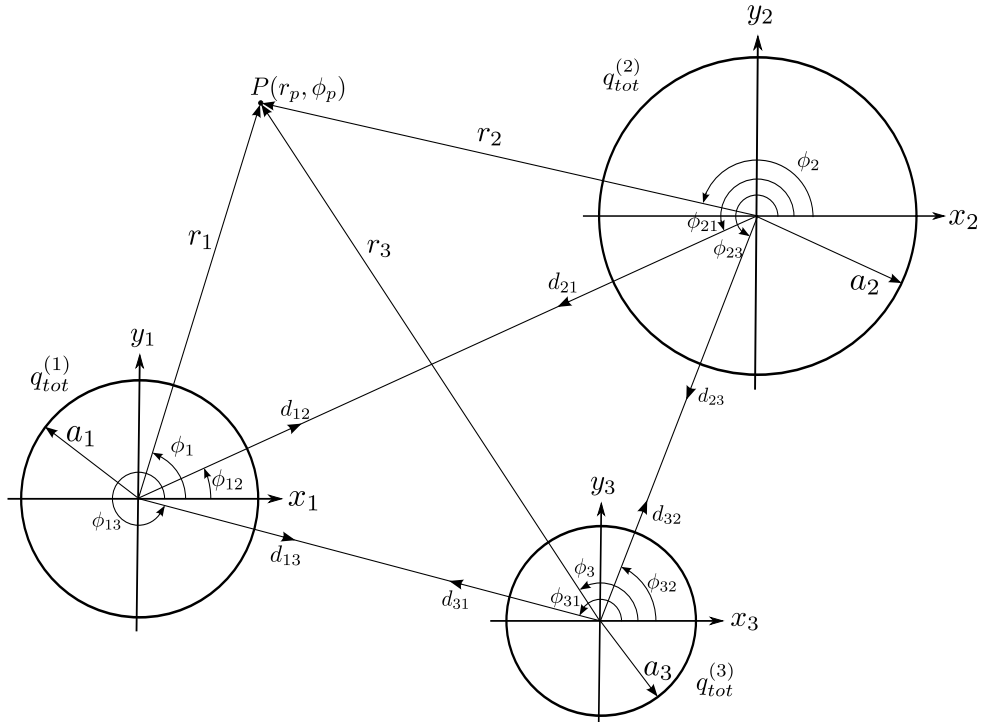


Figure 5.2.1: Three conducting cylinders arbitrarily located in space

Using (5.2.1) the individual potential distributions from each of the three cylinders,

in their respective coordinate systems, are

$$\begin{aligned}
u_1(r_1, \phi_1) &= C_A + A_0 \ln r_1 + \sum_{n=1}^{\infty} \left[A_n^C \left(\frac{a_1}{r_1} \right)^n \cos n\phi_1 + A_n^S \left(\frac{a_1}{r_1} \right)^n \sin n\phi_1 \right], \\
u_2(r_2, \phi_2) &= C_B + B_0 \ln r_2 + \sum_{n=1}^{\infty} \left[B_n^C \left(\frac{a_2}{r_2} \right)^n \cos n\phi_2 + B_n^S \left(\frac{a_2}{r_2} \right)^n \sin n\phi_2 \right], \\
u_3(r_3, \phi_3) &= C_C + C_0 \ln r_3 + \sum_{n=1}^{\infty} \left[C_n^C \left(\frac{a_3}{r_3} \right)^n \cos n\phi_3 + C_n^S \left(\frac{a_3}{r_3} \right)^n \sin n\phi_3 \right],
\end{aligned} \tag{5.2.4}$$

where the substitution $A^{(1)} = A$, $A^{(2)} = B$ and $A^{(3)} = C$ for the constants is made for simplification. As long as the sum of the charges on the conductors equals zero, $q_{tot}^{(1)} + q_{tot}^{(2)} + q_{tot}^{(3)} = 0$, the system will be complete ensuring the logarithmic potential vanishes at infinity. Then, setting the reference constant to zero $C \equiv C_A + C_B + C_C = 0$ and using (5.2.2) the coupled set of linear equations becomes

$$\begin{aligned}
& -A_0 \ln a_1 - B_0 \ln d_{21} - C_0 \ln d_{31} = -V_1 \\
& + \sum_{n=1}^{\infty} \left[B_n^C \tau_{21}^C(0, n, a_1) + B_n^S \tau_{21}^S(0, n, a_1) + C_n^C \tau_{31}^C(0, n, a_1) + C_n^S \tau_{31}^S(0, n, a_1) \right], \\
& -A_0 \ln d_{12} - B_0 \ln a_2 - C_0 \ln d_{32} = -V_2 \\
& + \sum_{n=1}^{\infty} \left[A_n^C \tau_{12}^C(0, n, a_2) + A_n^S \tau_{12}^S(0, n, a_2) + C_n^C \tau_{32}^C(0, n, a_2) + C_n^S \tau_{32}^S(0, n, a_2) \right], \\
& -A_0 \ln d_{13} - B_0 \ln d_{23} - C_0 \ln a_3 = -V_3 \\
& + \sum_{n=1}^{\infty} \left[A_n^C \tau_{13}^C(0, n, a_3) + A_n^S \tau_{13}^S(0, n, a_3) + B_n^C \tau_{23}^C(0, n, a_3) + B_n^S \tau_{23}^S(0, n, a_3) \right], \\
& -B_0 \gamma_{21}^C(m, a_1) - C_0 \gamma_{31}^C(m, a_1) = A_m^C \\
& + \sum_{n=1}^{\infty} \left[B_n^C \tau_{21}^C(m, n, a_1) + B_n^S \tau_{21}^S(m, n, a_1) + C_n^C \tau_{31}^C(m, n, a_1) + C_n^S \tau_{31}^S(m, n, a_1) \right], \\
& -B_0 \gamma_{21}^S(m, a_1) - C_0 \gamma_{31}^S(m, a_1) = A_m^S \\
& + \sum_{n=1}^{\infty} \left[B_n^C \tau_{21}^S(m, n, a_1) - B_n^S \tau_{21}^C(m, n, a_1) + C_n^C \tau_{31}^S(m, n, a_1) - C_n^S \tau_{31}^C(m, n, a_1) \right],
\end{aligned}$$

$$\begin{aligned}
& - A_0 \gamma_{12}^C(m, a_2) + C_0 \gamma_{32}^C(m, a_2) = B_m^C \\
& + \sum_{n=1}^{\infty} [A_n^C \tau_{12}^C(m, n, a_2) + A_n^S \tau_{12}^S(m, n, a_2) + C_n^C \tau_{32}^C(m, n, a_2) + C_n^S \tau_{32}^S(m, n, a_2)], \\
& - A_0 \gamma_{12}^S(m, a_2) - C_0 \gamma_{32}^S(m, a_2) = B_m^S \\
& + \sum_{n=1}^{\infty} [A_n^C \tau_{12}^S(m, n, a_2) - A_n^S \tau_{12}^C(m, n, a_2) + C_n^C \tau_{32}^S(m, n, a_2) - C_n^S \tau_{32}^C(m, n, a_2)], \\
& - A_0 \gamma_{13}^C(m, a_3) - B_0 \gamma_{23}^C(m, a_3) = C_m^C \\
& + \sum_{n=1}^{\infty} [A_n^C \tau_{13}^C(m, n, a_3) + A_n^S \tau_{13}^S(m, n, a_3) + B_n^C \tau_{23}^C(m, n, a_3) + B_n^S \tau_{23}^S(m, n, a_3)], \\
& - A_0 \gamma_{13}^S(m, a_3) - B_0 \gamma_{23}^S(m, a_3) = C_m^S \\
& + \sum_{n=1}^{\infty} [A_n^C \tau_{13}^S(m, n, a_3) - A_n^S \tau_{13}^C(m, n, a_3) + B_n^C \tau_{23}^S(m, n, a_3) - B_n^S \tau_{23}^C(m, n, a_3)],
\end{aligned}$$

where

$$\begin{aligned}
\tau_{21}^{C/S}(m, n, r_1) &= \frac{(-1)^m (n+m-1)!}{m!(n-1)!} \left(\frac{a_2}{d_{21}}\right)^n \left(\frac{r_1}{d_{21}}\right)^m \frac{\cos}{\sin}(n+m)\phi_{21}, \\
\gamma_{21}^{C/S}(n, r_1) &= -\frac{(-1)^n}{n} \left(\frac{r_1}{d_{21}}\right)^n \frac{\cos}{\sin} n\phi_{21}, \\
\tau_{31}^{C/S}(m, n, r_1) &= \frac{(-1)^m (n+m-1)!}{m!(n-1)!} \left(\frac{a_3}{d_{31}}\right)^n \left(\frac{r_1}{d_{31}}\right)^m \frac{\cos}{\sin}(n+m)\phi_{31}, \\
\gamma_{31}^{C/S}(n, r_1) &= -\frac{(-1)^n}{n} \left(\frac{r_1}{d_{31}}\right)^n \frac{\cos}{\sin} n\phi_{31}, \\
\tau_{12}^{C/S}(m, n, r_2) &= \frac{(-1)^m (n+m-1)!}{m!(n-1)!} \left(\frac{a_1}{d_{12}}\right)^n \left(\frac{r_2}{d_{12}}\right)^m \frac{\cos}{\sin}(n+m)\phi_{12}, \\
\gamma_{12}^{C/S}(n, r_2) &= -\frac{(-1)^n}{n} \left(\frac{r_2}{d_{12}}\right)^n \frac{\cos}{\sin} n\phi_{12}, \\
\tau_{32}^{C/S}(m, n, r_2) &= \frac{(-1)^m (n+m-1)!}{m!(n-1)!} \left(\frac{a_3}{d_{32}}\right)^n \left(\frac{r_2}{d_{32}}\right)^m \frac{\cos}{\sin}(n+m)\phi_{32}, \\
\gamma_{32}^{C/S}(n, r_2) &= -\frac{(-1)^n}{n} \left(\frac{r_2}{d_{32}}\right)^n \frac{\cos}{\sin} n\phi_{32},
\end{aligned}$$

$$\begin{aligned}\tau_{13}^{C/S}(m, n, r_3) &= \frac{(-1)^m(n+m-1)!}{m!(n-1)!} \left(\frac{a_1}{d_{13}}\right)^n \left(\frac{r_3}{d_{13}}\right)^m \frac{\cos(n+m)\phi_{13}}{\sin(n+m)\phi_{13}}, \\ \gamma_{13}^{C/S}(n, r_3) &= -\frac{(-1)^n}{n} \left(\frac{r_3}{d_{13}}\right)^n \frac{\cos n\phi_{13}}{\sin n\phi_{13}}, \\ \tau_{23}^{C/S}(m, n, r_3) &= \frac{(-1)^m(n+m-1)!}{m!(n-1)!} \left(\frac{a_2}{d_{23}}\right)^n \left(\frac{r_3}{d_{23}}\right)^m \frac{\cos(n+m)\phi_{23}}{\sin(n+m)\phi_{23}}, \\ \gamma_{23}^{C/S}(n, r_3) &= -\frac{(-1)^n}{n} \left(\frac{r_3}{d_{23}}\right)^n \frac{\cos n\phi_{23}}{\sin n\phi_{23}}.\end{aligned}$$

The set of linear equations is truncated to $n = m = M$ to solve for the constants of integration. The total charges per unit length of the cylinders are, respectively,

$$q_{tot}^{(1)} = -2\pi\epsilon A_0, \quad q_{tot}^{(2)} = -2\pi\epsilon B_0, \quad q_{tot}^{(3)} = -2\pi\epsilon C_0,$$

which are used to determine A_0 , B_0 and C_0 for the linear set of equations.

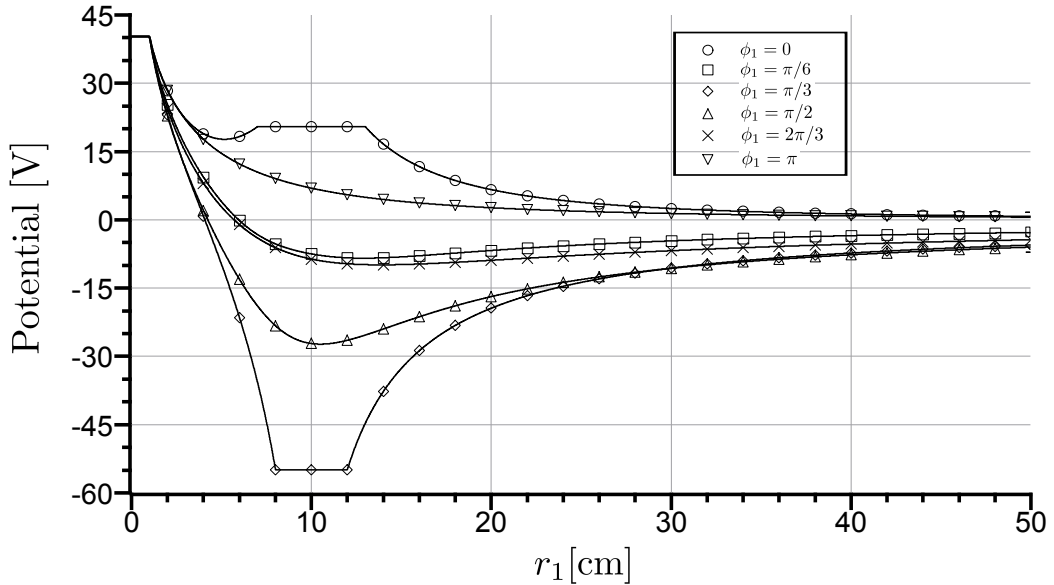


Figure 5.2.2: Potential distribution with respect to r_1 for angles $\phi_1 = 0, \pi/6, \pi/3, \pi/2, 2\pi/3$ and π , when $a_1 = 1$ cm, $a_2 = 2$ cm, $a_3 = 3$ cm, $d_{12} = d_{23} = d_{13} = 10$ cm, $q_{tot}^{(1)} = 1$ nC/m, $q_{tot}^{(2)} = -2$ nC/m, $q_{tot}^{(3)} = 1$ nC/m and $M = 15$

Numerical results are obtained for the case when $a_1 = 1$ cm, $a_2 = 2$ cm, $a_3 = 3$ cm, $d_{12} = d_{13} = d_{23} = 10$ cm, $\phi_{12} = \pi/3$, $\phi_{13} = 0$, $\phi_{21} = 4\pi/3$, $\phi_{23} = 5\pi/3$, $\phi_{31} = \pi$ and $\phi_{32} = 2\pi/3$, that is the axes of the cylinders form an equilateral

triangle, and the charges $q_{tot}^{(1)} = 1$ nC/m, $q_{tot}^{(2)} = -2$ nC/m and $q_{tot}^{(3)} = 1$ nC/m are placed on the conductors. Figure 5.2.2 shows plots of the potential with respect to the (r_1, ϕ_1) coordinates as it varies radial out from cylinder 1 on the lines defined by $\phi_1 = 0, \pi/6, \pi/3, \pi/2, 2\pi/3$ and π over the range $0 < r_1 < 50$ cm for a truncation of $M = 15$. The calculated potentials on the cylinders are $V_1 = 40.2284$ V, $V_2 = -54.8842$ V and $V_3 = 20.4456$ V.

Chapter 6

Application of the translational addition theorems to the solution of magnetostatic fields

The magnetic field can be defined in terms of a magnetic scalar potential u_m , for regions where $\mathbf{J} = 0$ and, within homogeneous materials, satisfies Laplace's equation as in the electrostatic case. Thus,

$$\nabla^2 u_m = 0, \quad \text{wherever } \mathbf{J} = 0. \quad (6.0.1)$$

The solution is obtained, as before, by using the method of separation of variables in circular coordinates. The magnetic field intensity \mathbf{H} is then found by

$$\mathbf{H} = -\nabla u_m. \quad (6.0.2)$$

6.1 Two perfectly conducting cylinders in an external magnetic field parallel to the plane of their axes and normal to them

Consider two perfectly conducting cylinders of radii a_1 and a_2 with a separation d between their axes, as shown in the Figure 6.1.1. The cylinders are placed in an external magnetic field oriented along the common x -axis of the cylinders $\mathbf{H}_0 = H_0 \mathbf{a}_x$. We define the external magnetic field as the only contribution to

the magnetic scalar potential at infinity, i.e., the magnetic potentials from the cylinders vanish at infinity. The medium surrounding the cylinders is homogeneous, of permeability μ .

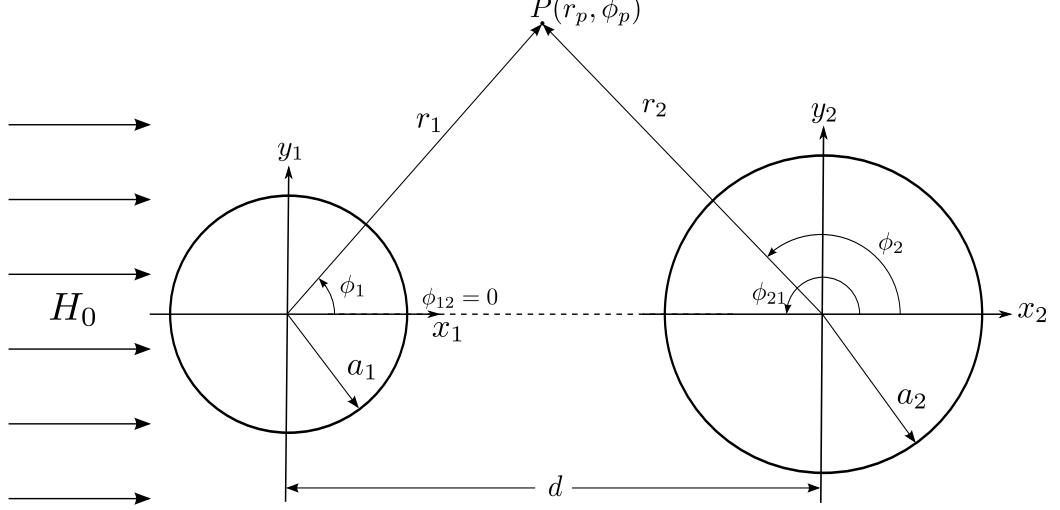


Figure 6.1.1: Two conducting cylinders in external magnetic field, $\mathbf{H}_0 = H_0 \mathbf{a}_x$

The magnetic scalar potentials of each of the cylinders expressed in their attached coordinate systems are

$$u_{m_1}(r_1, \phi_1) = C_A + A_0 \ln r_1 + \sum_{n=1}^{\infty} A_n \left(\frac{a_1}{r_1} \right)^n \cos n\phi_1, \quad r_1 > a_1, \quad (6.1.1)$$

$$u_{m_2}(r_2, \phi_2) = C_B + B_0 \ln r_2 + \sum_{n=1}^{\infty} B_n \left(\frac{a_2}{r_2} \right)^n \cos n\phi_2, \quad r_2 > a_2. \quad (6.1.2)$$

The magnetic potential due the external magnetic field $\mathbf{H}_0 = H_0 \mathbf{a}_x$ in the local coordinates of each cylinder is

$$u_{m_1}^{ex}(r_1, \phi_1) = -H_0 r_1 \cos \phi_1 + C_{ex}, \quad (6.1.3)$$

$$u_{m_2}^{ex}(r_2, \phi_2) = -H_0 r_2 \cos \phi_2 + C_{ex} - H_0 d, \quad (6.1.4)$$

where C_{ex} is a constant of reference.

To impose the boundary condition at $r_1 = a_1$, the translational addition theorems (3.2.6) and (3.4.5), with the substitutions $r_q \equiv r_2$, $\phi_q \equiv \phi_2$, $r_p \equiv r_1$, $\phi_p \equiv \phi_1$,

$r_{qp} \equiv d$ and $\phi_{qp} = \pi$ are reduced to

$$\begin{aligned}\ln r_2 &= \ln d - \sum_{n=1}^{\infty} \frac{1}{n} \left(\frac{r_1}{d}\right)^n \cos n\phi_1, \\ \left(\frac{1}{r_2}\right)^n \cos n\phi_2 &= \sum_{m=0}^{\infty} \frac{(-1)^n (n+m-1)!}{m!(n-1)!} \left(\frac{1}{d}\right)^n \left(\frac{r_1}{d}\right)^m \cos m\phi_1,\end{aligned}$$

where again, for convenience, we denote

$$\tau_B(m, n, r_1, a_2, d) = \frac{(-1)^n (n+m-1)!}{m!(n-1)!} \left(\frac{a_2}{d}\right)^n \left(\frac{r_1}{d}\right)^m, \quad (6.1.5a)$$

$$\gamma_B(n, r_1, d) = -\frac{1}{n} \left(\frac{r_1}{d}\right)^n. \quad (6.1.5b)$$

Therefore the total magnetic scalar potential in the coordinates of cylinder 1 is

$$\begin{aligned}u_{m_{tot}}^{(1)}(r_1, \phi_1) &= A_0 \ln r_1 + B_0 \ln d + \sum_{n=1}^{\infty} \left\{ \left[A_n \left(\frac{a_1}{r_1}\right)^n + B_0 \gamma_B(n, r_1, d) \right] \cos n\phi_1 \right\} \\ &+ \sum_{n=1}^{\infty} \sum_{m=0}^{\infty} B_n \tau_B(m, n, r_1, a_2, d) \cos m\phi_1 + C - H_0 r_1 \cos \phi_1,\end{aligned} \quad (6.1.6)$$

where $C \equiv C_A + C_B + C_{ex}$. The boundary condition on the surface of cylinder 1 requires that the normal component of the magnetic field intensity to be zero. Therefore, the Neumann boundary condition to be imposed on the surface of cylinder 1 is

$$\frac{\partial u_{m_{tot}}^{(1)}}{\partial r_1} = 0. \quad (6.1.7)$$

Taking the derivative of (6.1.6) with respect to r_1 gives

$$\begin{aligned}\frac{\partial u_{m_{tot}}^{(1)}}{\partial r_1} &= -H_0 \cos \phi_1 + \frac{A_0}{r_1} + \sum_{n=1}^{\infty} \frac{n}{r_1} \left[B_0 \gamma_B(n, r_1, d) - A_n \left(\frac{a_1}{r_1}\right)^n \right] \cos n\phi_1 \\ &+ \sum_{n=1}^{\infty} \sum_{m=0}^{\infty} \frac{m}{r_1} B_n \tau_B(m, n, r_1, a_2, d) \cos m\phi_1.\end{aligned} \quad (6.1.8)$$

Applying the boundary condition on cylinder 1 gives

$$0 = -H_0 \cos \phi_1 + \frac{A_0}{a_1} + \sum_{n=1}^{\infty} \frac{n}{a_1} \left[B_0 \gamma_B(n, a_1, d) - A_n \right] \cos n\phi_1$$

$$+ \sum_{n=1}^{\infty} \sum_{m=1}^{\infty} \frac{m}{a_1} B_n \tau_B(m, n, a_1, a_2, d) \cos m\phi_1. \quad (6.1.9)$$

Using the orthogonal properties of the trigonometric functions, (6.1.9) gives the set of infinite equations

$$A_0 = 0, \quad m = 0, \quad (6.1.10a)$$

$$A_1 - \sum_{n=1}^{\infty} B_n \tau_B(1, n, a_1, a_2, d) = -H_0 a_1, \quad m = 1, \quad (6.1.10b)$$

$$A_m - \sum_{n=1}^{\infty} B_n \tau_B(m, n, a_1, a_2, d) = 0, \quad m = 2, 3, \dots \quad (6.1.10c)$$

The same steps taken to apply the boundary conditions at cylinder 1 are followed for cylinder 2. Now $u_{m_1}(r_1, \phi_1)$ is translated into the coordinate system (r_2, ϕ_2) and the boundary conditions at $r_2 = a_2$ are imposed, that is,

$$\frac{\partial m_{m_{tot}}^{(2)}}{\partial r_2} = 0, \quad (6.1.11)$$

which gives the infinite set of equations

$$B_0 = 0, \quad m = 0, \quad (6.1.12a)$$

$$B_1 - \sum_{n=1}^{\infty} A_n \tau_B(1, n, a_2, a_1, d) = -H_0 a_2, \quad m = 1, \quad (6.1.12b)$$

$$B_m - \sum_{n=1}^{\infty} A_n \tau_B(m, n, a_2, a_1, d) = 0, \quad m = 2, 3, \dots \quad (6.1.12c)$$

where

$$\tau_A(m, n, r_2, a_1, d) = \frac{(-1)^m (n+m-1)!}{m!(n-1)!} \left(\frac{a_1}{d} \right)^n \left(\frac{r_2}{d} \right)^m, \quad (6.1.13a)$$

$$\gamma_A(n, r_2, d) = -\frac{(-1)^n}{n} \left(\frac{r_2}{d} \right)^n. \quad (6.1.13b)$$

Like in the electrostatic cases the infinite set of equations is truncated to $n = m = M$ and then using Gaussian elimination, we solve for the constants of integration. Once the constants are obtained the magnetic field intensity is found from

$$\begin{aligned}\mathbf{H} &= -\nabla u_{m_{tot}}(r_1, \phi_1 | r_2, \phi_2) \\ &= H_0 \mathbf{a}_x - \left[\nabla_1 u_{m_1}(r_1, \phi_1) + \nabla_2 u_{m_2}(r_2, \phi_2) \right],\end{aligned}$$

where the subscripts on the ∇ operator indicate that the gradient is taken with respect to the respective coordinate system. The magnetic field components are found to be

$$\begin{aligned}H_x &= H_0 + \sum_{n=1}^{\infty} \left[A_n \left(\frac{n}{r_1} \right) \left(\frac{a_1}{r_1} \right)^n \cos(n+1)\phi_1 + B_n \left(\frac{n}{r_2} \right) \left(\frac{a_2}{r_2} \right)^n \cos(n+1)\phi_2 \right], \\ H_y &= \sum_{n=1}^{\infty} \left[A_n \left(\frac{n}{r_1} \right) \left(\frac{a_1}{r_1} \right)^n \sin(n+1)\phi_1 + B_n \left(\frac{n}{r_2} \right) \left(\frac{a_2}{r_2} \right)^n \sin(n+1)\phi_2 \right].\end{aligned}$$

Two-dimensional bipolar coordinate solution

The scalar magnetic potential obtained using the separation of variables in bipolar coordinates [15], yields

$$u_{m_{tot}}^{bi}(\eta, \xi) = H_0 a + 2H_0 a \sum_{n=1}^{\infty} \left\{ e^{n\eta} - \frac{e^{-n\eta_1}}{\cosh n\eta_1} \sinh n\eta \right\} \cos n\xi, \quad (6.1.14)$$

$$u_{m_{tot}}^{bi}(\eta, \xi) = -H_0 a + 2H_0 a \sum_{n=1}^{\infty} \left\{ e^{-n\eta} + \frac{e^{-n\eta_2}}{\cosh n\eta_2} \sinh n\eta \right\} \cos n\xi. \quad (6.1.15)$$

To obtain the magnetic field intensity the gradient of the magnetic potential is taken, in bipolar coordinates, giving

$$\mathbf{H} = -\nabla u_{m_{tot}}^{bi}(\eta, \xi) = -\frac{1}{h_\eta} \frac{\partial u_{m_{tot}}^{bi}}{\partial \eta} \mathbf{a}_\eta - \frac{1}{h_\xi} \frac{\partial u_{m_{tot}}^{bi}}{\partial \xi} \mathbf{a}_\xi, \quad (6.1.16)$$

where we use the scale factors and geometrical relations between the bipolar and Cartesian unit vectors in Appendix B to obtain the magnetic field components in

terms of unit vectors \mathbf{a}_x and \mathbf{a}_y .

Numerical results of the two perfectly conducting cylinder system in the presence of an external magnetic field

Numerical results are obtained for the case when $a_1 = 1$ cm, $a_2 = 2$ cm, $H_0 = 1$ A/m, and truncation $M = 50$ for varying separation distances d in free space. Figure 6.1.2 shows plots of the magnetic field intensity components H_x and H_y around the surface of cylinder 1, i.e. $r_1 = a_1$, for the separation distances $d = 5$ cm, 10 cm and 20 cm.

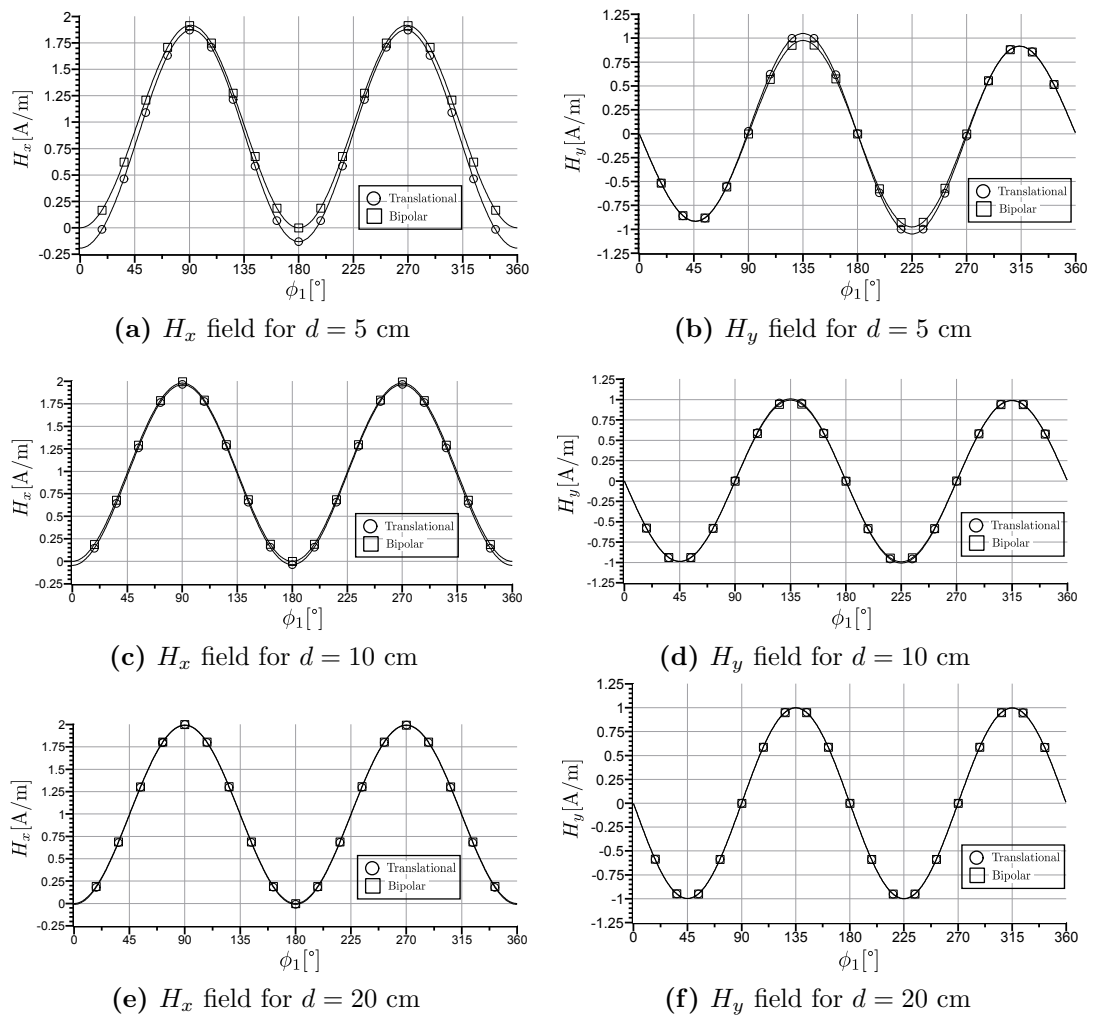


Figure 6.1.2: Magnetic field intensity components H_x and H_y plots around cylinder 1, $r_1 = a_1$ for different separation distances $d = 5$ cm, 10 cm and 20 cm between the translational and bipolar methods for $a_1 = 1$ cm, $a_2 = 2$ cm, $H_0 = 1$ A/m, and $M = 50$

Notice as the separation distance decreases the translational method is no longer

as good an approximation for the magnetic field components, especially near $\phi_1 = 0$ and 180° for the H_x component in Figure 6.1.2a. However, as the separation distance increase in relation to the cylinder radii we see the translational method results are in excellent agreement with the results from the bipolar method.

6.2 Two perfectly conducting cylinders in an external magnetic field normal to the plane of their axes

Now let the direction of the external magnetic field be oriented in the y -direction, $\mathbf{H}_0 = H_0 \mathbf{a}_y$, as shown in Figure 6.2.1 for the same two cylinder system in Section 6.1.

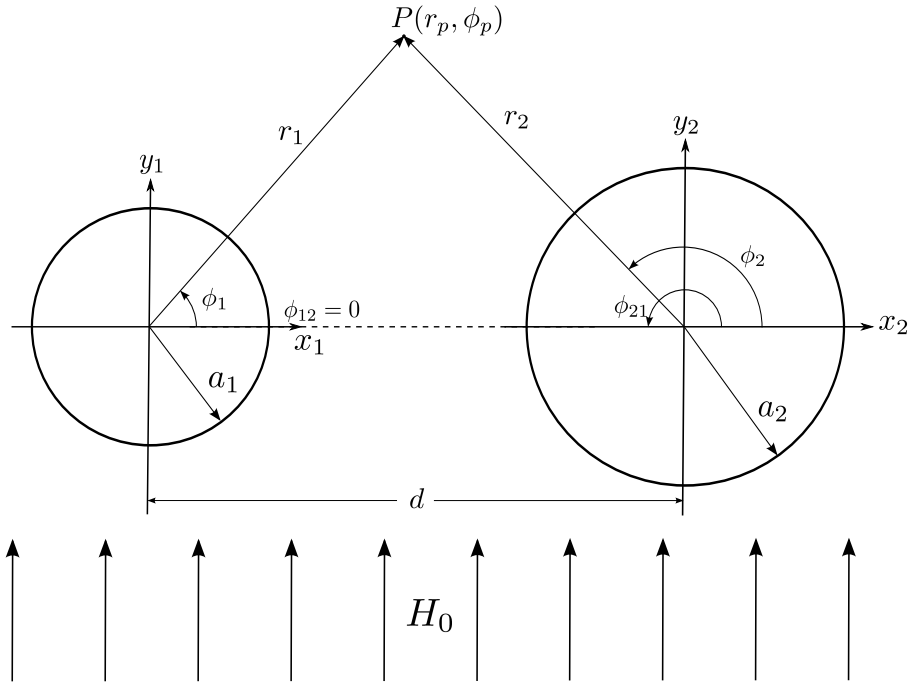


Figure 6.2.1: Two conducting cylinders in external magnetic field, $\mathbf{H}_0 = H_0 \mathbf{a}_y$

The harmonic potential of each cylinder expressed in its attached coordinate system are, then

$$u_{m_1}(r_1, \phi_1) = C_A + A_0 \ln r_1 + \sum_{n=1}^{\infty} \left(\frac{a_1}{r_1} \right)^n \left\{ A_n^C \cos n\phi_1 + A_n^S \sin n\phi_1 \right\}, \quad (6.2.1)$$

$$u_{m_2}(r_2, \phi_2) = C_B + B_0 \ln r_2 + \sum_{n=1}^{\infty} \left(\frac{a_2}{r_2} \right)^n \left\{ B_n^C \cos n\phi_2 + B_n^S \sin n\phi_2 \right\}. \quad (6.2.2)$$

The magnetic potential due the external magnetic field $\mathbf{H}_0 = H_0 \mathbf{a}_y$ in the local coordinates of each cylinder is

$$u_{m_1}^{ex} = -H_0 r_1 \sin \phi_1 + C_{ex}, \quad (6.2.3)$$

$$u_{m_2}^{ex} = -H_0 r_2 \sin \phi_2 + C_{ex}, \quad (6.2.4)$$

where C_{ex} is a constant of reference. To impose the boundary condition at $r_1 = a_1$, the translational addition theorems (3.2.5), (3.2.6) and (3.4.5), with the substitutions $r_q \equiv r_2$, $\phi_q \equiv \phi_2$, $r_p \equiv r_1$, $\phi_p \equiv \phi_1$, $r_{qp} \equiv d$ and $\phi_{qp} = \pi$ to translate u_{m_2} into the coordinate system (r_1, ϕ_1) . Thus, the total magnetic potential is

$$\begin{aligned} u_{m_{tot}}^{(1)}(r_1, \phi_1) &= C - H_0 r_1 \sin \phi_1 + A_0 \ln r_1 + B_0 \ln d \\ &+ \sum_{n=1}^{\infty} \left\{ \left[A_n^C \left(\frac{a_1}{r_1} \right)^n + B_0 \gamma_B(n, r_1, d) \right] \cos n\phi_1 + A_n^S \left(\frac{a_1}{r_1} \right)^n \sin n\phi_1 \right\} \\ &+ \sum_{n=1}^{\infty} \sum_{m=0}^{\infty} \left\{ B_n^C \tau_B(m, n, r_1, a_2, d) \cos m\phi_1 - B_n^S \tau_B(m, n, r_1, a_2, d) \sin m\phi_1 \right\}, \end{aligned} \quad (6.2.5)$$

where $C \equiv C_A + C_B + C_{ex}$ and the functions $\gamma_B(n, r_1, d)$ and $\tau_B(m, n, r_1, a_2, d)$ are defined in (6.1.5). The derivative of (6.2.5) with respect to r_1 is taken so the boundary condition, i.e., the magnetic field intensity normal to the surface of the cylinder, $r_1 = a_1$, is zero. Thus,

$$\begin{aligned} 0 &= -H_0 \sin \phi_1 + \frac{A_0}{a_1} + \sum_{n=1}^{\infty} \frac{n}{a_1} \left\{ [B_0 \gamma_B(n, r_1, d) - A_n^C] \cos n\phi_1 - A_n^S \left(\frac{a_1}{r_1} \right)^n \sin n\phi_1 \right\} \\ &+ \sum_{n=1}^{\infty} \sum_{m=0}^{\infty} \frac{m}{a_1} \left\{ B_n^C \tau_B(m, n, r_1, a_2, d) \cos m\phi_1 - B_n^S \tau_B(m, n, r_1, a_2, d) \sin m\phi_1 \right\}, \end{aligned} \quad (6.2.6)$$

Using the orthogonal properties of the trigonometric functions, (6.2.6) gives the

set of infinite equations

$$A_0 = 0, \quad m = 0, \quad (6.2.7a)$$

$$A_m^C - \sum_{n=1}^{\infty} B_n^C \tau_B(m, n, a_1) = 0, \quad m = 1, 2, \dots, \quad (6.2.7b)$$

$$A_1^S + \sum_{n=1}^{\infty} B_n^S \tau_B(1, n, a_1) = -H_0 a_1, \quad m = 1, \quad (6.2.7c)$$

$$A_m^S + \sum_{n=1}^{\infty} B_n^S \tau_B(m, n, a_1) = 0, \quad m = 2, 3, \dots \quad (6.2.7d)$$

In the same way, imposing the boundary condition at the surface of cylinder 2 gives the set of infinite equations

$$B_0 = 0, \quad m = 0, \quad (6.2.8a)$$

$$B_m^C - \sum_{n=1}^{\infty} A_n^C \tau_A(m, n, a_2) = 0, \quad m = 1, 2, \dots, \quad (6.2.8b)$$

$$B_1^S + \sum_{n=1}^{\infty} A_n^S \tau_A(1, n, a_2) = -H_0 a_2, \quad m = 1, \quad (6.2.8c)$$

$$B_m^S + \sum_{n=1}^{\infty} A_n^S \tau_A(m, n, a_2) = 0, \quad m = 2, 3, \dots, \quad (6.2.8d)$$

where the functions $\gamma_A(n, r_2, d)$ and $\tau_A(m, n, r_2, a_1, d)$ are defined in (6.1.13). The infinite set of equations is truncated to $n = m = M$ and then using Gaussian elimination, we solve for the constants of integration. Once the constants are obtained we use $\mathbf{H} = -\nabla u_{m_{tot}}$ to find the magnetic field intensity.

Solving this same problem in bipolar coordinates, assuming the magnetic potential vanishes at infinity, yields

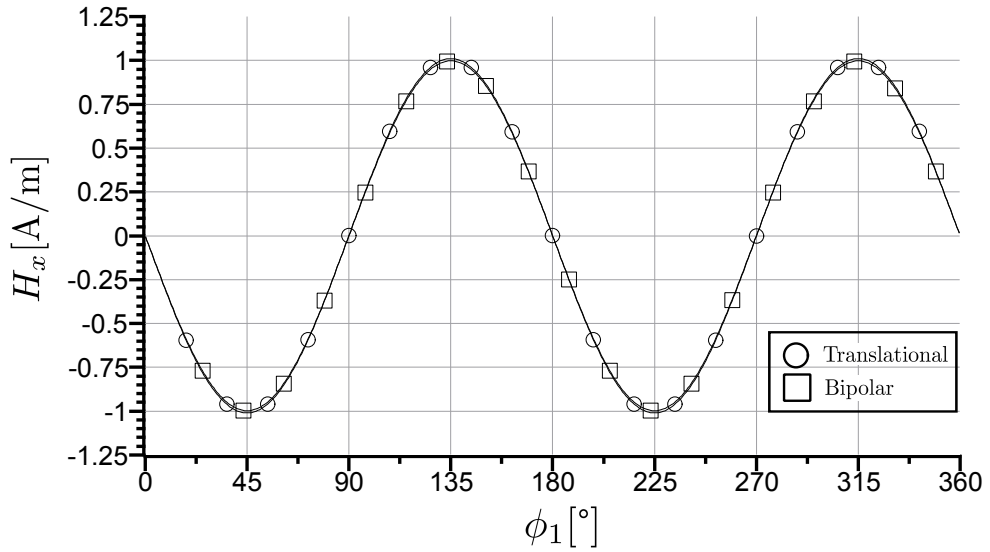
$$u_{m_{tot}}^{bi}(\eta, \xi) = -2H_0 a \sum_{n=1}^{\infty} \left\{ e^{n\eta} - \frac{e^{-n\eta_1}}{\cosh n\eta_1} \sinh n\eta \right\} \sin n\xi, \quad (6.2.9)$$

$$u_{m_{tot}}^{bi}(\eta, \xi) = -2H_0 a \sum_{n=1}^{\infty} \left\{ e^{-n\eta} + \frac{e^{-n\eta_2}}{\cosh n\eta_2} \sinh n\eta \right\} \sin n\xi. \quad (6.2.10)$$

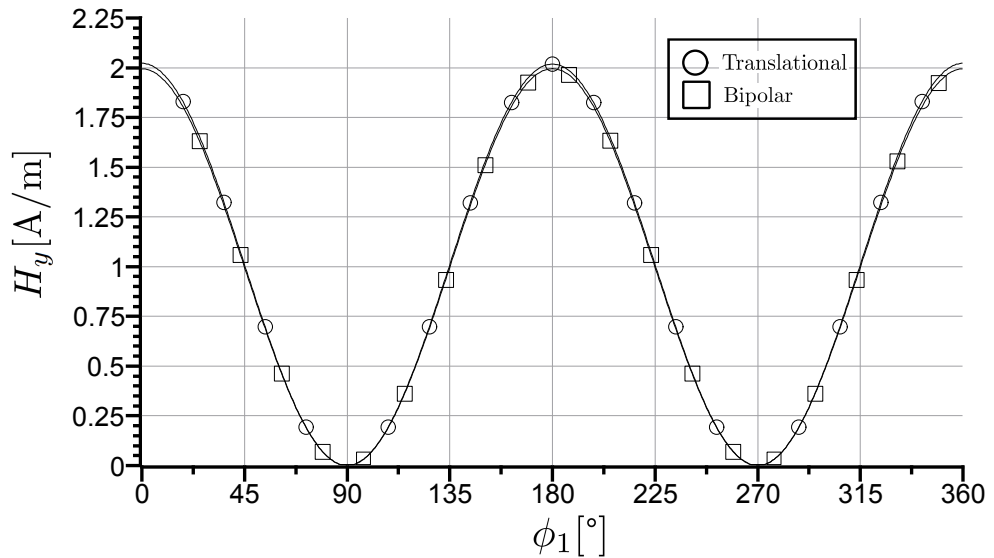
Again, as in the previous section, we use $\mathbf{H} = -\nabla u_{m_{tot}}^{bi}(\eta, \xi)$ to find the magnetic

field intensity in terms of the unit vectors \mathbf{a}_η and \mathbf{a}_ξ , then, using the relations in Appendix B to find the magnetic field in terms of Cartesian unit vectors.

Numerical results are obtained for the case when $a_1 = 1$ cm, $a_2 = 2$ cm, $d = 20$ cm, $H_0 = 1$ A/m and truncation $M = 50$ in free space. Figure 6.2.2 shows plots of the magnetic field intensity components H_x and H_y around the surface of cylinder 1, i.e. $r_1 = a_1$.



(a) H_x field



(b) H_y field

Figure 6.2.2: Magnetic field intensity component plots around cylinder 1, $r_1 = a_1$ between the translational and bipolar methods for $a_1 = 1$ cm, $a_2 = 2$ cm, $d = 20$ cm, $H_0 = 1$ A/m and $M = 50$

6.3 The magnetic vector potential

The magnetic field can be defined in terms of a magnetic vector potential $\mathbf{B} = \nabla \times \mathbf{A}$, since one of Maxwell's equations states that the divergence of \mathbf{B} is zero. Maxwell's other equation to do with magnetic fields states

$$\begin{aligned}\nabla \times \mathbf{B} &= \mu \mathbf{J}, \\ \nabla \times (\nabla \times \mathbf{A}) &= \mu \mathbf{J},\end{aligned}$$

where μ is the permeability and \mathbf{J} is the current distribution. If we use the vector relation $\nabla \times (\nabla \times \mathbf{A}) = \nabla(\nabla \cdot \mathbf{A}) - \nabla^2 \mathbf{A}$ and conveniently have $\nabla \cdot \mathbf{A} = 0$ this gives

$$\nabla^2 \mathbf{A} = -\mu \mathbf{J}. \quad (6.3.1)$$

For two-dimensional magnetostatic problems it can be assumed that the fields are not functions of the z -coordinate, as a result the magnetic vector potential can have only the component A_z , tangential to the cylindrical surfaces. The magnetic problems will assume the region free from current $\mathbf{J} = 0$, so the solution reduces to the electrostatic case

$$\nabla^2 A_z = 0, \quad \text{wherever } \mathbf{J} = 0, \quad (6.3.2)$$

and using the separation of variables method in circular coordinates to (6.3.2) allows us to find the magnetic fields.

The boundary condition for a perfect conductor is $\mathbf{a}_n \times \mathbf{B} = \mu \mathbf{J}_S$ where \mathbf{a}_n is the unit outward normal to the surface and \mathbf{J}_S is the surface current, where the total current on the p^{th} cylinder is I_p . Therefore, the Neumann boundary condition on the surface of cylinder the p^{th} is

$$\int_0^{2\pi} \left. \frac{\partial A_{z_{tot}}^{(p)}}{\partial r_p} d\phi_p \right|_{r_p=a_p} = -\frac{I_p}{a_p}. \quad (6.3.3)$$

Chapter 7

Conclusion and Future Work

7.1 Conclusion

In this thesis, a novel analytic method is formulated for the solution of scalar Laplacian field problems for arbitrary configurations of parallel, infinitely long conducting cylinders. These exact analytic solutions are intended to be used as benchmark solutions, with controllable accuracies, to validate more general approximate numerical methods. In the real world, we understand the two-dimensional field problem solutions to be good approximations for long conductors only in the region between or sufficiently close to conductors, neglecting the end effects.

For the boundary value problem with many parallel cylinders, the field contributions from all the other cylinders were expressed in the polar coordinates attached to each cylinder by using the translational addition theorems for polar Laplacian functions derived from the cylindrical scalar wave addition theorems [6,9]. Then, the boundary conditions were imposed at each cylinder surface resulting in an infinite set of algebraic equations for the constants of integration, which were appropriately truncated in terms of the desired accuracy.

The validity of the series in the addition theorems for polar Laplacian functions was confirmed with numerical results showing excellent convergence. Then, the addition theorems were applied to obtain numerical solutions to some electrostatic and magnetostatic field problems relative to complete systems of cylinders, i.e., when the sum of the charges on all the conductors is equal to zero, and as a consequence,

the potential vanishes at infinity. For the case of two cylinders, we compared the results with the existing exact results obtained by applying the method of separation of variables in two-dimensional bipolar coordinates [14,15], with excellent agreement. Numerical results are also calculated for various configurations with three parallel cylinders using the translational addition theorem method.

7.2 Continued research

The research presented in this thesis was confined to complete systems of conducting cylinders. One of the first areas to explore is to extend this research to systems of conducting cylinders describing actual real world arrangements of cables and transmission lines in the presence of grounded conductors or planes. Another engineering application is to consider a grounded array of conductors in the presence of an external field in order to determine associated shielding effects.

A second area of study would be to use the results from this thesis to describe fields in the presence of penetrable cylinders, dielectric or magnetic, where the boundary conditions are more complex. Another extension would be to apply the derived addition theorems to other engineering and physics disciplines, such as, fluid dynamics and steady state temperature distributions in conducting bodies.

All the cylinders considered in the work presented are circular cylinders, but for the more general case of elliptical cylinders, work can be done to derive translational addition theorems for Laplacian elliptical cylindrical functions. Similarly, this can be done for the Laplacian parabolic cylindrical functions.

Appendix A

Circular cylindrical harmonics

Laplace's equation in plane circular coordinates (r, ϕ) is

$$r \frac{\partial}{\partial r} \left(r \frac{\partial u}{\partial r} \right) + \frac{\partial^2 u}{\partial \phi^2} = 0. \quad (\text{A.1})$$

To solve Laplace's equation the separation method is used, let $u(r, \phi) = R(r)\Phi(\phi)$, substitute in (A.1) and divide by u . This gives

$$\frac{r}{R} \frac{\partial}{\partial r} \left(r \frac{\partial R}{\partial r} \right) + \frac{1}{\Phi} \frac{\partial^2 \Phi}{\partial \phi^2} = 0. \quad (\text{A.2})$$

The two terms must be individually constant, therefore the separation parameter $-n^2$, where n represents only positive integer values, is chosen such that the circular function, $R(r)\Phi(\phi)$, is periodic in angle ϕ . The result is two ordinary differential equations

$$\frac{d^2 \Phi}{d\phi^2} + n^2 \Phi = 0, \quad (\text{A.3a})$$

$$r \frac{d}{dr} \left(r \frac{dR}{dr} \right) - n^2 R = 0. \quad (\text{A.3b})$$

The solutions to (A.3) for $n \neq 0$ are

$$R_n = A_n r^n + B_n r^{-n},$$

$$\Phi_n = C_n \cos n\phi + D_n \sin n\phi,$$

and for $n = 0$,

$$R_0 = A_0 + B_0 \ln r,$$

$$\Phi_0 = C_0 + D_0 \phi.$$

The general harmonic solution is obtained by linear superposition to give

$$\begin{aligned} u(r, \phi) &= \sum_{n=0}^{\infty} R_n \Phi_n \\ &= (A_0 + B_0 \ln r)(C_0 + D_0 \phi) + \sum_{n=1}^{\infty} (A_n r^n + B_n r^{-n}) (C_n \cos n\phi + D_n \sin n\phi). \end{aligned} \quad (\text{A.4})$$

A necessary regularity condition of the harmonic solutions is for them to be periodic over period 2π thus (A.4) is reduced to

$$u(r, \phi) = A_0 + B_0 \ln r + \sum_{n=1}^{\infty} (A_n r^n + B_n r^{-n}) (C_n \cos n\phi + D_n \sin n\phi). \quad (\text{A.5})$$

Appendix B

Two-dimensional bipolar coordinates

Bipolar Laplacian harmonics

Laplace's equation in two-dimensional bipolar coordinates (η, ξ) is

$$\nabla^2 u_{bi}(\eta, \xi) = \left(\frac{\cosh \eta - \cos \xi}{a} \right)^2 \left[\frac{\partial^2 u_{bi}}{\partial \eta^2} + \frac{\partial^2 u_{bi}}{\partial \xi^2} \right] = 0. \quad (\text{B.1})$$

Note here the that $\left(\frac{\cosh \eta - \cos \xi}{a} \right)^2$ at infinity ($\eta = 0, \xi = 0$) is zero, therefore no solution to (B.1) exists at infinity. However, for all other points Laplace's equation reduces to

$$\nabla^2 u_{bi}(\eta, \xi) = \frac{\partial^2 u_{bi}}{\partial \eta^2} + \frac{\partial^2 u_{bi}}{\partial \xi^2} = 0. \quad (\text{B.2})$$

To solve Laplace's equation the separation method is used, let $u(\eta, \xi) = N(\eta)\Xi(\xi)$, substitute in (B.2) and divide by u . This gives

$$\frac{1}{n} \frac{\partial^2 u}{\partial \eta^2} + \frac{1}{\Xi} \frac{\partial^2 u}{\partial \xi^2} = 0. \quad (\text{B.3})$$

Thus using the separation parameter $-n^2$, the resulting ordinary differential equations are

$$\frac{d^2 \Xi}{d\xi^2} + n^2 \Xi = 0, \quad (\text{B.4a})$$

$$\frac{d^2 N}{d\eta^2} + n^2 N = 0. \quad (\text{B.4b})$$

The general harmonic solution is then by linear superposition

$$\begin{aligned}
u(\eta, \xi) &= \sum_{n=0}^{\infty} N_n \Xi_n \\
&= (A_0 + B_0 \eta)(C_0 + D_0 \xi) + \sum_{n=1}^{\infty} (A_n e^{n\eta} + B_n e^{-n\eta}) (C_n \cos n\xi + D_n \sin n\xi).
\end{aligned} \tag{B.5}$$

A necessary regularity condition of the harmonic solutions is for them to be periodic over period 2π thus (B.5) is reduced to

$$u(r, \phi) = A_0 + B_0 \eta + \sum_{n=1}^{\infty} (A_n e^{n\eta} + B_n e^{-n\eta}) (C_n \cos n\xi + D_n \sin n\xi). \tag{B.6}$$

Bipolar coordinates relation to Cartesian coordinates

To relate bipolar coordinates to Cartesian coordinates we define the points $(-a, 0)$, $(a, 0)$ and (x, y) [14], where a is the semi-foci distances of the bipolar coordinates, as shown in Figure B.1. Then the relationship between (η, ξ) and (x, y) can be

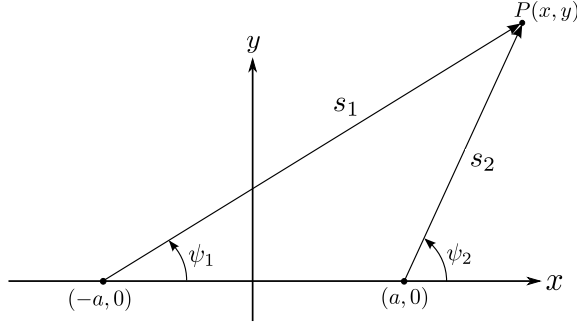


Figure B.1: Relation between bipolar and Cartesian coordinates

shown to be

$$\eta = \ln \left(\frac{s_1}{s_2} \right) = \ln \left(\frac{\sqrt{(x-a)^2 + y^2}}{\sqrt{(x+a)^2 + y^2}} \right) \tag{B.7}$$

and

$$\xi = \psi_1 - \psi_2 = \tan^{-1} \left(\frac{y}{x-a} \right) - \tan^{-1} \left(\frac{y}{x+a} \right). \tag{B.8}$$

Bipolar coordinates unit vectors and scale factors

The unit vectors and scale factors associated with these coordinates are

$$d\mathbf{S} = \mathbf{a}_n h_\xi d\xi dz, \quad (\text{B.9a})$$

$$\mathbf{a}_\eta = \frac{-\mathbf{a}_x (\cosh \eta \cos \xi - 1) - \mathbf{a}_y \sinh \eta \sin \xi}{\cosh \eta - \cos \xi}, \quad (\text{B.9b})$$

$$\mathbf{a}_\xi = \frac{-\mathbf{a}_x \sinh \eta \sin \xi + \mathbf{a}_y (\cosh \eta \cos \xi - 1)}{\cosh \eta - \cos \xi}, \quad (\text{B.9c})$$

$$h_\eta = h_\xi = \frac{a}{\cosh \eta - \cos \xi}. \quad (\text{B.9d})$$

Bibliography

- [1] E. Weber, *Electromagnetic Fields: Theory and Applications*. John Wiley & Sons, Inc, 1950.
- [2] M. Abd-El-Malek, I. El-Awadi, and S. El-Mansi, “Electro-static potential between two conducting cylinders via the group method approach,” *Proceedings of Institute of Mathematics of NAS of Ukraine*, vol. 30, no. 1, pp. 60–67, 2000.
- [3] M. P. Sarma and W. Janishchewskyj, “Electrostatic field of a system of parallel cylindrical conductors,” *IEEE Transactions on Power Apparatus and Systems*, no. 7, pp. 1069–1078, 1969.
- [4] S. C. K. M. Kotuwage, “Application of translational addition theorems to electric and magnetic field analysis in many-sphere systems,” Master’s thesis, The University of Manitoba, 2011.
- [5] A.-K. M. Hamid, *Electromagnetic Wave Scattering by Many-Sphere Systems with Application to Simulation of Three-Dimensional Bodies*. PhD thesis, The University of Manitoba, 1991.
- [6] H. A. Ragheb, *Simulation of Cylindrical Reflector Antennas*. PhD thesis, The University of Manitoba, May 1987.
- [7] M. N. Sadiku, *Numerical Techniques in Electromagnetics*. CRC Press, LLC, second edition ed., 2001.
- [8] J. A. Stratton, *Electromagnetic Theory*. IEEE Press Series on Electromagnetic Wave Theory, Hoboken, New Jersey: John Wiley & Sons, Inc, 2007.

- [9] V. Twersky, “Multiple scattering of radiation by an arbitrary configuration of parallel cylinders,” *The Journal of the Acoustical Society of America*, vol. 24, pp. 42–46, Jan. 1952.
- [10] W. R. Smythe, *Static and Dynamic Electricity*. International Series in Pure and Applied Physics, McGraw-Hill, Inc, third edition ed., 1968.
- [11] I. M. Ryzhik and I. S. Gradshteyn, *Table of Integrals, Series, and Products: Corrected and Enlarged Edition*. Academic Press, Inc, 1980.
- [12] M. Abramowitz and I. A. Stegun, eds., *Handbook of Mathematical Functions: with Formulas, Graphs, and Mathematical Tables*. Dover Books on Mathematics, Dover Publications, Inc, 1965.
- [13] L. Greengard and V. Rokhlin, “A fast algorithm for particle simulations,” *Journal of Computational Physics*, vol. 135, no. 2, pp. 280–292, 1997.
- [14] G. Arfken, *Mathematical Methods for Physicists*. IEEE Press Series on Electromagnetic Wave Theory, Academic Press, Inc., second edition ed., 1970.
- [15] A. A. Ashour, “The magnetic field of an infinite plane current sheet uniform except for two circular insertions of different uniform conductivities,” *Geophysical Journal of the Royal Astronomical Society*, vol. 83, pp. 127–142, May 1985.